Search for di-Higgs production at the ATLAS experiment

DIS 2021

ATLAS EXPERIMENT

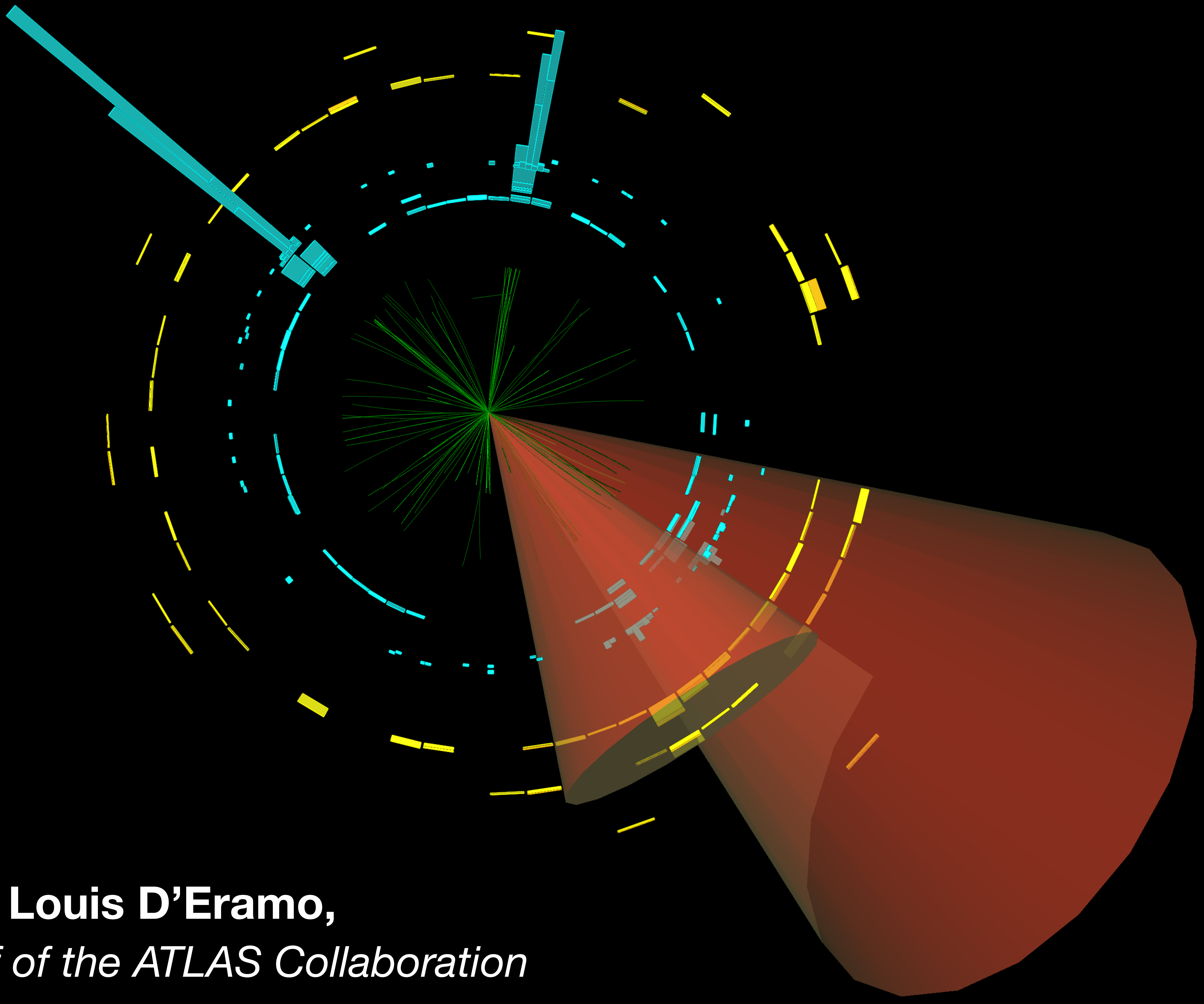

Louis D'Eramo,

On behalf of the ATLAS Collaboration

Northern Illinois University

NIU

Investigating the Higgs potential

The full expression of the Higgs potential is encoded with parameters μ and λ as:

[Phys. Rev. D 101, 075023]

$$V(\phi^\dagger\phi) = -\mu^2\phi^\dagger\phi + \lambda(\phi^\dagger\phi)^2$$

$$\supset \boxed{\underbrace{\mu^2}_{\frac{1}{2}m_H^2} H^2} + \boxed{\sqrt{\frac{\lambda}{2}}\mu\, H^3} + \boxed{\frac{\lambda}{4}H^4}$$

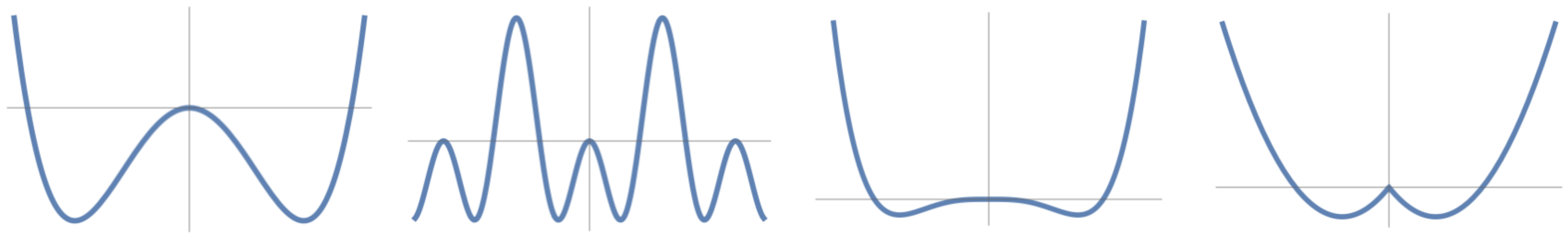

Landau-Ginzburg Higgs | Nambu-Goldstone Higgs | Coleman-Weinberg Higgs | Tadpole-Induced Higgs

These parameters are defining the vacuum expected value ν:

$$\boxed{\nu = \sqrt{\frac{\mu^2}{2\lambda}} \simeq 246\ \text{GeV}}$$

Determined from the EW precise measurements

- First estimation from the Higgs mass measurement:
  - Combined with the v.e.v computation: $\lambda_{SM} \sim 0.13$

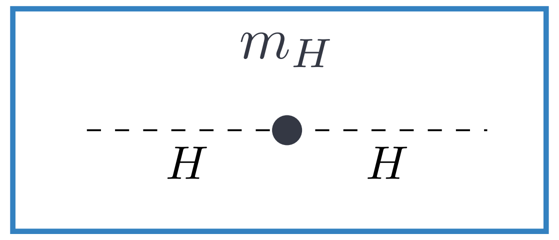

- Quartic interaction even rarer : out of reach even for HL-LHC
  - Contribution increases with $\sqrt{s}$

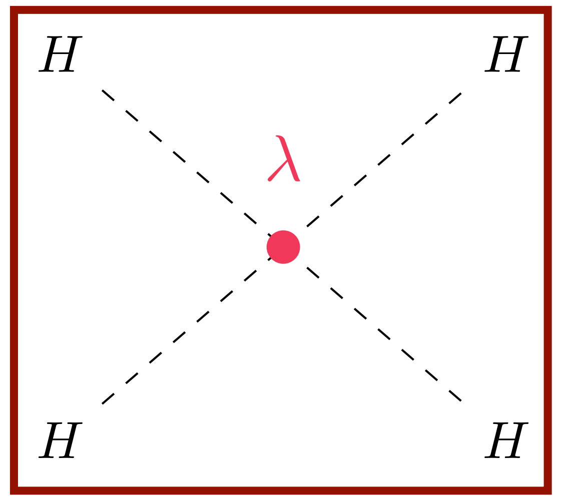

- Direct access to λ through Higgs pair creation:

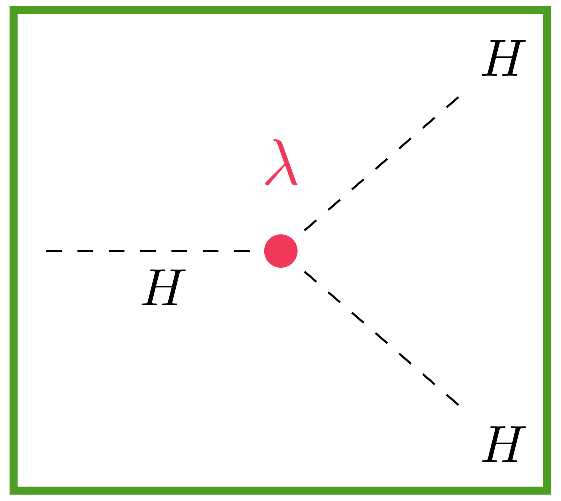

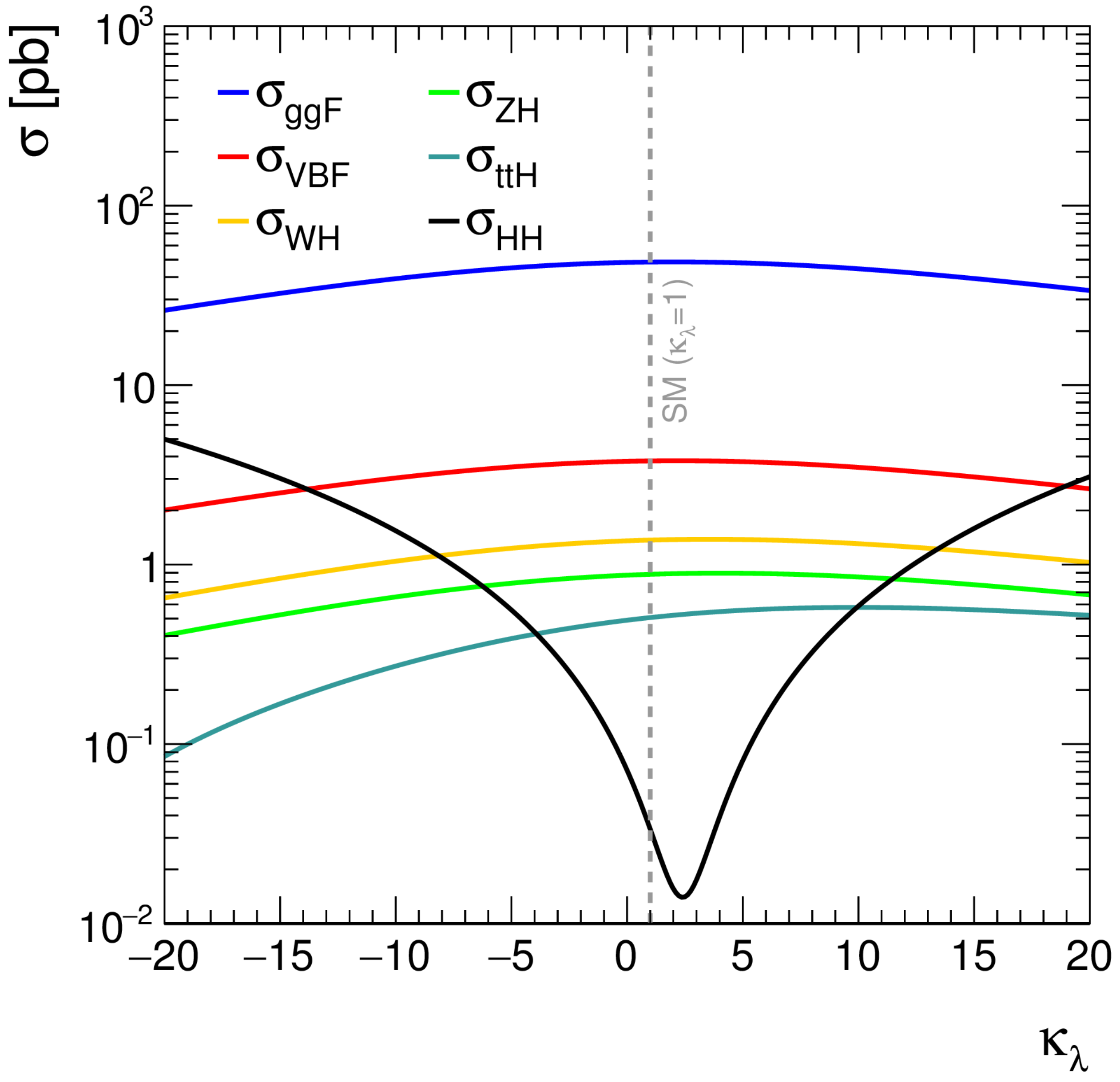

- Coupling strength denoted as $\kappa_\lambda = \lambda_{HHH}/\lambda_{SM}$
- Wide range of BSM models predicting different shapes and thus values for κ_λ
- Some constraints from Single Higgs production, small effect on cross-section → looking for pair production.

How are Higgs pairs produced?

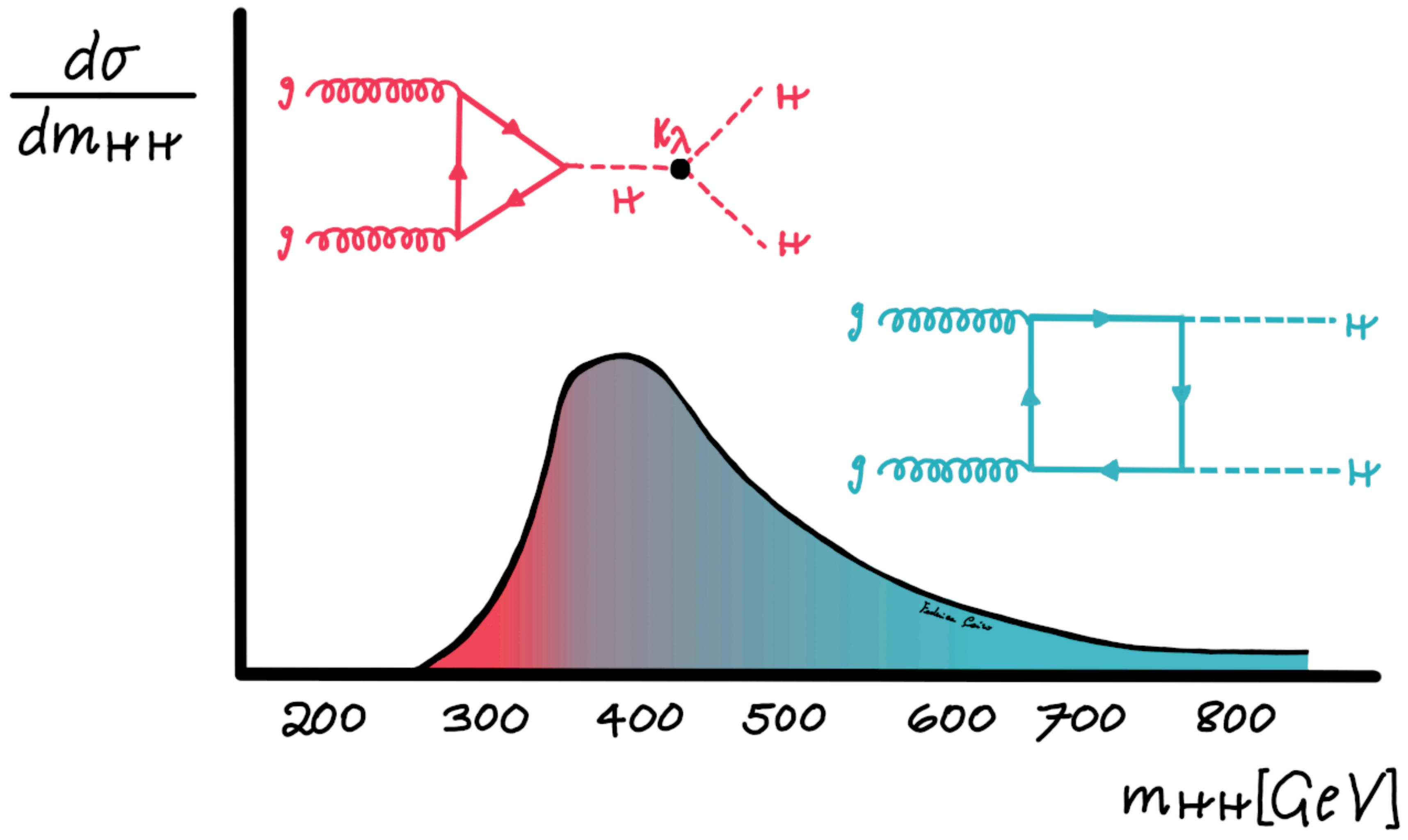

- **gluon-gluon Fusion (ggF)**: $\sigma_{HH}^{ggF} = 31.02$ fb
  - Destructive interference between triangle and box diagrams makes the cross-section tiny (1000x smaller than single Higgs).
  - Low masses essential to constrain trilinear coupling κ_λ
  - m_{HH} shape very dependent on the κ_λ

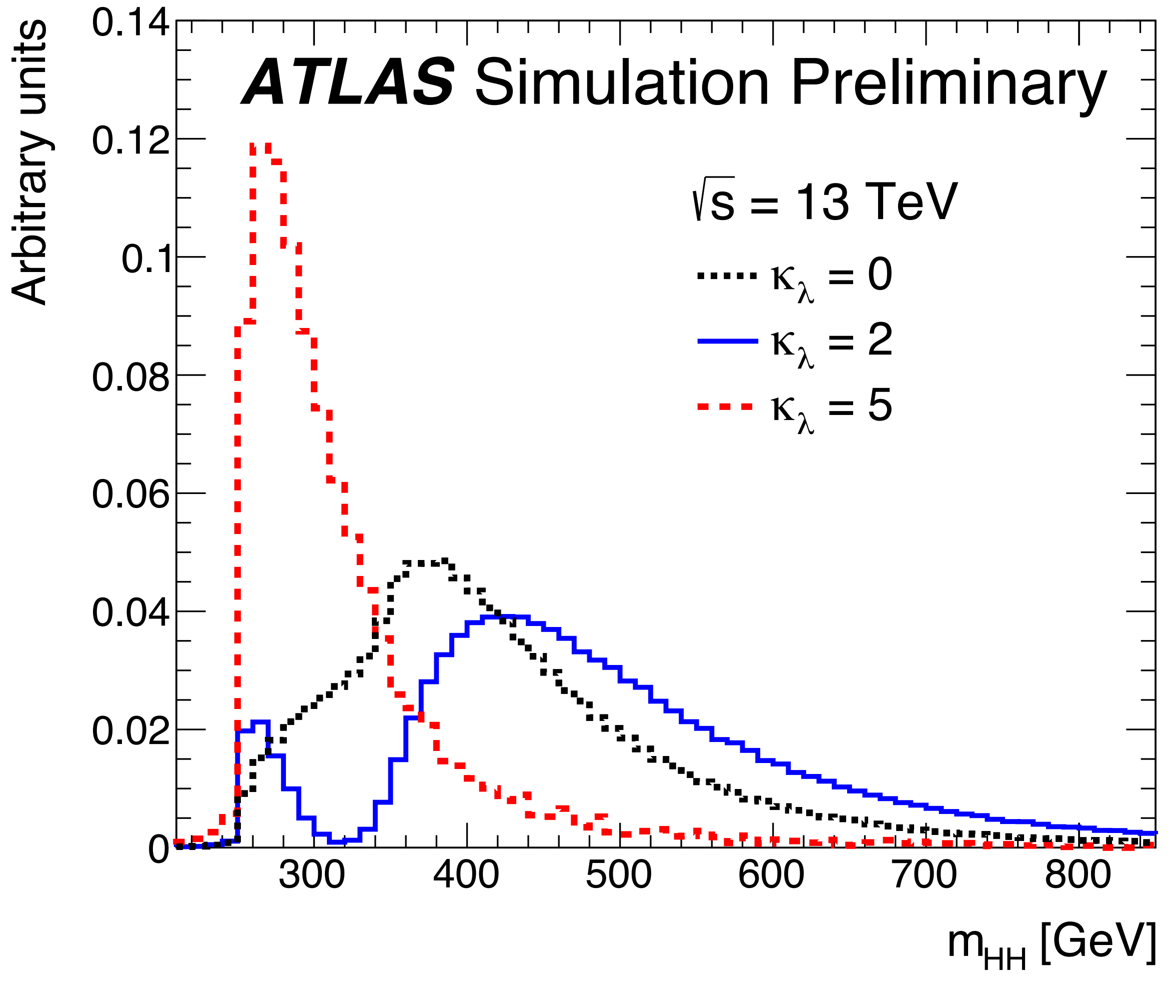

- **Vector Boson Fusion (VBF):** $\sigma_{HH}^{VBF} = 1.72$ fb

Second order contribution to total production, but direct handle to vector boson coupling modifiers κ_{2V} and κ_V:

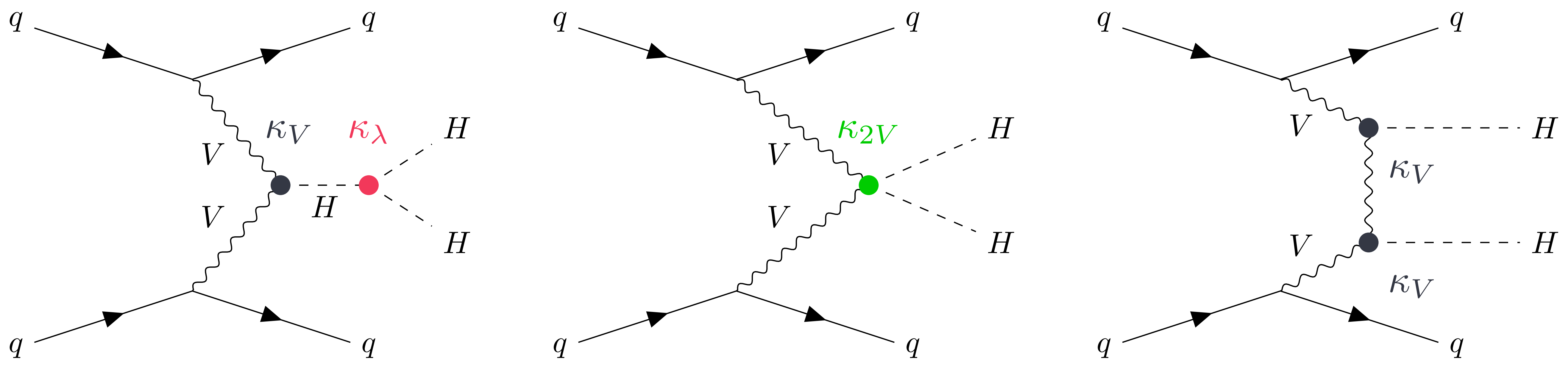

- **BSM resonances:**

Possible increase in signal from new physics benchmarks:

- Spin-0: predicted by Two-Higgs-Doublet-Models and Electroweak Singlet models
- Spin-2: predicted by Randall-Sundrum (RS) model of warped extra dimensions

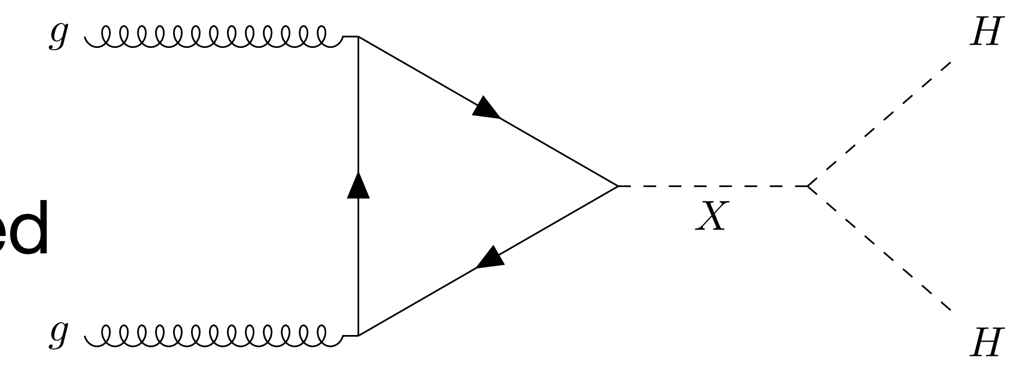

Where to look for Higgs pairs?

No clear *Golden channel*, but several promising signatures:

$BR(HH \to XXYY)$

	bb	WW	gg	ττ	cc	ZZ	γγ	Zγ	μμ
bb	33%								
WW	25%	4.6%							
gg									
ττ	7.4%								
cc									
ZZ	3.1%								
γγ	0.26%	0.1%							
Zγ									
μμ									

□ = results from ATLAS

Combining the results is necessary **for observation**.

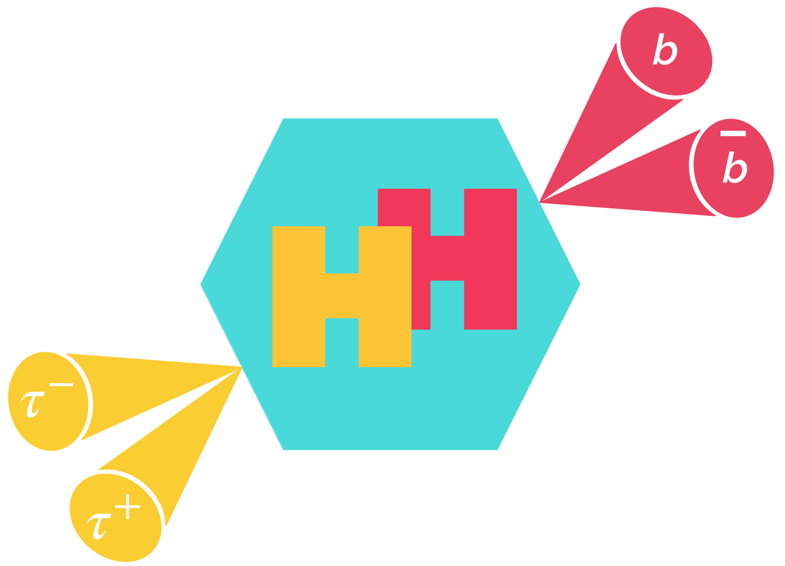

$HH \to b\bar{b}\tau^+\tau^-$

- $H \to b\bar{b}$: High BR
- $H \to \tau^+\tau^-$: Low background

Resolved: $\mathscr{L} = 36\text{fb}^{-1}$ Phys. Rev. Lett. 121, 191801

Boosted: $\mathscr{L} = 139\text{fb}^{-1}$ JHEP 11 (2020) 163

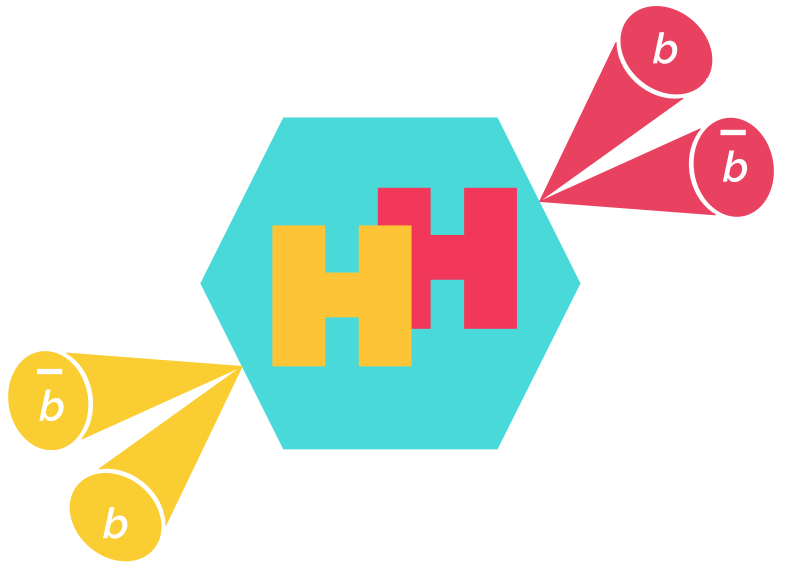

$HH \to b\bar{b}b\bar{b}$

- $H \to b\bar{b}$: High BR
- Large hadronic background

ggF: $\mathscr{L} = 36\text{fb}^{-1}$ JHEP 01 (2019) 030

VBF: $\mathscr{L} = 126\text{fb}^{-1}$ JHEP 07 (2020) 108

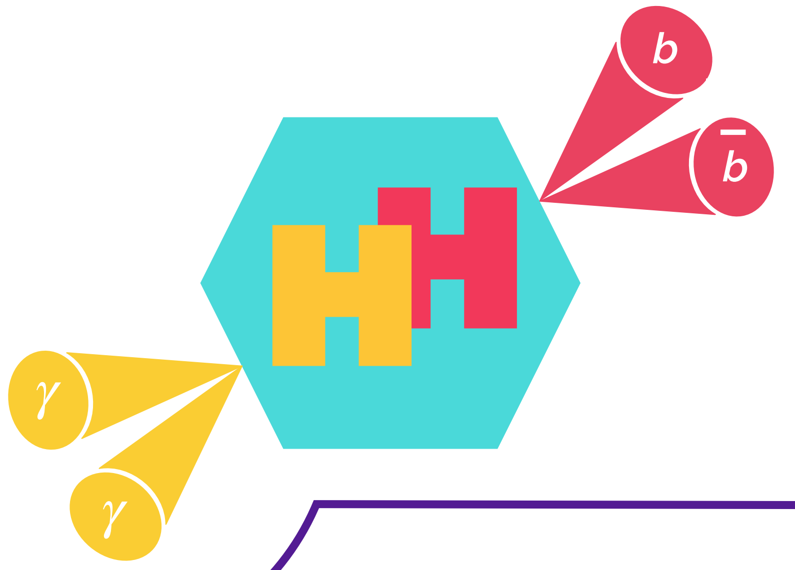

$HH \to b\bar{b}\gamma\gamma$ NEW

- $H \to b\bar{b}$: High BR
- $H \to \gamma\gamma$: Good mass resolution/sensitive to low m_{HH}

$\mathscr{L} = 139\text{fb}^{-1}$ ATLAS-CONF-2021-016

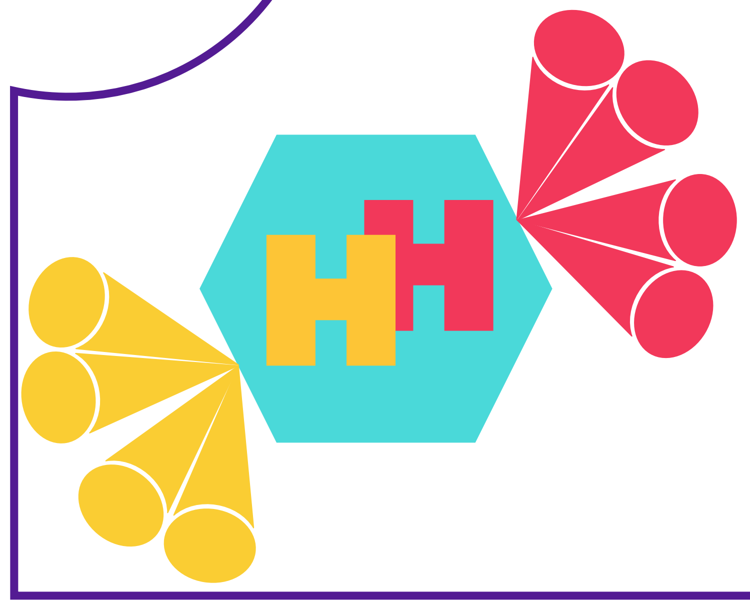

$HH \to W^+W^- + XX$ / $HH \to b\bar{b}ZZ$

- Decent BR from $H \to VV$
- Complex final signatures due to the decay of Vs

$b\bar{b}l\nu l\nu$: $\mathscr{L} = 139\text{fb}^{-1}$ Phys. Lett. B 801 (2020) 135145

$\gamma\gamma WW^*$: $\mathscr{L} = 36\text{fb}^{-1}$ Eur. Phys. J. C 78 (2018) 1007

$b\bar{b}l\nu q\bar{q}$: $\mathscr{L} = 36\text{fb}^{-1}$ JHEP 04 (2019) 092

WW^*WW^*: $\mathscr{L} = 36\text{fb}^{-1}$ JHEP 05 (2019) 124

Not shown today

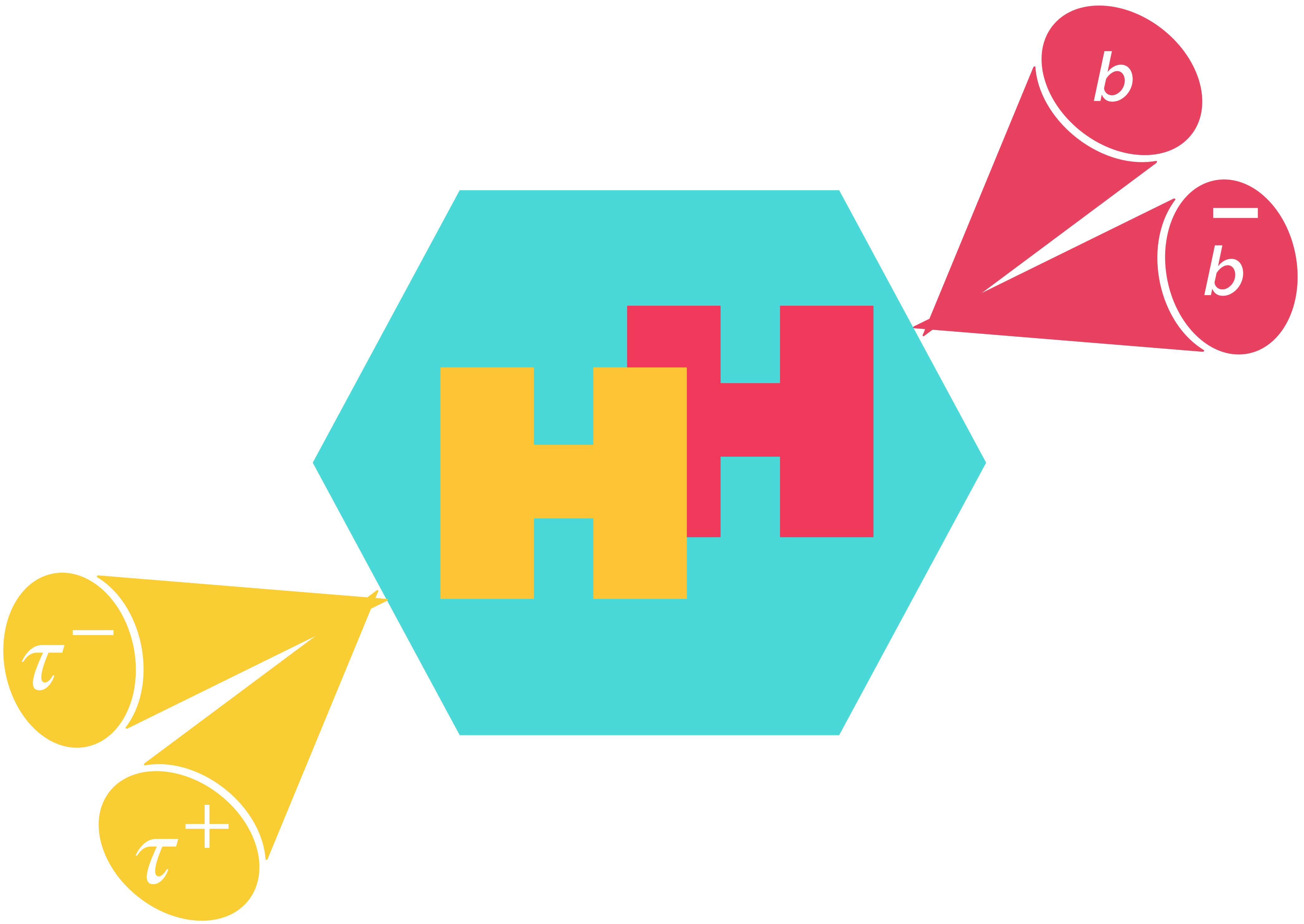

$$HH \to b\bar{b}\tau^+\tau^-$$

Strategy

Resolved: $\mathscr{L} = 36\text{fb}^{-1}$ Phys. Rev. Lett. 121, 191801
Boosted: $\mathscr{L} = 139\text{fb}^{-1}$ JHEP 11 (2020) 163

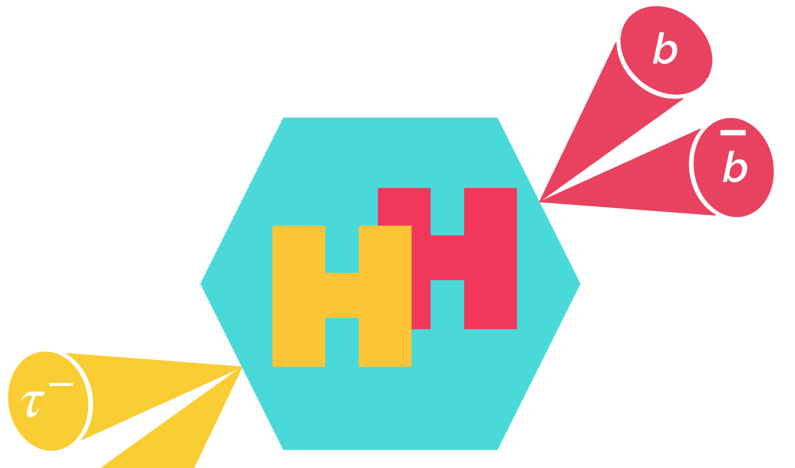

Two strategies aiming at different regimes:

- **Resolved**: low momenta, single objects can be defined → non-resonant & resonant searches;
- **Boosted**: high momenta, objects are merged → resonant searches.

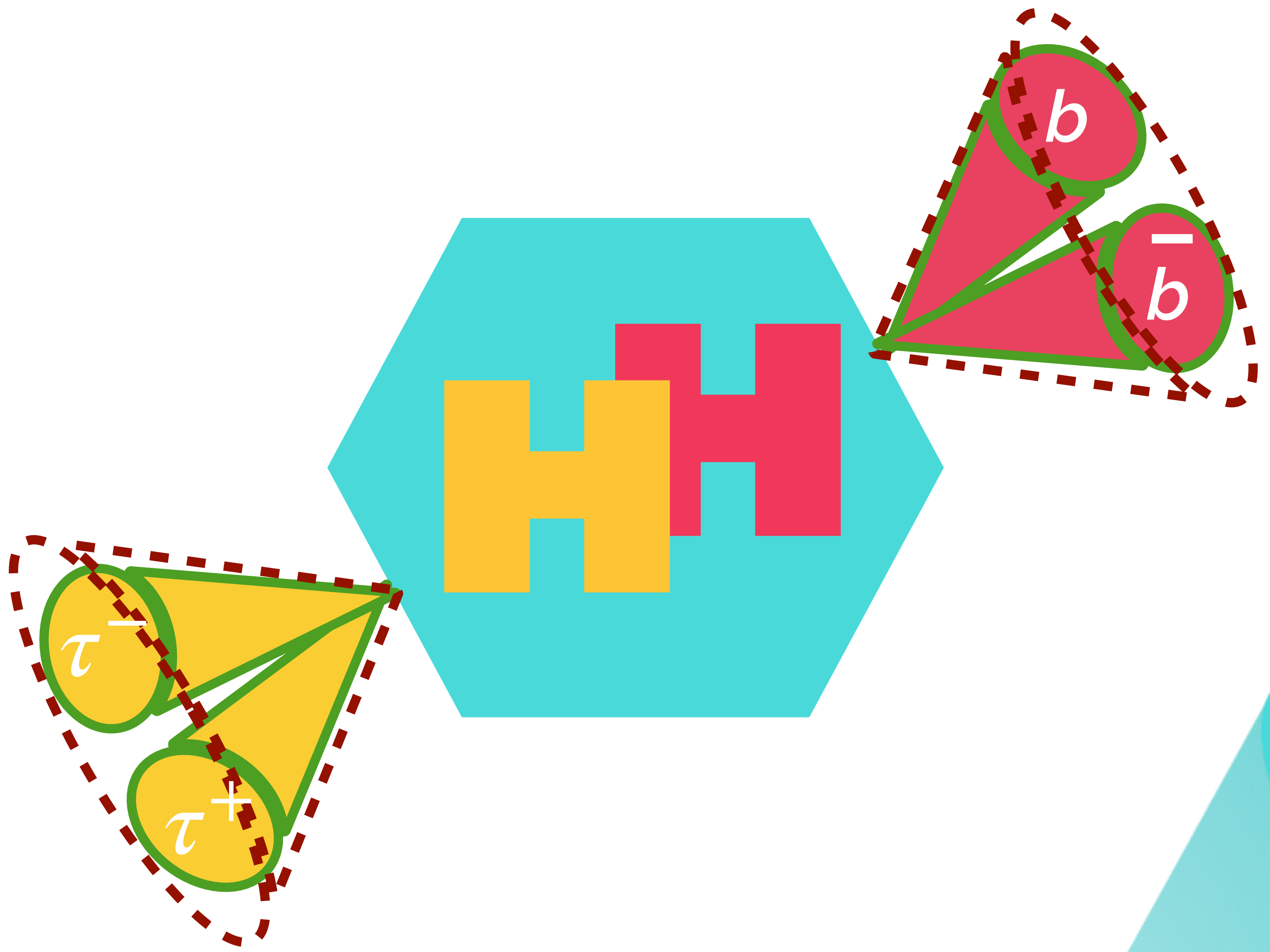

Resolved:
Exactly 2 b-jets
Boosted:
- ≥ 1 extra large R jet;
- 2 variable radius b-tagged jets inside.

Resolved:
Based on the decay of taus:
- $\tau_{\text{lep}}\tau_{\text{had}}$: exactly 1 lepton + 1 hadronic τ;
- $\tau_{\text{had}}\tau_{\text{had}}$: exactly two hadronic τs.

Boosted:
Novel Boosted Decision Tree (BDT) reconstruction and identification of di-τ in large R jets:
- ≤ 3 sub-jets, sum of track charge ± 1 in each sub-τ.

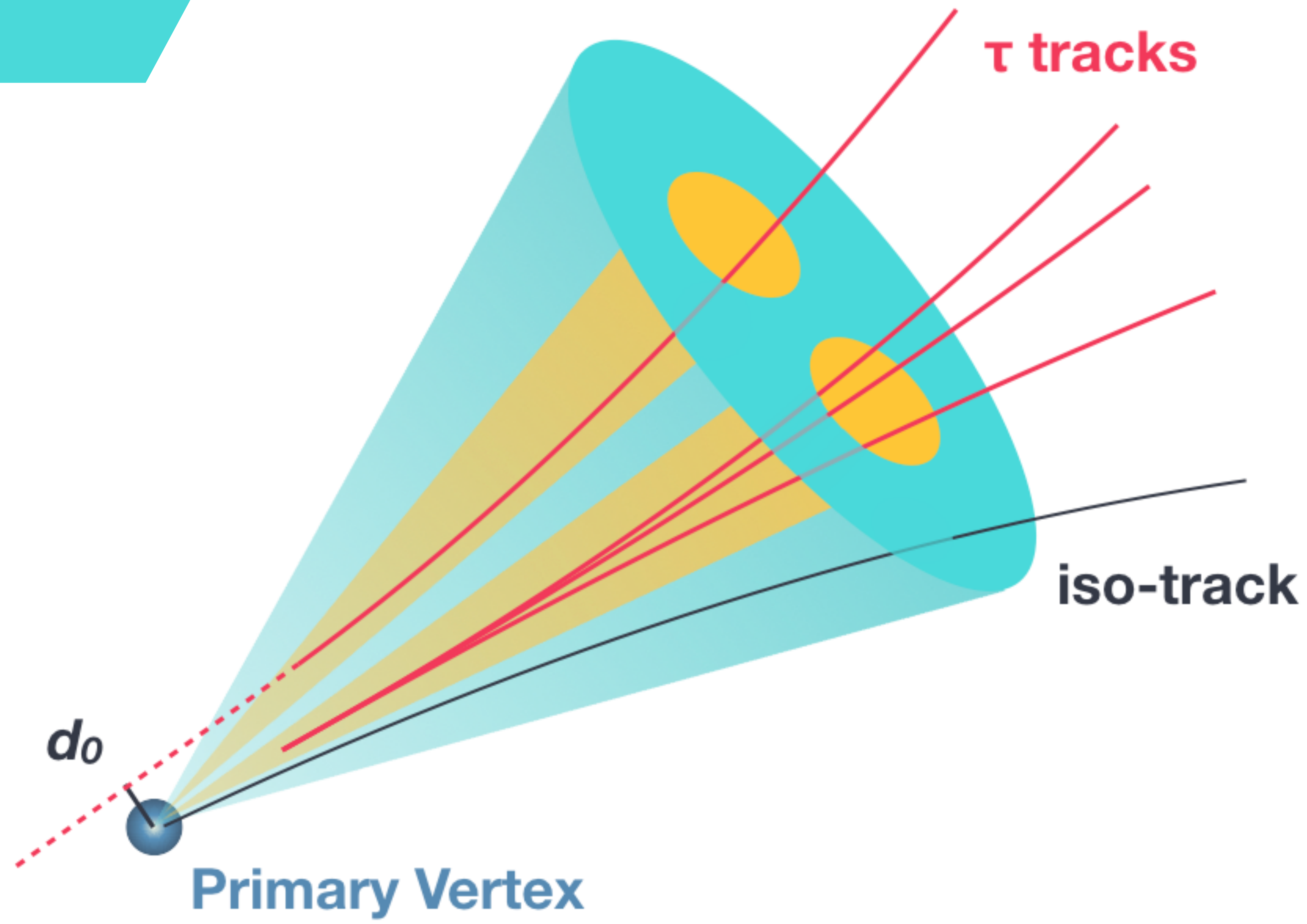

How to look for signal?

Resolved: $\mathscr{L} = 36\text{fb}^{-1}$ Phys. Rev. Lett. 121, 191801
Boosted: $\mathscr{L} = 139\text{fb}^{-1}$ JHEP 11 (2020) 163

$HH \to b\bar{b}\tau^+\tau^-$

Resolved:

Fit: based on a BDT distribution trained in 3 SRs:

- $\tau_{lep}\tau_{had}$: Single Lepton Trigger (STT), Lepton + Tau Trigger (LTT);
- $\tau_{had}\tau_{had}$: Single/Di Tau Triggers.

Non-resonant

Signal: SM ggF HH.

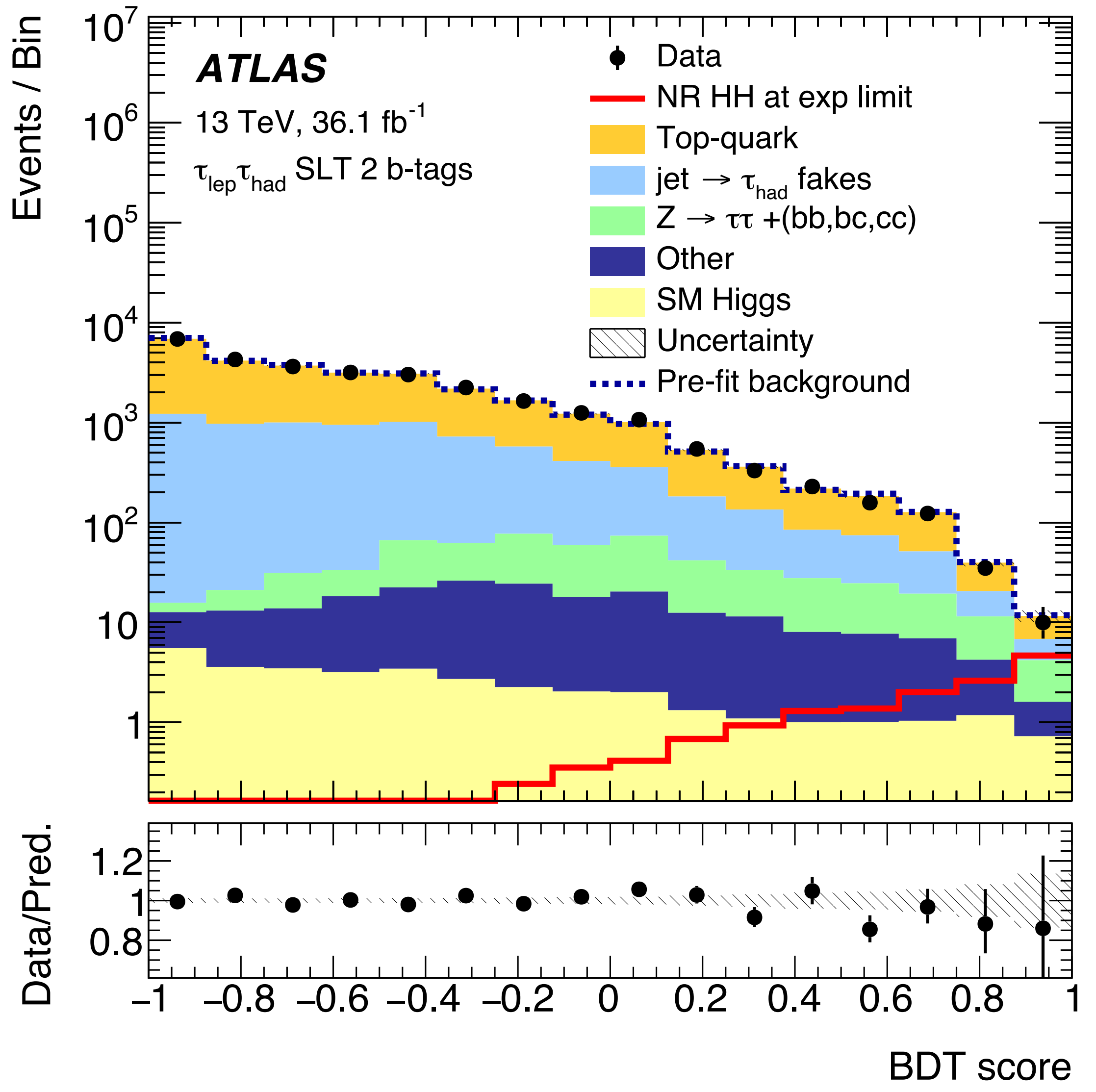

Resonant

Signals: Spin-0 and Spin-2.

- 1 training/mass (260-1000 GeV)

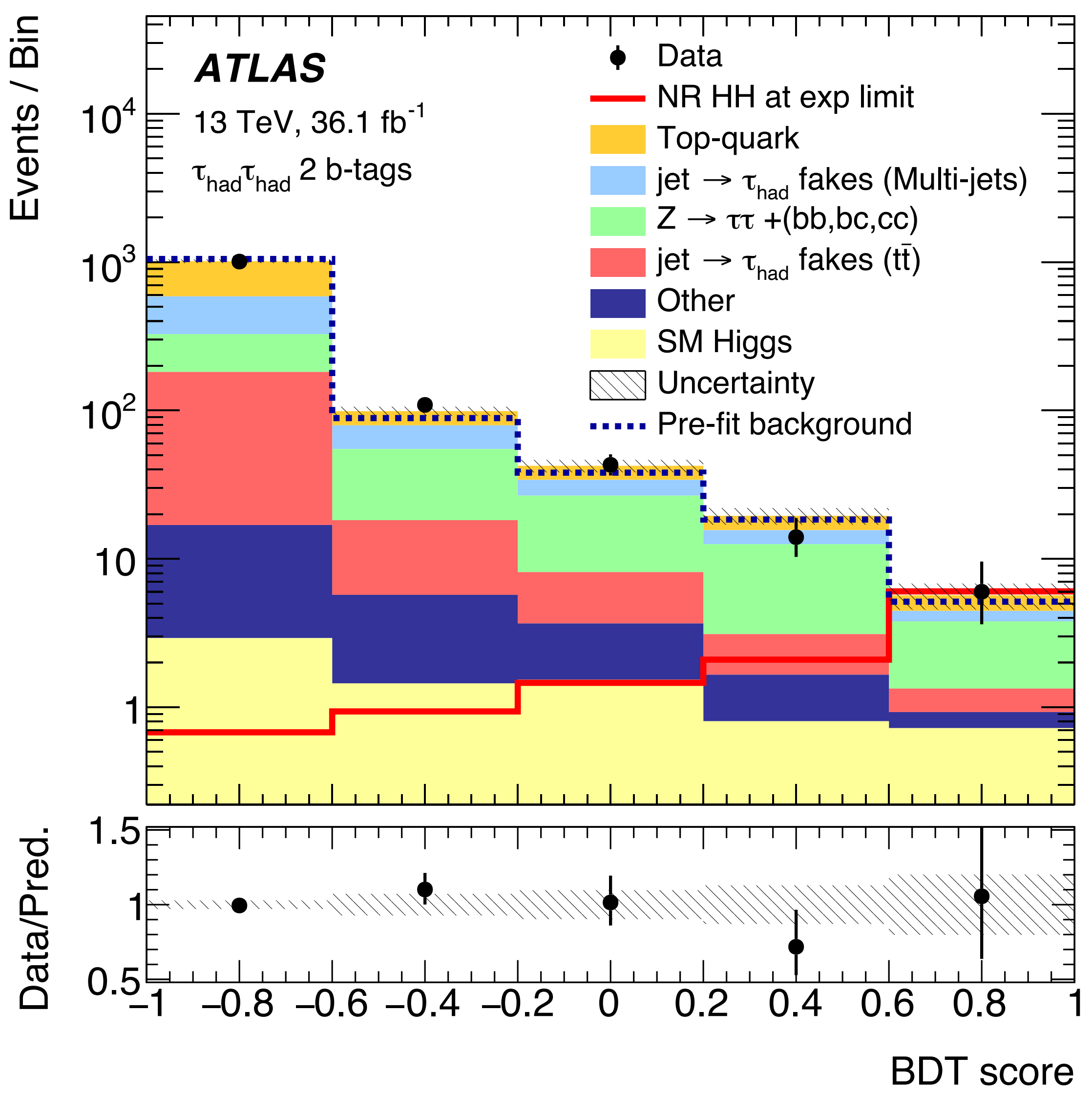

dedicated Control Regions for:

$t\bar{t}$, $Z \to \tau\tau$, multi-jets (evaluated from data-driven ABCD method)

Boosted:

Fit: Single bin fit for different *resonant* masses.

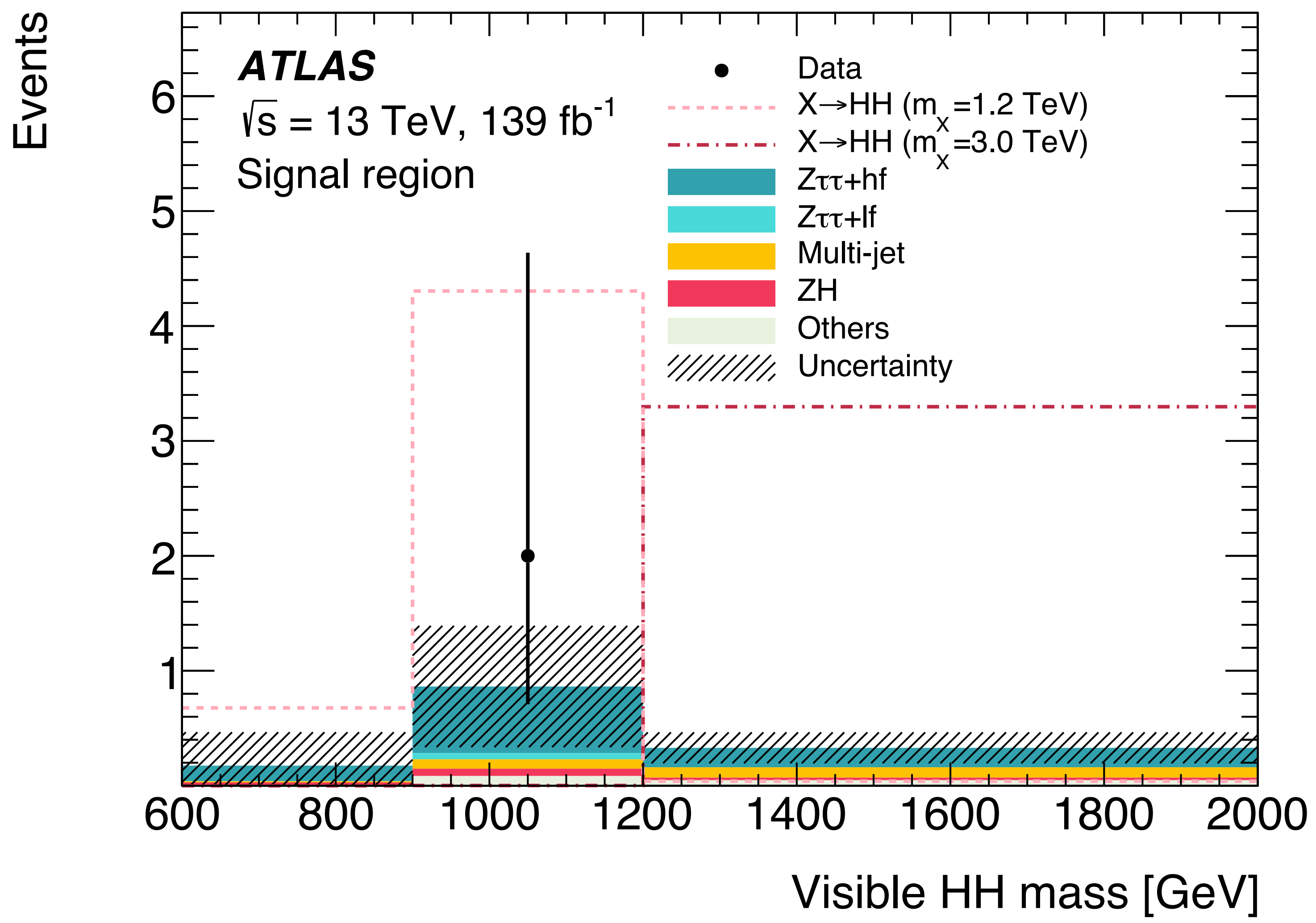

Selections based on:

- Mass of Large R jet;
- visible di-Higgs mass m_{HH}^{vis}.

dedicated Control Regions for:

$Z \to \tau\tau$ + jets, multi-jets (evaluated from data-driven ABCD method)

Results

Resolved: $\mathscr{L} = 36\text{fb}^{-1}$ Phys. Rev. Lett. 121, 191801
Boosted: $\mathscr{L} = 139\text{fb}^{-1}$ JHEP 11 (2020) 163

$HH \to b\bar{b}\tau^+\tau^-$

Resolved: No significant excess found

Non-resonant

$\sigma^{ggF}_{HH} \times BR(HH \to b\bar{b}\tau\tau)$ **observed (expected)** limit is **12.7 (14.8)** times the SM prediction.

Resonant

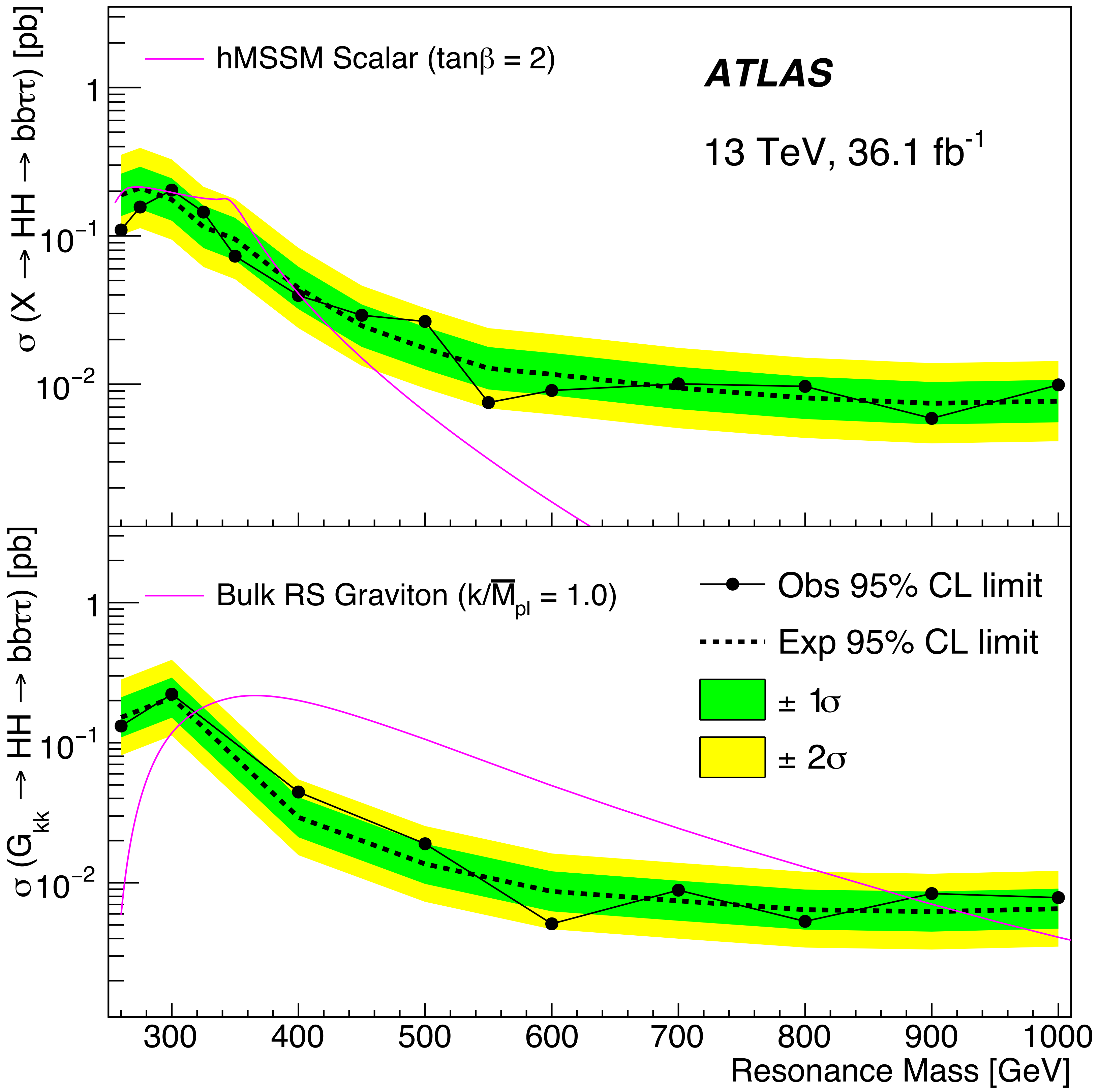

Limits set on $\sigma(X/G_{KK} \to HH \to b\bar{b}\tau\tau)$

- X is for the hMSSM scalar production.
- G_{KK} for the bulk RS Kaluza–Klein (KK) graviton production.

Boosted: No significant excess found

Limits set on $\sigma(X \to HH \to b\bar{b}\tau\tau)$ where X is a narrow-width scalar resonance:

- Two regimes based on the cut on m^{vis}_{HH}

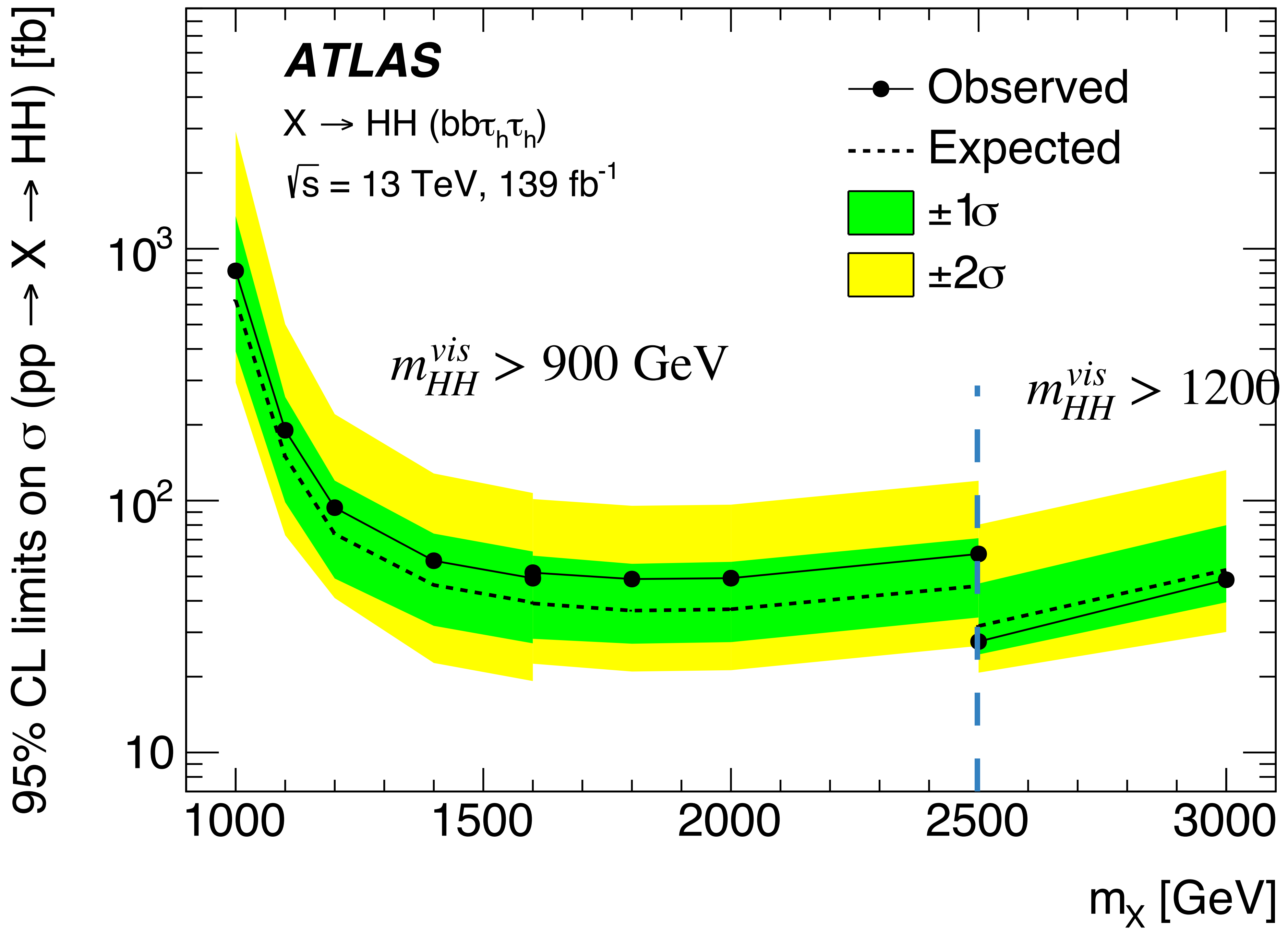

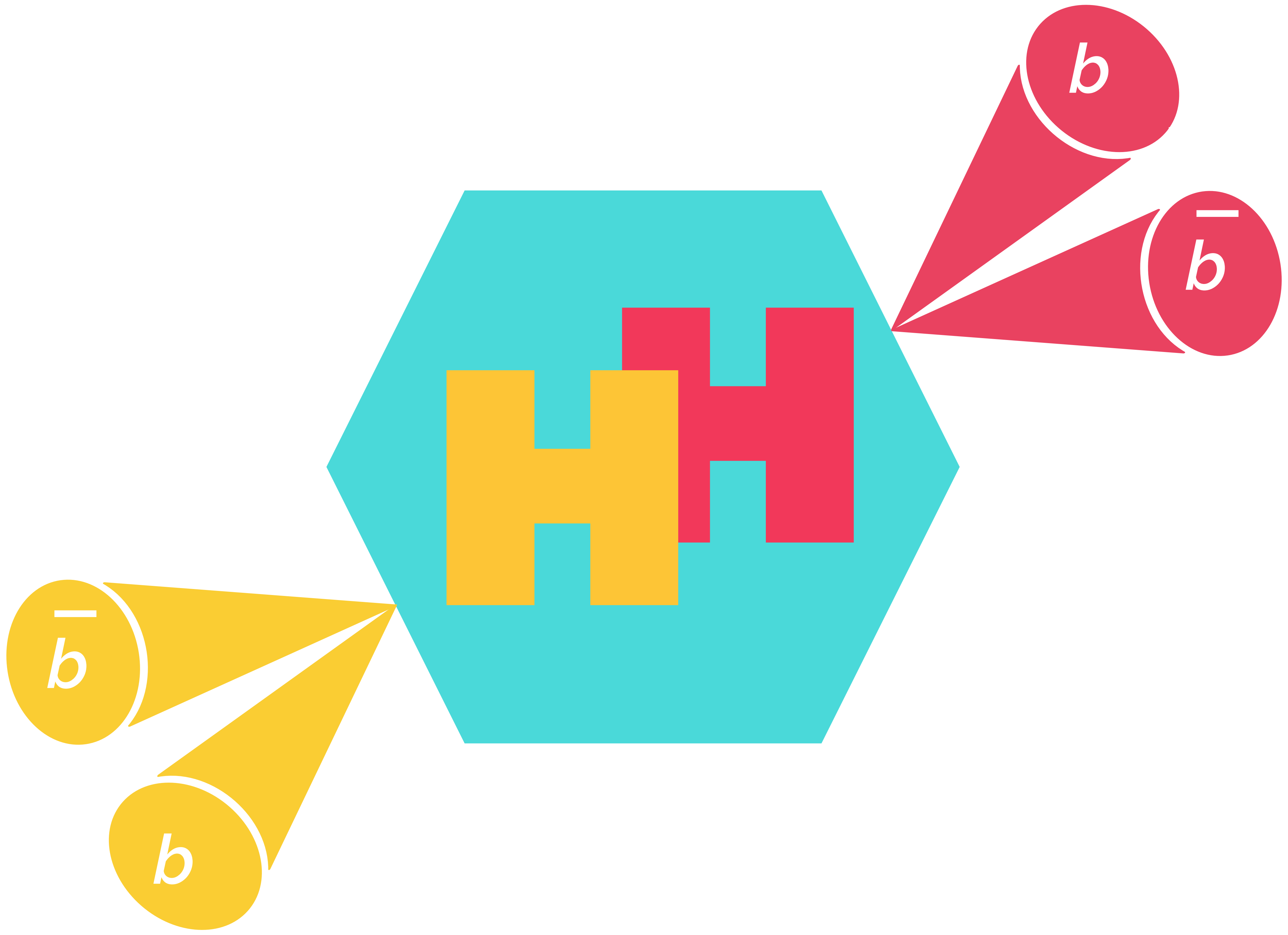

$$HH \rightarrow b\bar{b}b\bar{b}$$

Strategy

ggF: $\mathscr{L} = 36\text{fb}^{-1}$ JHEP 01 (2019) 030
VBF: $\mathscr{L} = 126\text{fb}^{-1}$ JHEP 07 (2020) 108

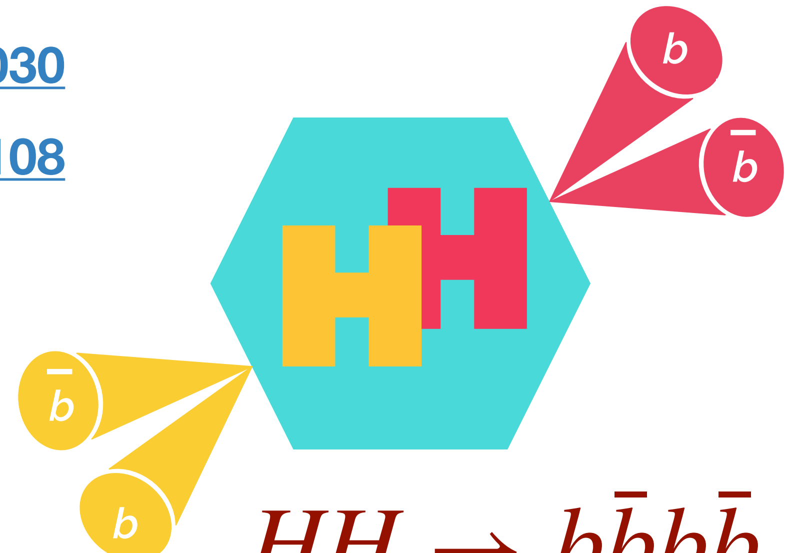

$HH \rightarrow b\bar{b}b\bar{b}$

On top of the two regimes (**Resolved**/**Boosted**), different signals are aimed for:

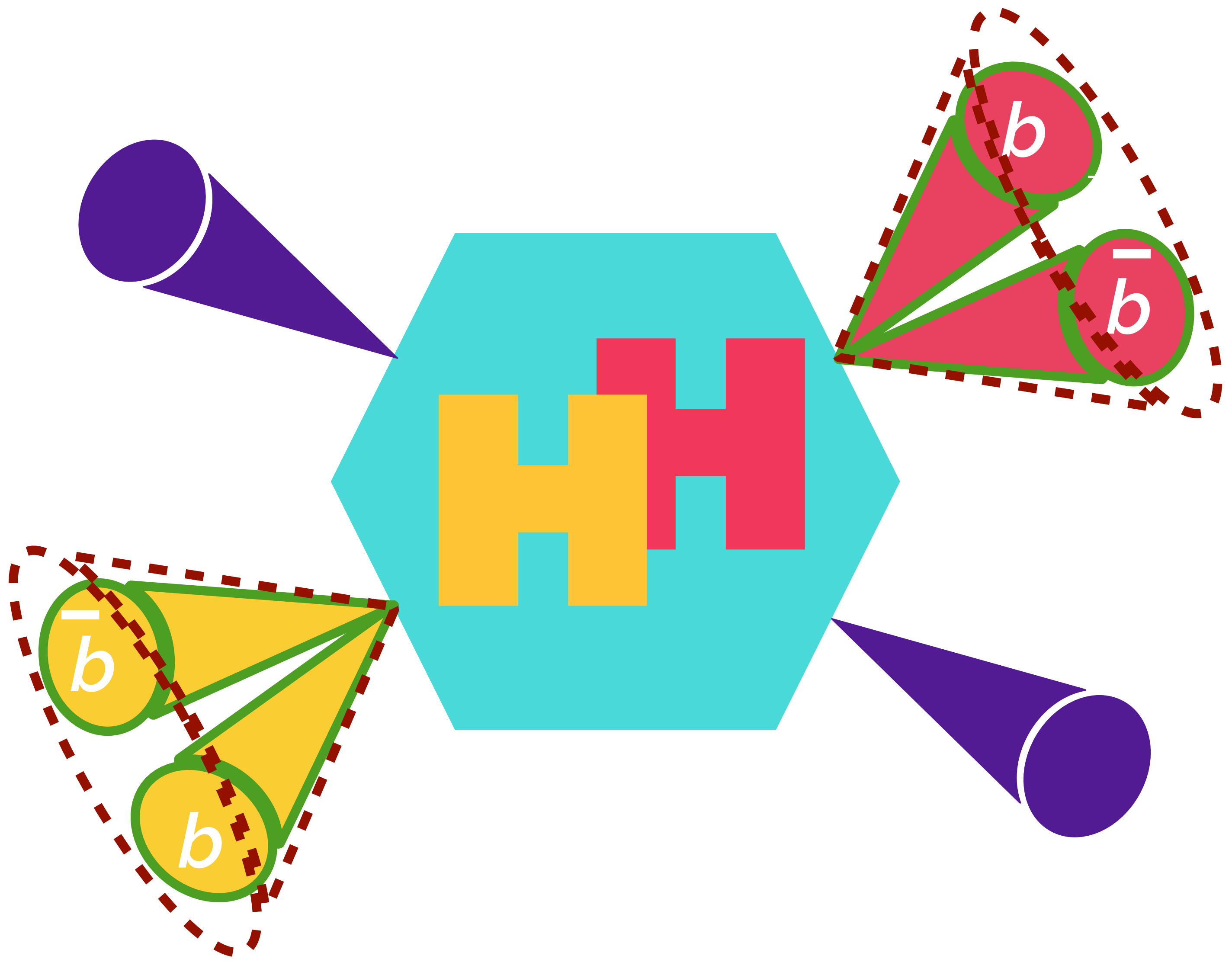

ggF

Resolved:
- At least 4 central b-tagged jets.

Boosted:
- At least 2 large R jets;
- At least 1 variable radius b-tagged jet in each large R jet.

VBF

Central jets:
- At least 4 central b-tagged jets.

VBF jets:
- At least 2 forward jets with opposite η sign.

Pairing Jets

1. Angular distance between jets in each Higgs candidate $|\Delta R_{jj}|$ is compared to the 4 bodies invariant mass m_{4j}

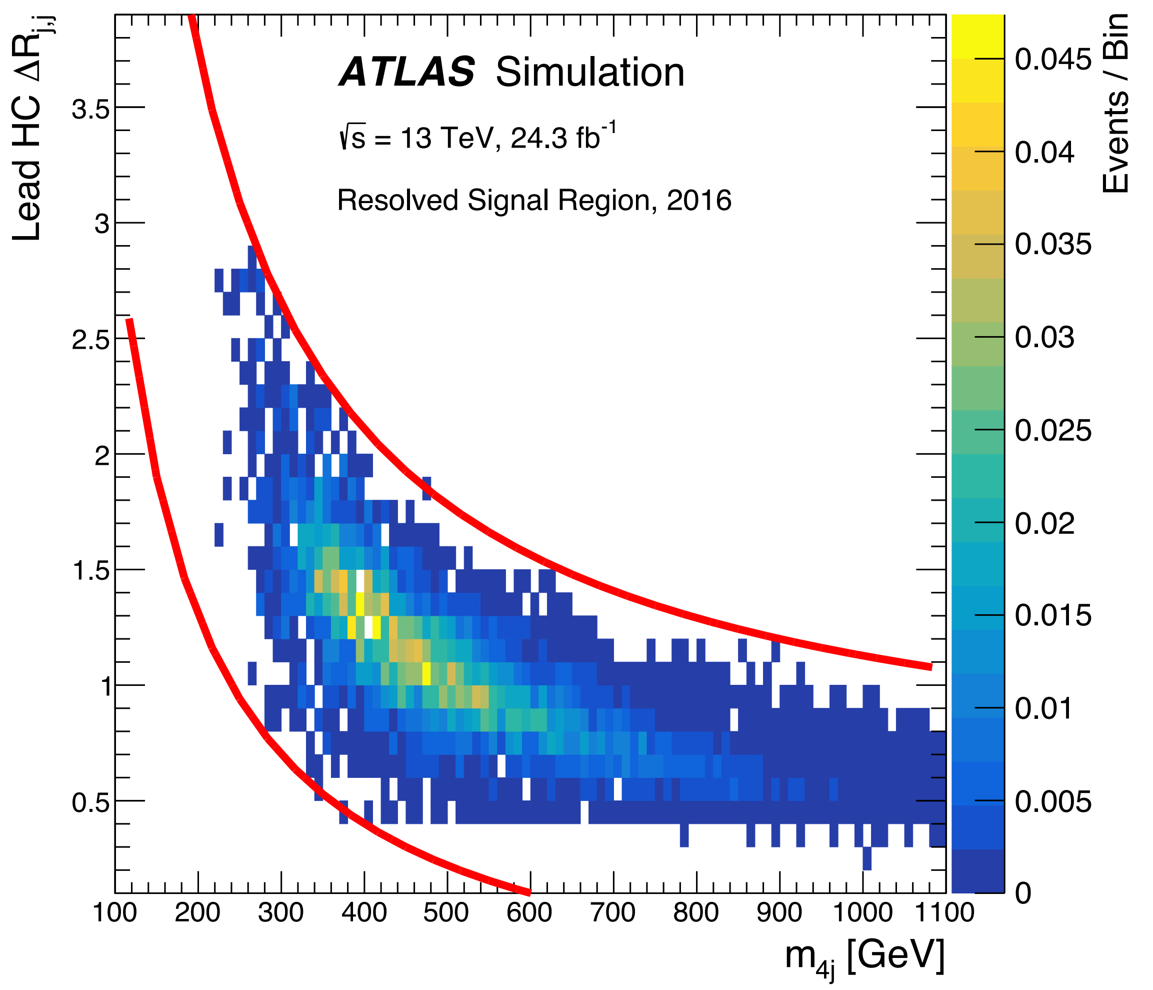

2. Given that the reconstructed masses should be similar, the distance to median of the signal expectation is minimised.

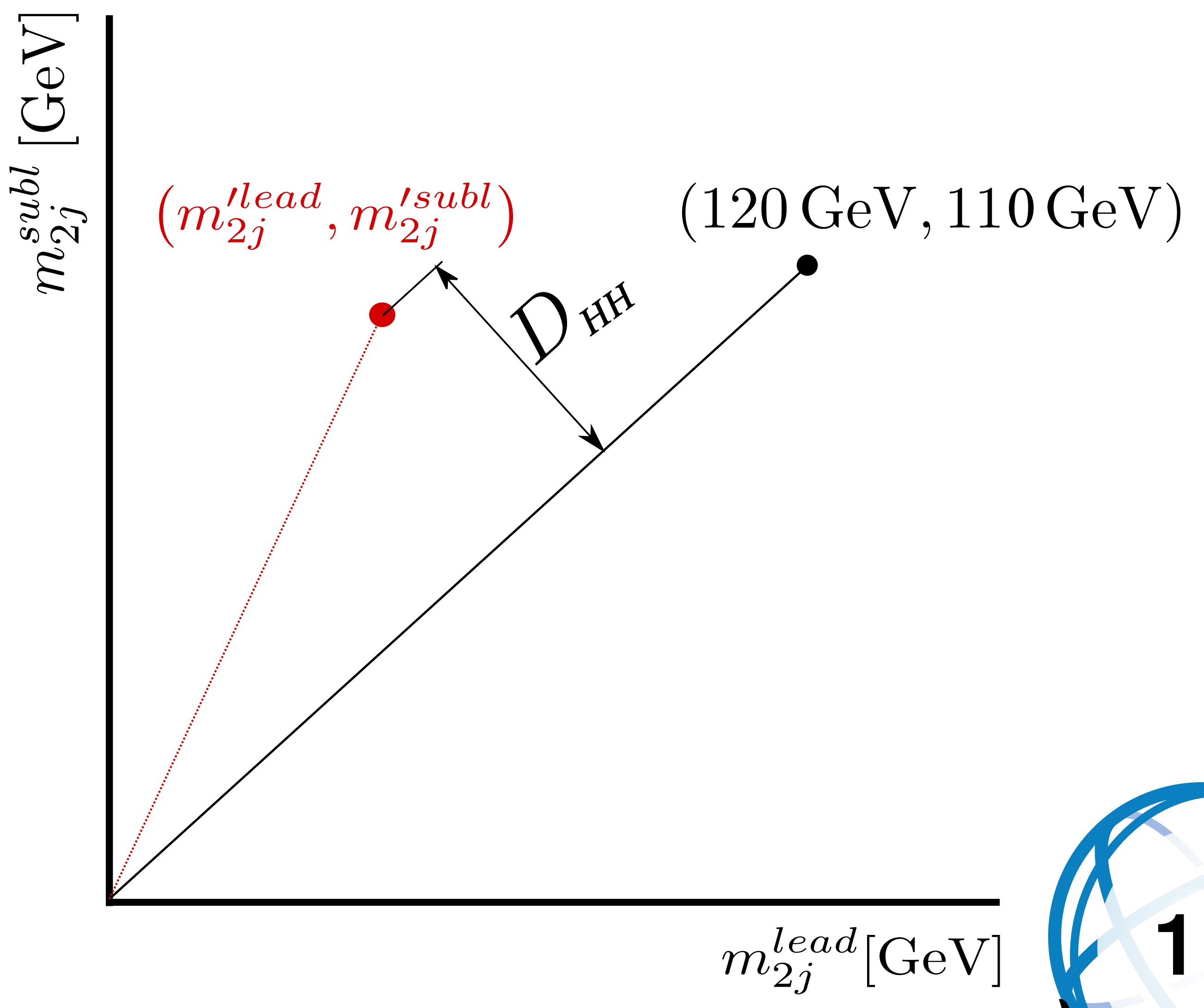

How to look for signal?

ggF: $\mathscr{L} = 36\text{fb}^{-1}$ JHEP 01 (2019) 030
VBF: $\mathscr{L} = 126\text{fb}^{-1}$ JHEP 07 (2020) 108

$HH \rightarrow b\bar{b}\tau^+\tau^-$

ggF

Resolved:

Fit: using the *HH invariant mass*

Main backgrounds:

- $t\bar{t}$: Consistency of jet originating from top quark checked through specific variable
- multi-jets:
  - $|\Delta\eta_{HH}| < 1.5$, 4-jets mass dependent Higgs p_T cut;
  - Dedicated Signal, Validation and Control Regions based Higgs bosons masses and b-tagging requirements (2-tag vs 4-tag).

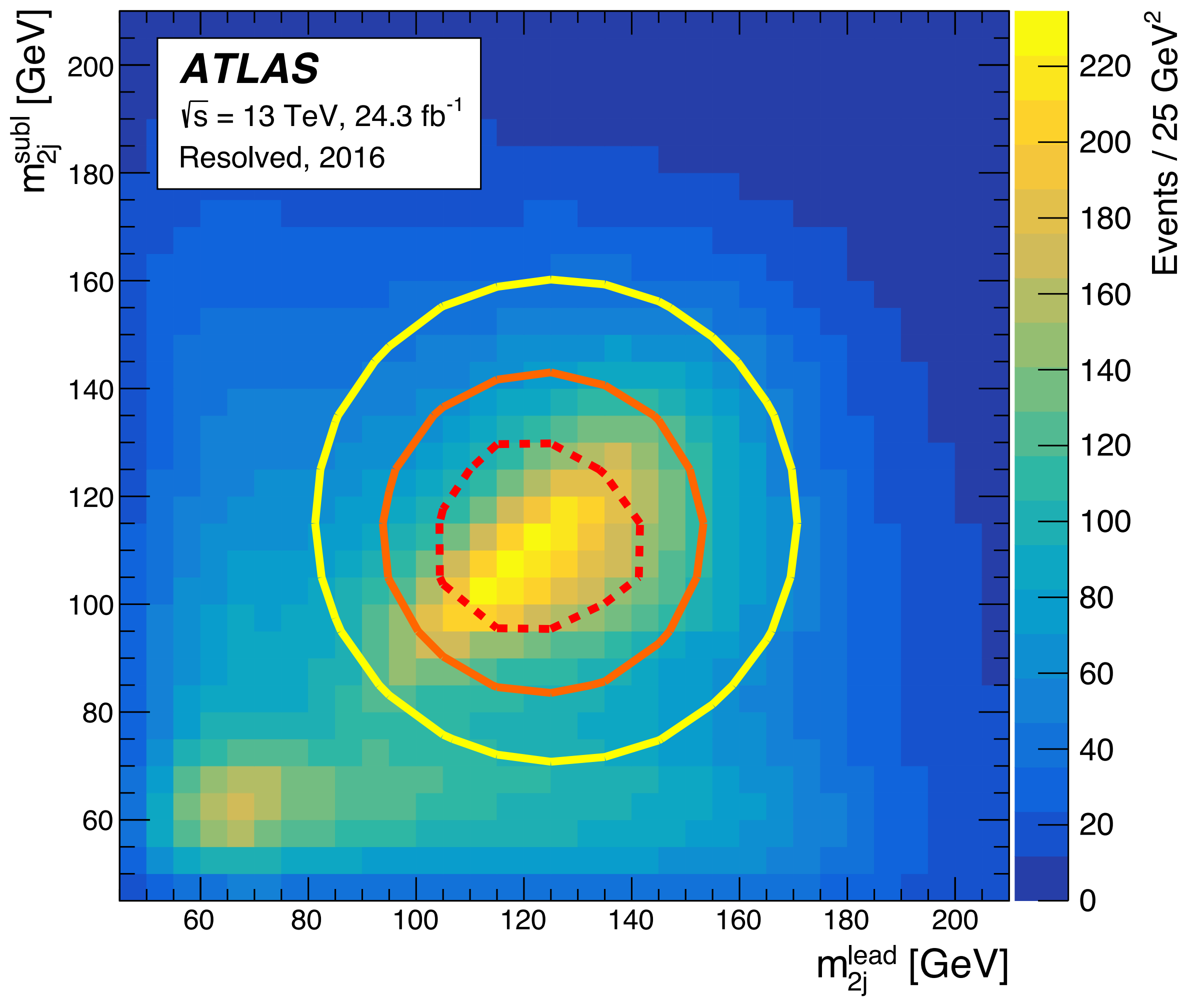

Boosted:

Fit: due to low b-tagging efficiency in large jets, 3 signal regions are defined:

2-tagged sub-jets.

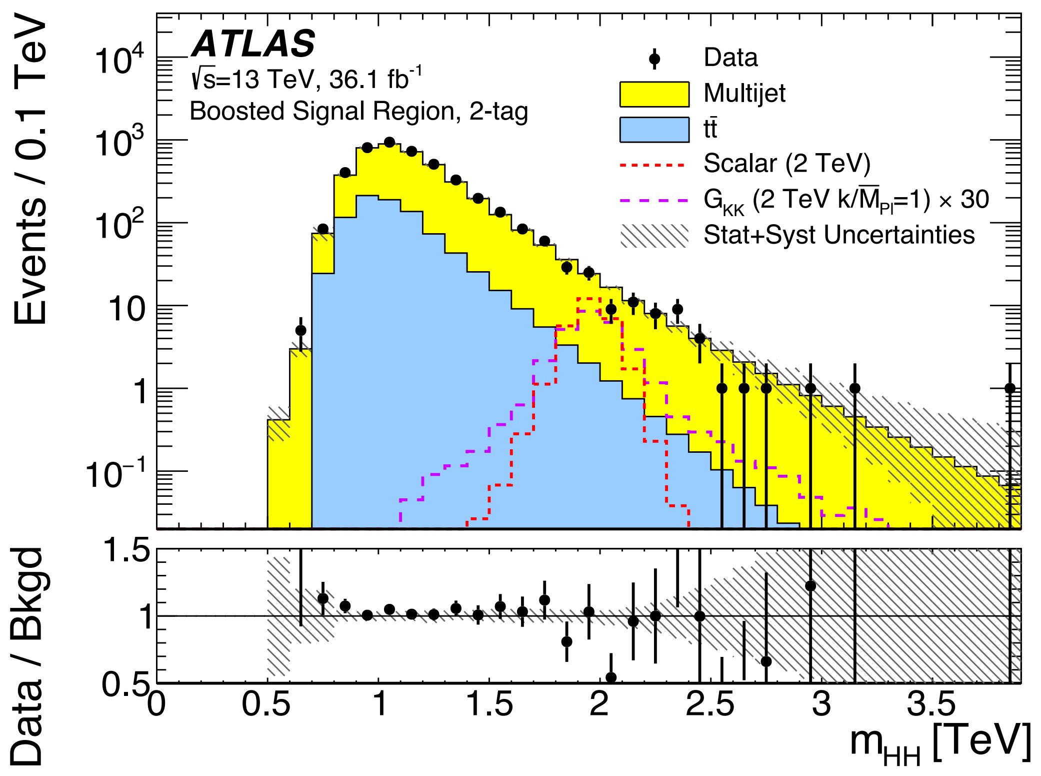

3-tagged sub-jets.

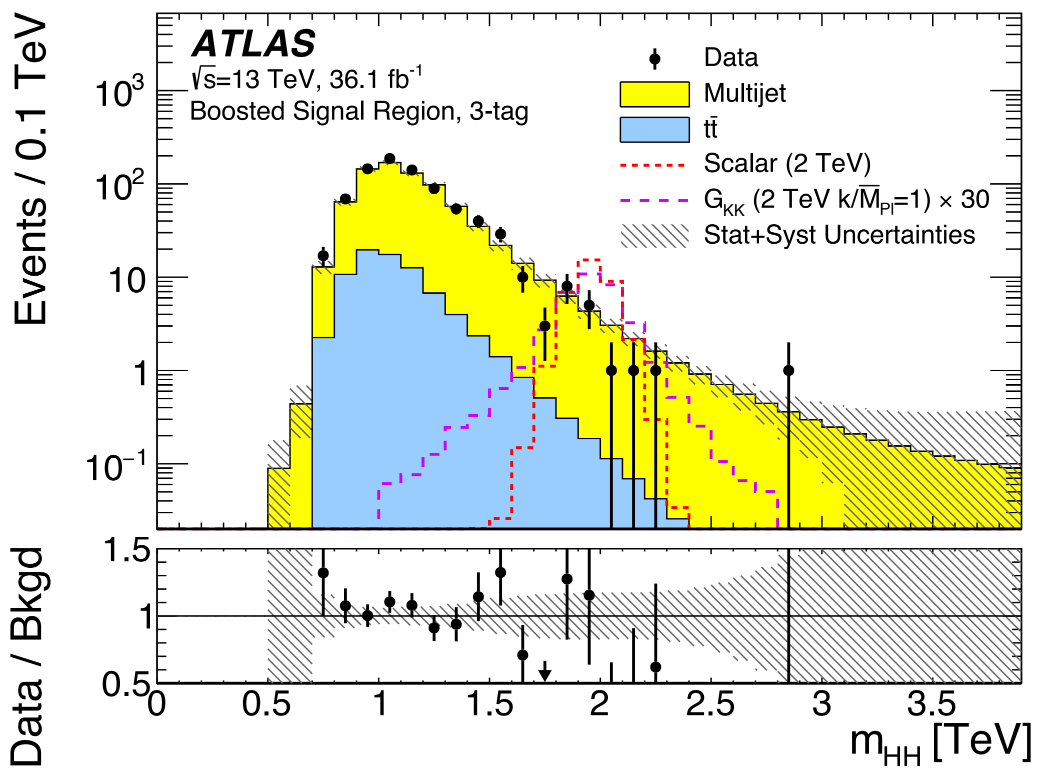

4-tagged sub-jets.

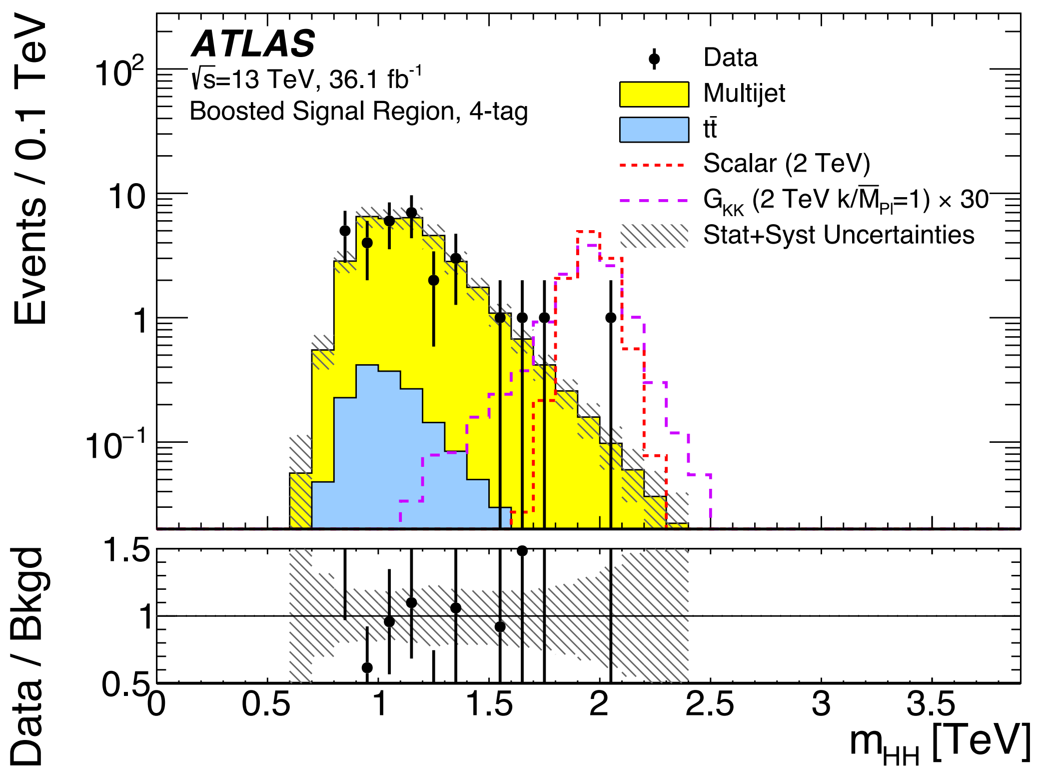

VBF

Similar cuts as for the ggF resolved analysis.

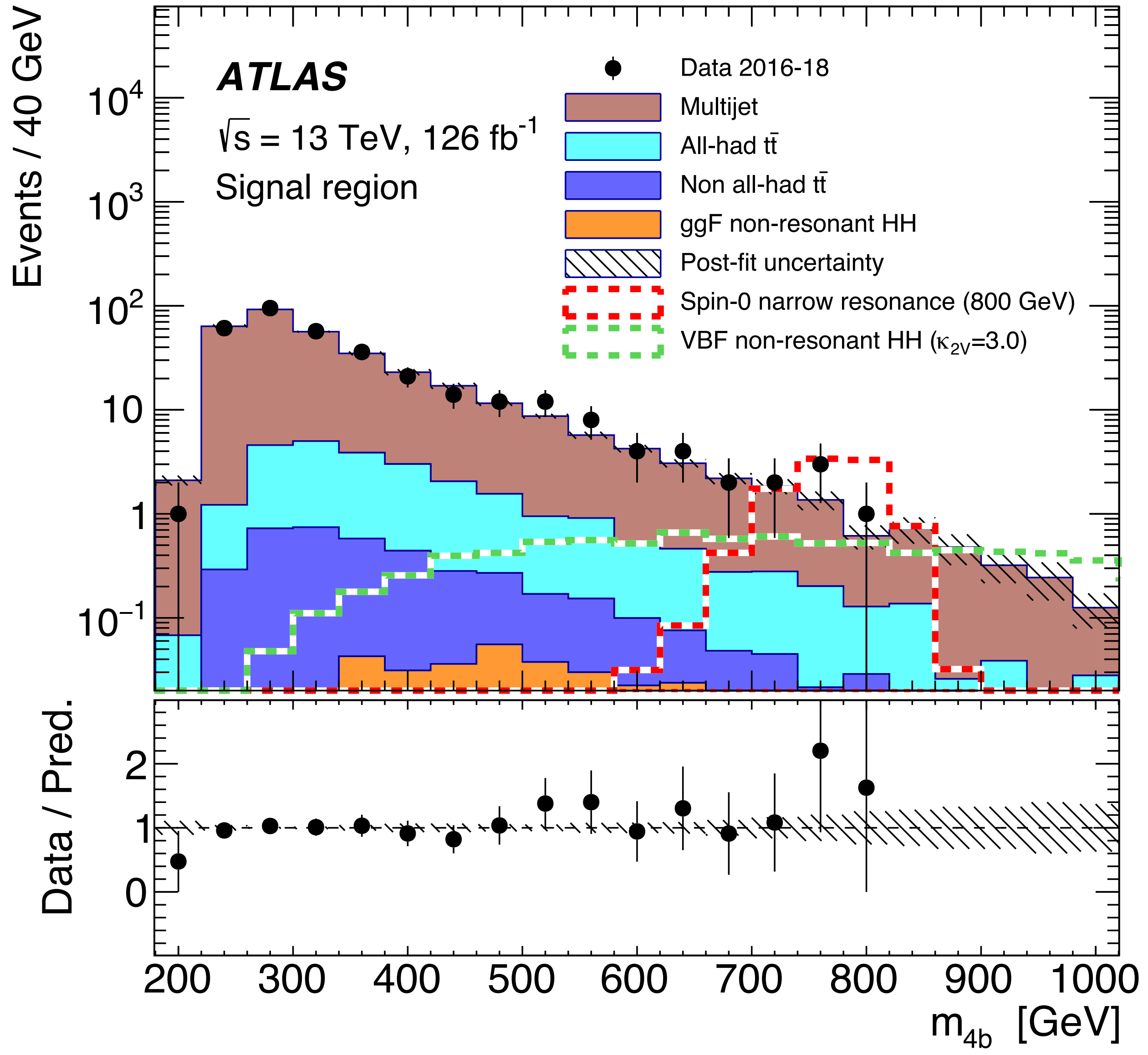

Results

ggF: $\mathscr{L} = 36\text{fb}^{-1}$ JHEP 01 (2019) 030
VBF: $\mathscr{L} = 126\text{fb}^{-1}$ JHEP 07 (2020) 108

$HH \rightarrow b\bar{b}b\bar{b}$

ggF

No significant excess found

Non-resonant **Resolved**

$\sigma_{HH}^{ggF} \times BR(HH \rightarrow b\bar{b}b\bar{b})$ **observed (expected)** limit is **12.9 (14.8)** times the SM prediction.

Resonant **Resolved** (260–1400 GeV) **Boosted** (800–3000 GeV)

Limits set on $\sigma(X/G_{KK} \rightarrow HH \rightarrow b\bar{b}b\bar{b})$:

- X is a narrow-width scalar resonance.
- G_{KK} for the bulk RS Kaluza–Klein (KK) graviton production.

Small excess at 280 GeV with local (global) significance of **3.6 (2.3) σ**

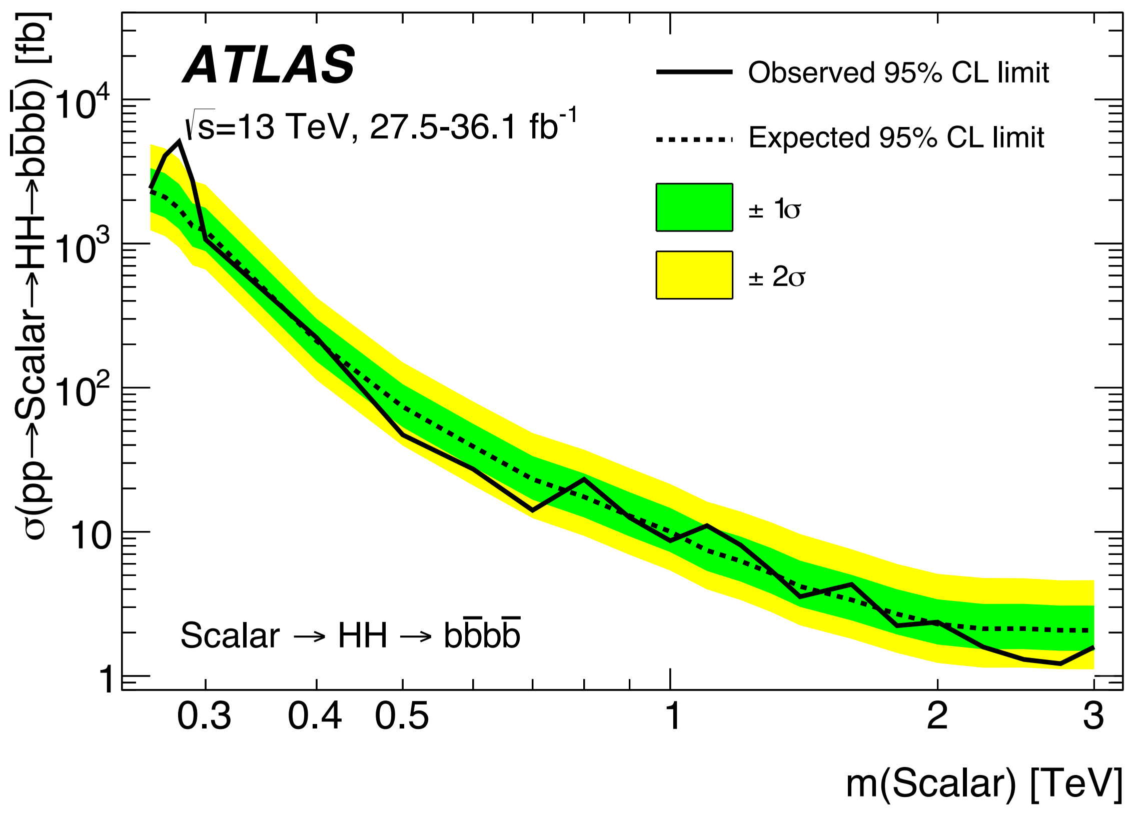

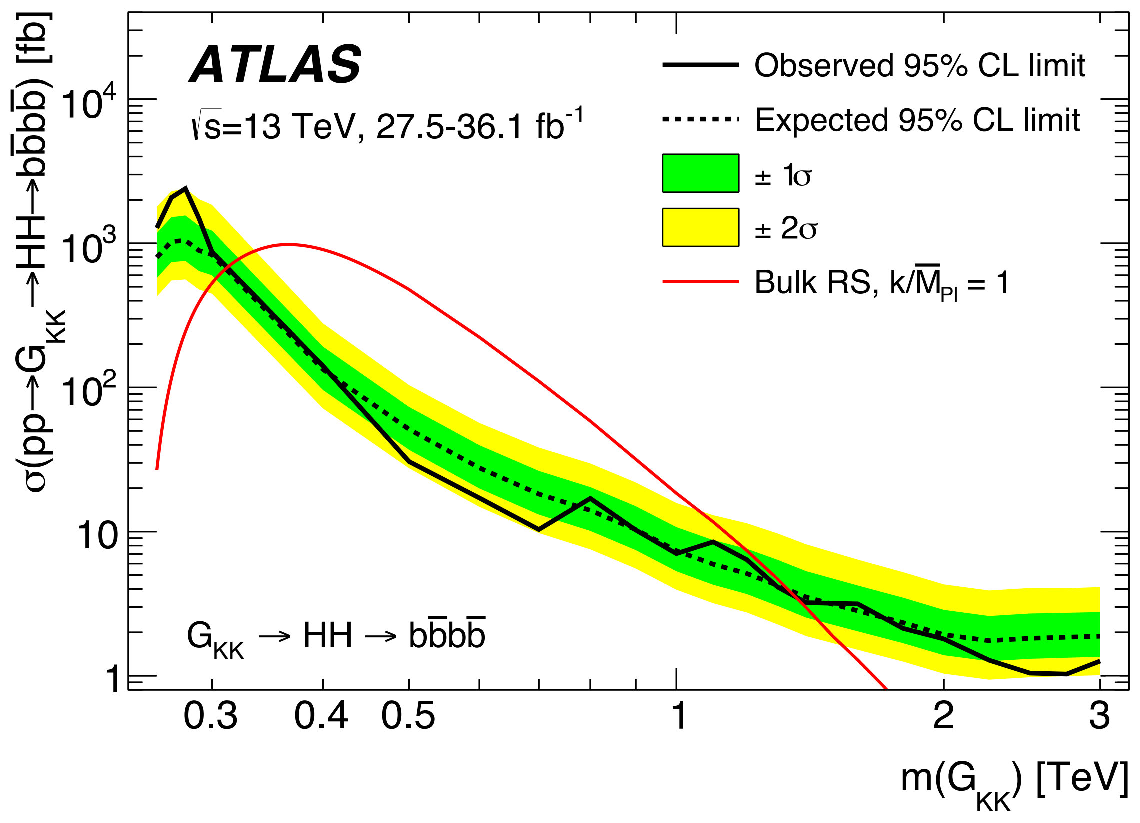

VBF

No significant excess found

Non-resonant

σ_{HH}^{VBF} **observed (expected)** limit is **840 (550)** times the SM prediction.

Limits are set on κ_{2V}:
$-0.43 < \kappa_{2V} < 2.56$ (observed),
$-0.55 < \kappa_{2V} < 2.72$ (expected).

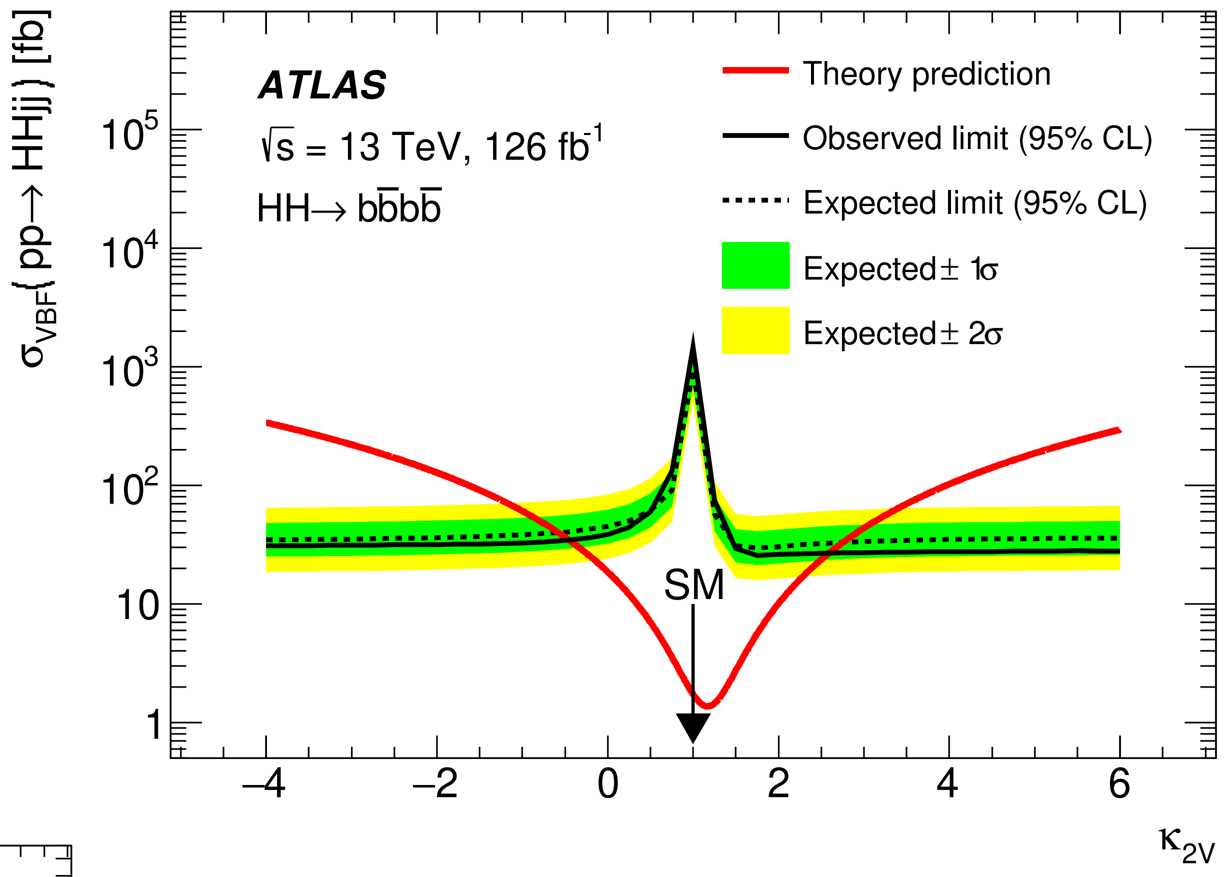

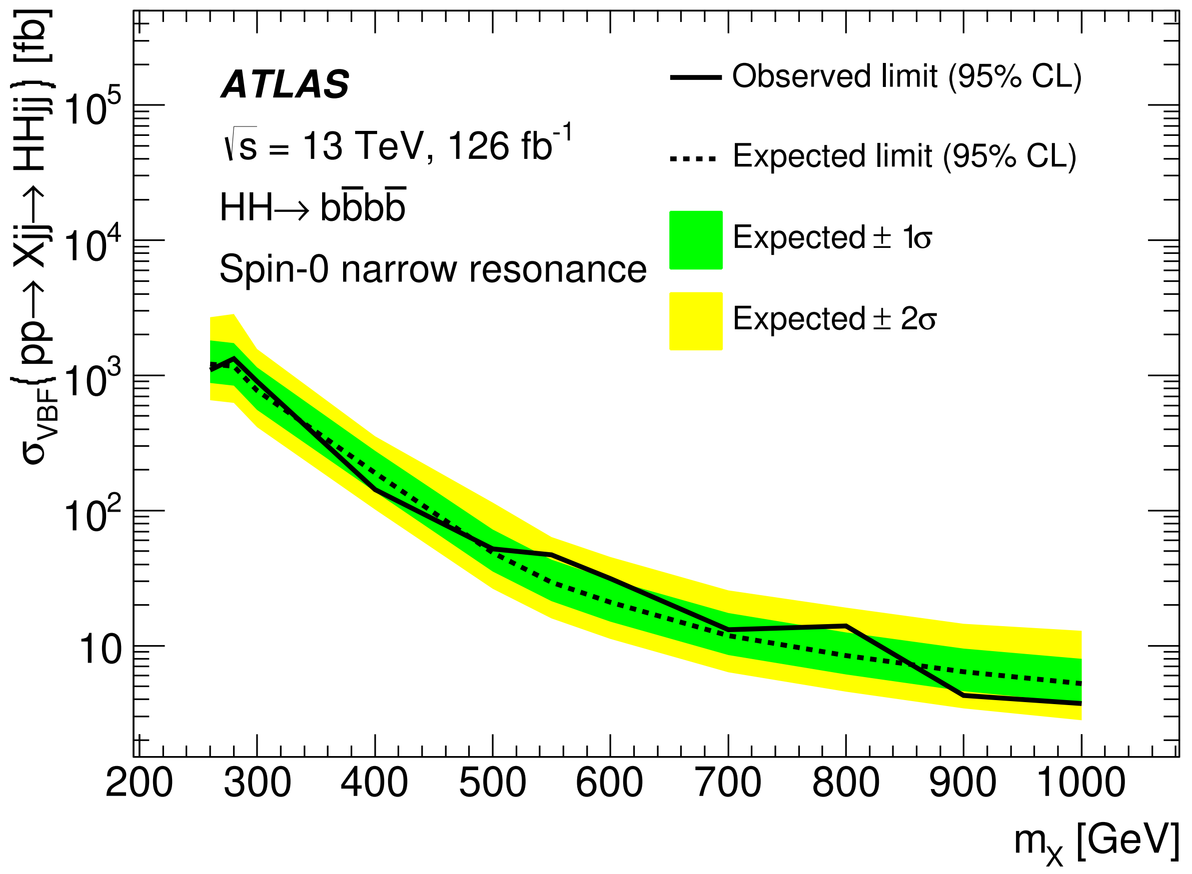

Resonant

Limits set on $\sigma_{VBF}(X \rightarrow HH)$ where X is either a narrow- or broad-width scalar resonance

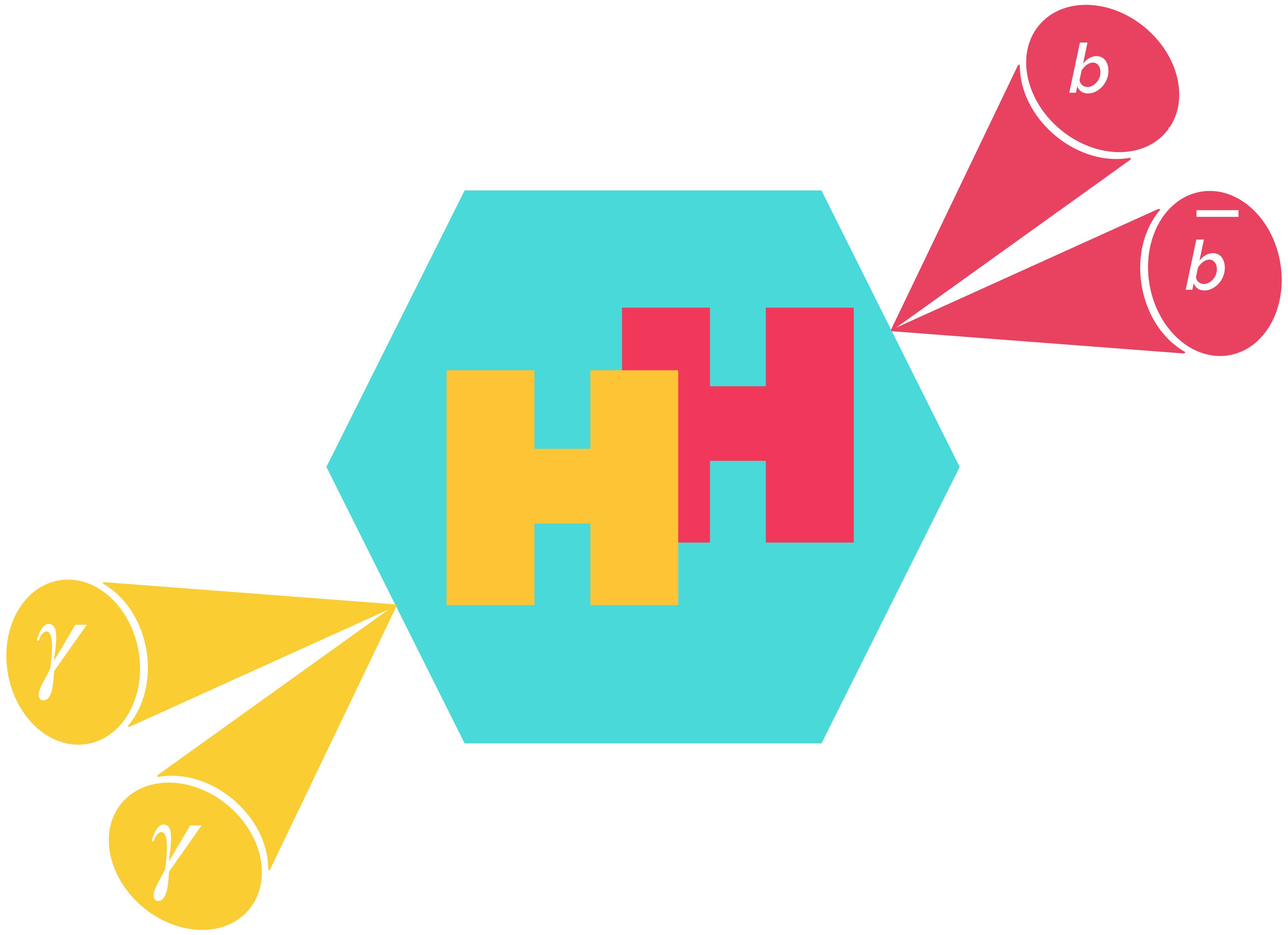

$$HH \to b\bar{b}\gamma\gamma$$

Strategy

Non-resonant and resonant search: $\mathscr{L} = 139\text{fb}^{-1}$ ATLAS-CONF-2021-016

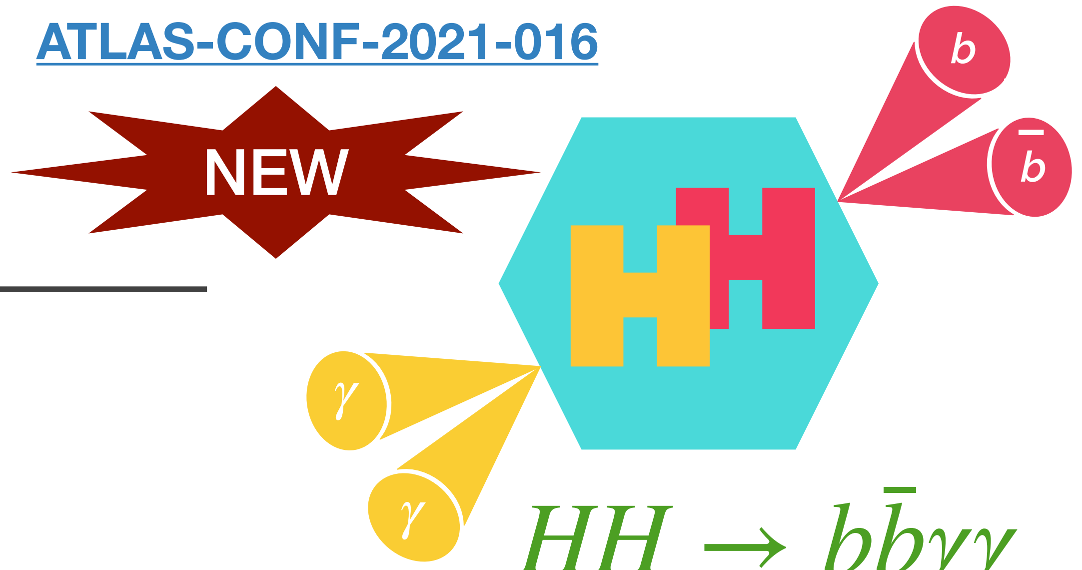

$HH \rightarrow b\bar{b}\gamma\gamma$

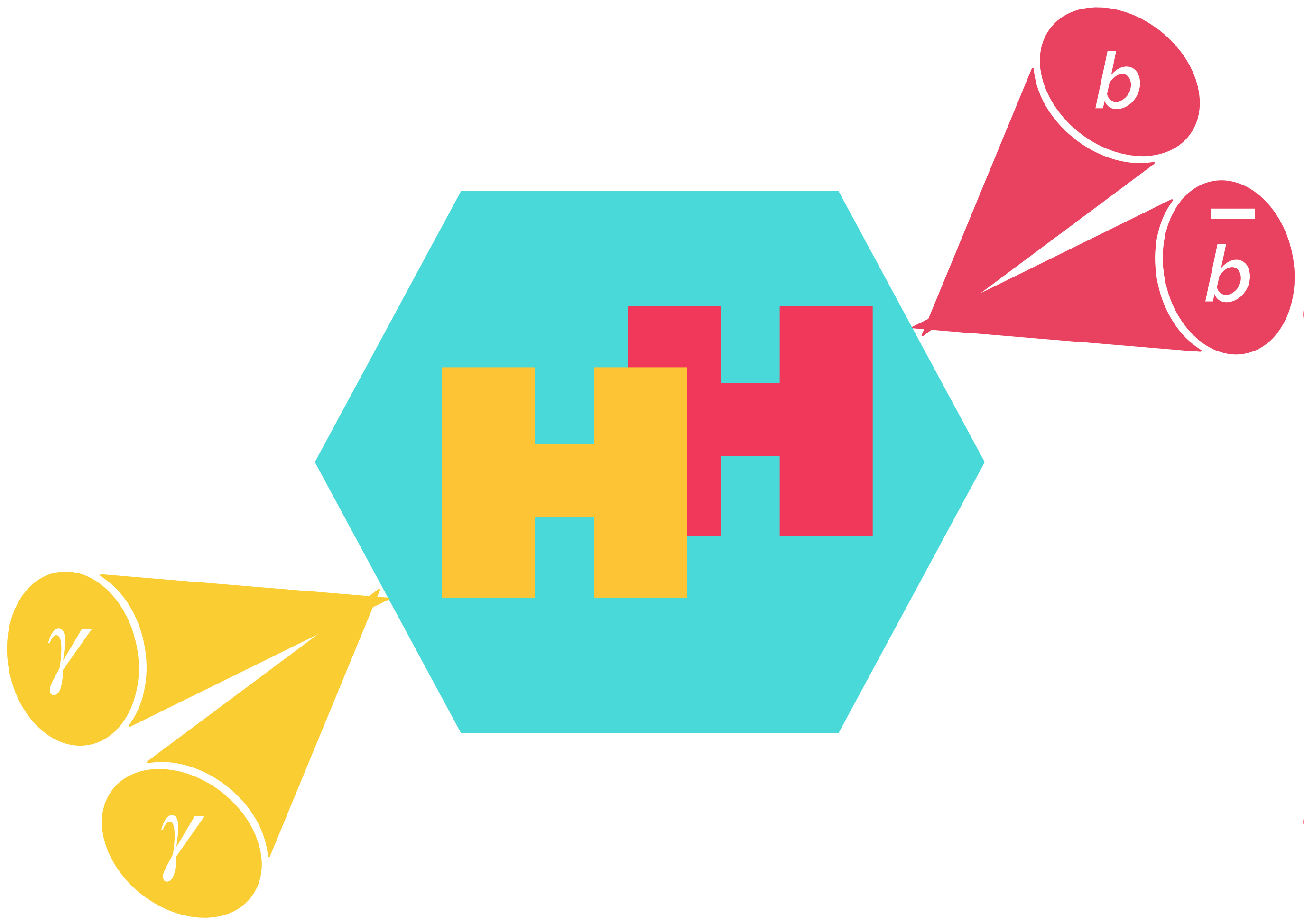

- Exactly 2 High quality photons

- Exactly 2 b-jets:
  - Dedicated energy correction from semileptonic decay effect (muon and neutrino) → similar to what applied in $VH \rightarrow b\bar{b}$

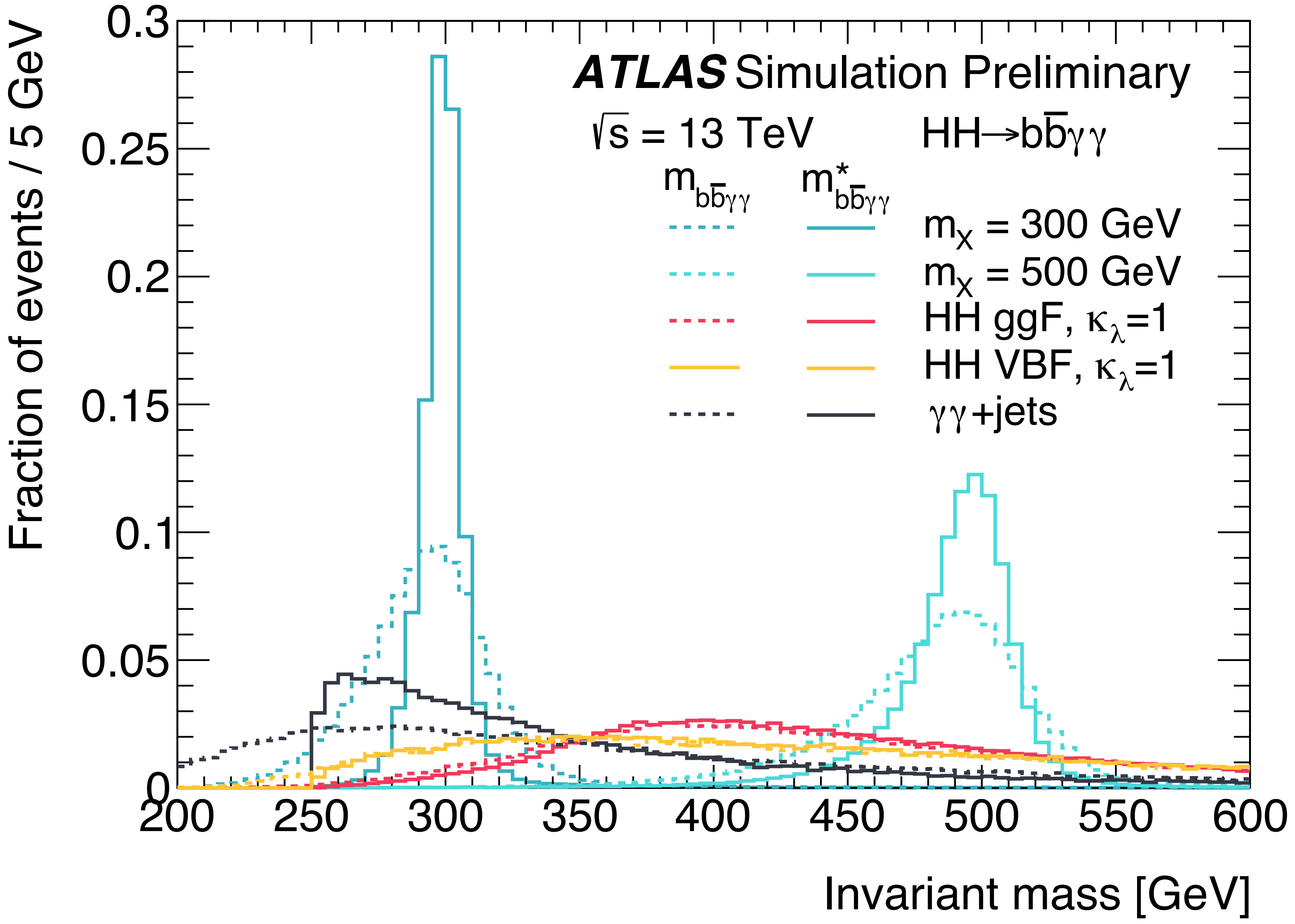

While the $m_{\gamma\gamma}$ variable is now used for the fit, the HH invariant mass $m_{b\bar{b}\gamma\gamma}$ is still useful for both the:

- Non-resonant search (sensitive to κ_λ);
- Resonant searches (sensitive to mass of resonance).

Due to experimental resolution effects, this can be corrected, assuming the two sub-systems are originating from Higgs bosons:

$$m^*_{b\bar{b}\gamma\gamma} = m_{b\bar{b}\gamma\gamma} - m_{b\bar{b}} - m_{\gamma\gamma} + 250$$

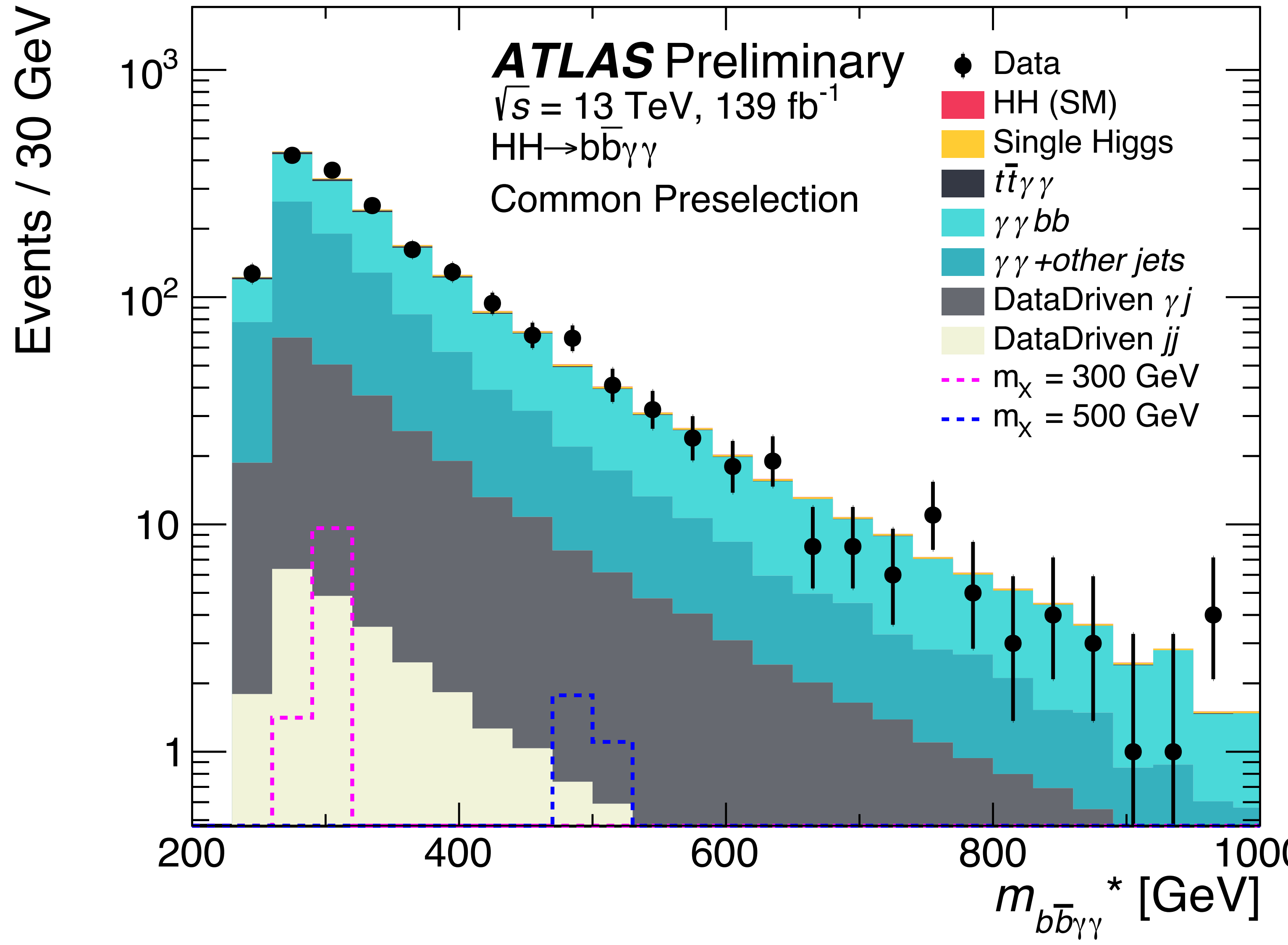

How to look for signal?

Non-resonant and resonant search: $\mathscr{L} = 139\text{fb}^{-1}$ ATLAS-CONF-2021-016

NEW

$HH \to b\bar{b}\gamma\gamma$

Non Resonant

A *BDT* is used to select signal like events w.r.t di-photon + single Higgs. Categories are created from $m^*_{b\bar{b}\gamma\gamma}$:

- High mass, focussed on SM
  - $\kappa_\lambda = 1$ ggF HH used as signal;
- Low mass, focussed on BSM
  - $\kappa_\lambda = 10$ ggF HH used as signal.

350 GeV

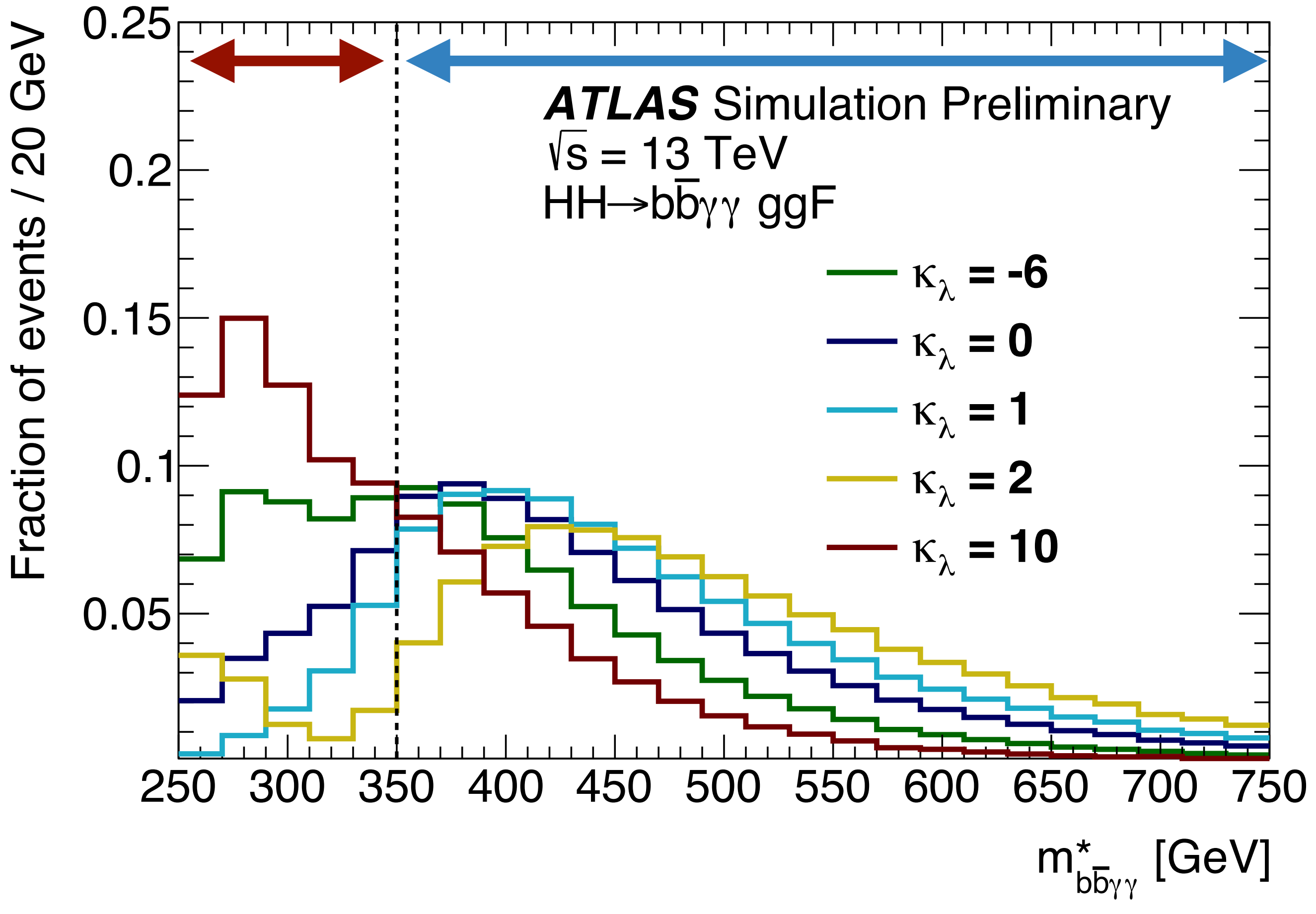

In each mass category, two regions are created: Loose/Tight BDT cut

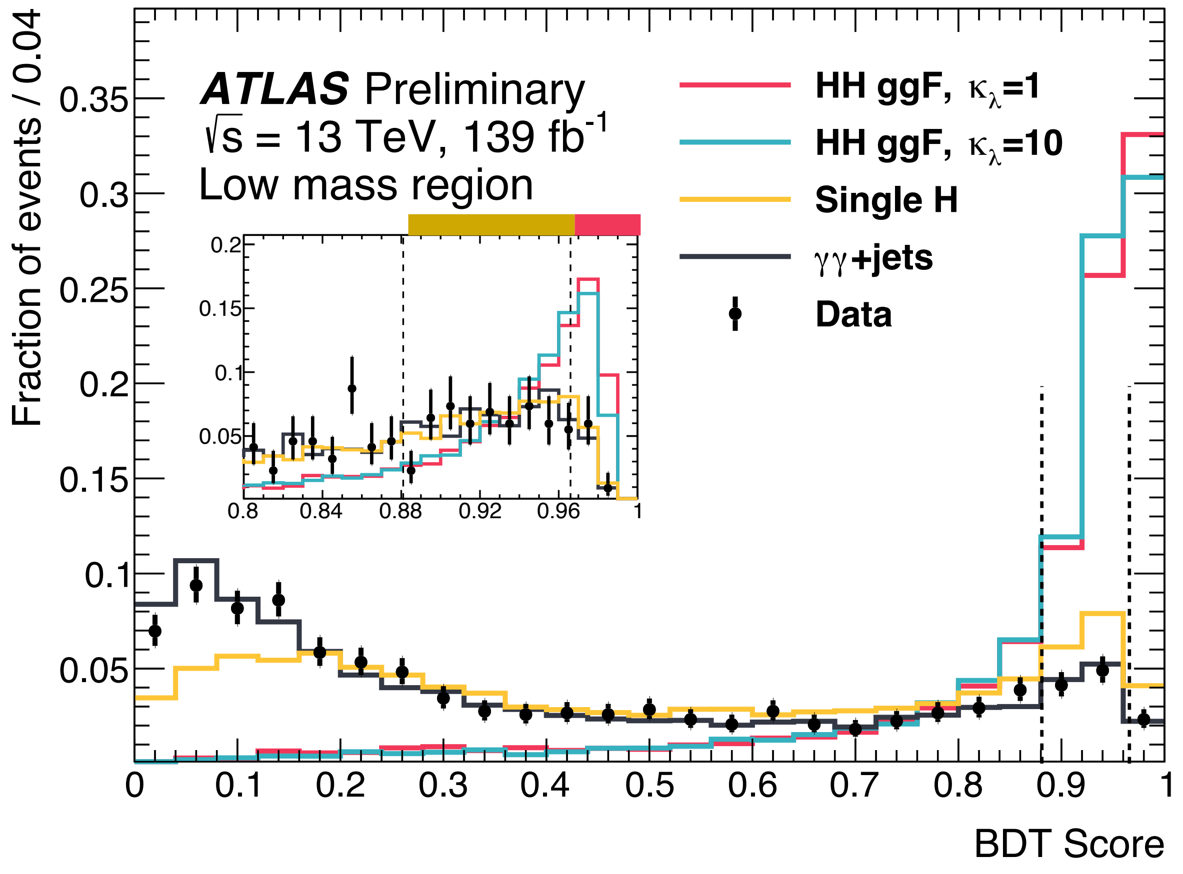

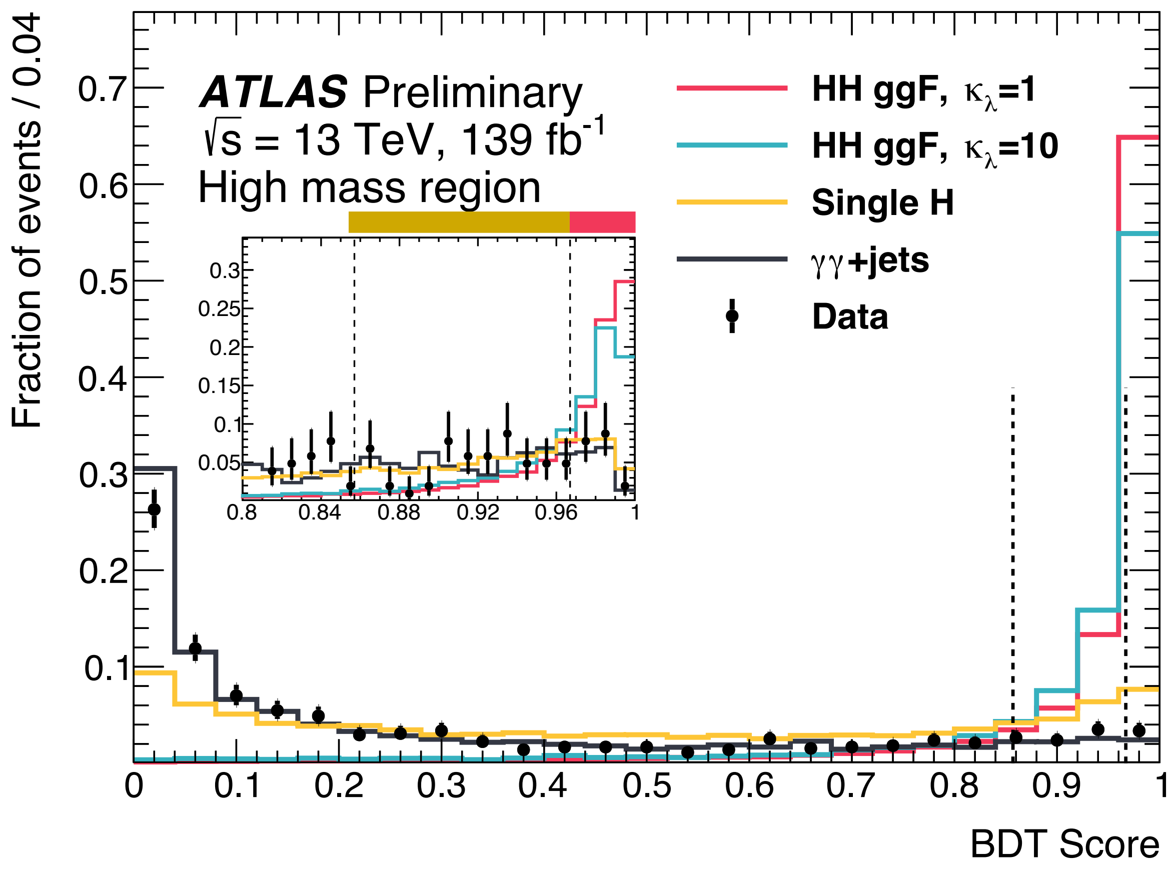

Resonant:

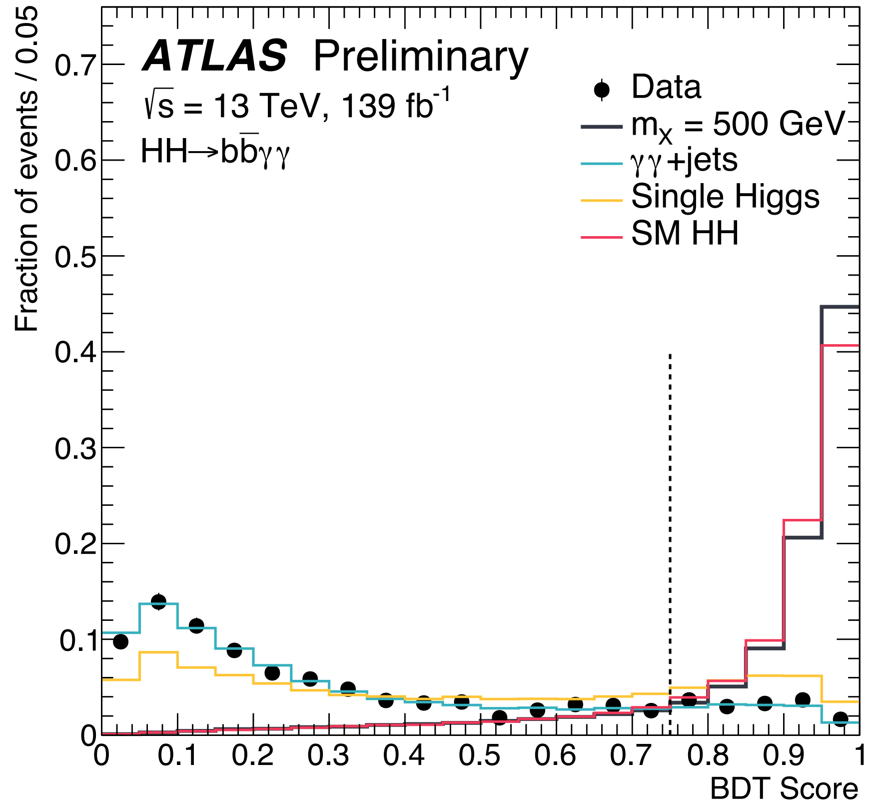

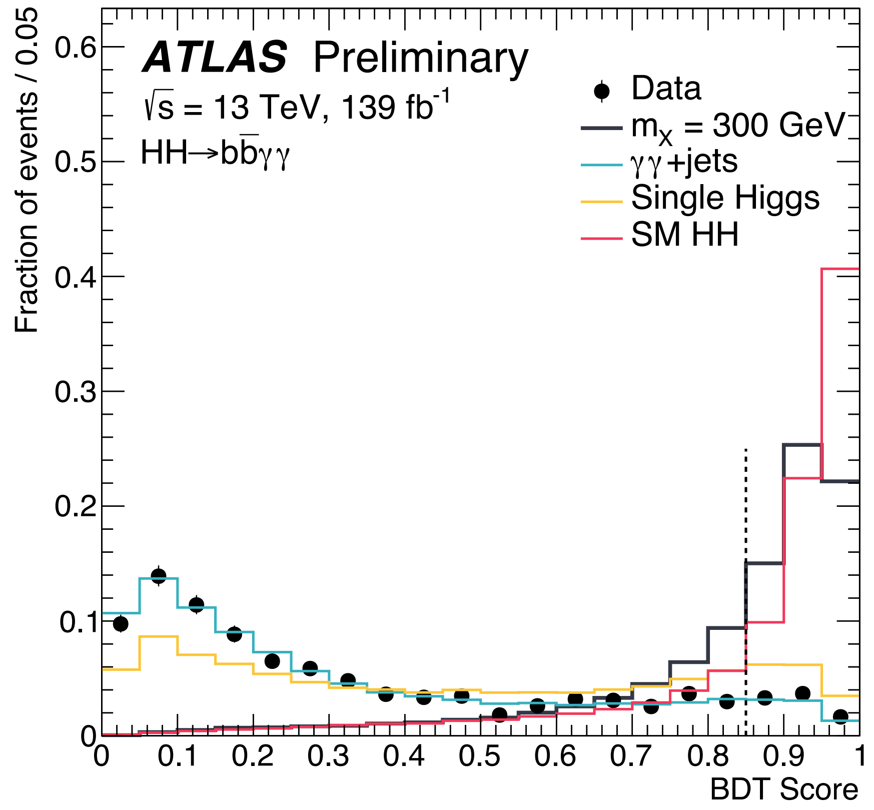

1. 2 separate *BDTs* are used to separate resonant signals from di-photon and single Higgs:
   - All resonances are combined and reweighted to show same $m^*_{b\bar{b}\gamma\gamma}$ as background;
   - BDT scores combined:

$$\text{BDT}_{\text{tot}} = \frac{1}{\sqrt{C_1^2 + C_2^2}} \sqrt{C_1^2 \left(\frac{\text{BDT}_{\gamma\gamma}+1}{2}\right)^2 + C_2^2 \left(\frac{\text{BDT}_{\text{Single}H}+1}{2}\right)^2}$$

$C_1 = 1 - C_2 = 0.65$ to maximise significance

   - Mass dependent cut on BDT score
   - 22 mass categories created.

2. Cut is set on the $m^*_{b\bar{b}\gamma\gamma}$ mass for each resonant search:

$$[mean - 2 \times RMS;\ mean + 2 \times RMS]^*$$

* extended to 4 x RMS for $m_X \geq 900$ GeV

Modelling

Non-resonant and resonant search: $\mathscr{L} = 139\text{fb}^{-1}$ ATLAS-CONF-2021-016

NEW

$HH \rightarrow b\bar{b}\gamma\gamma$

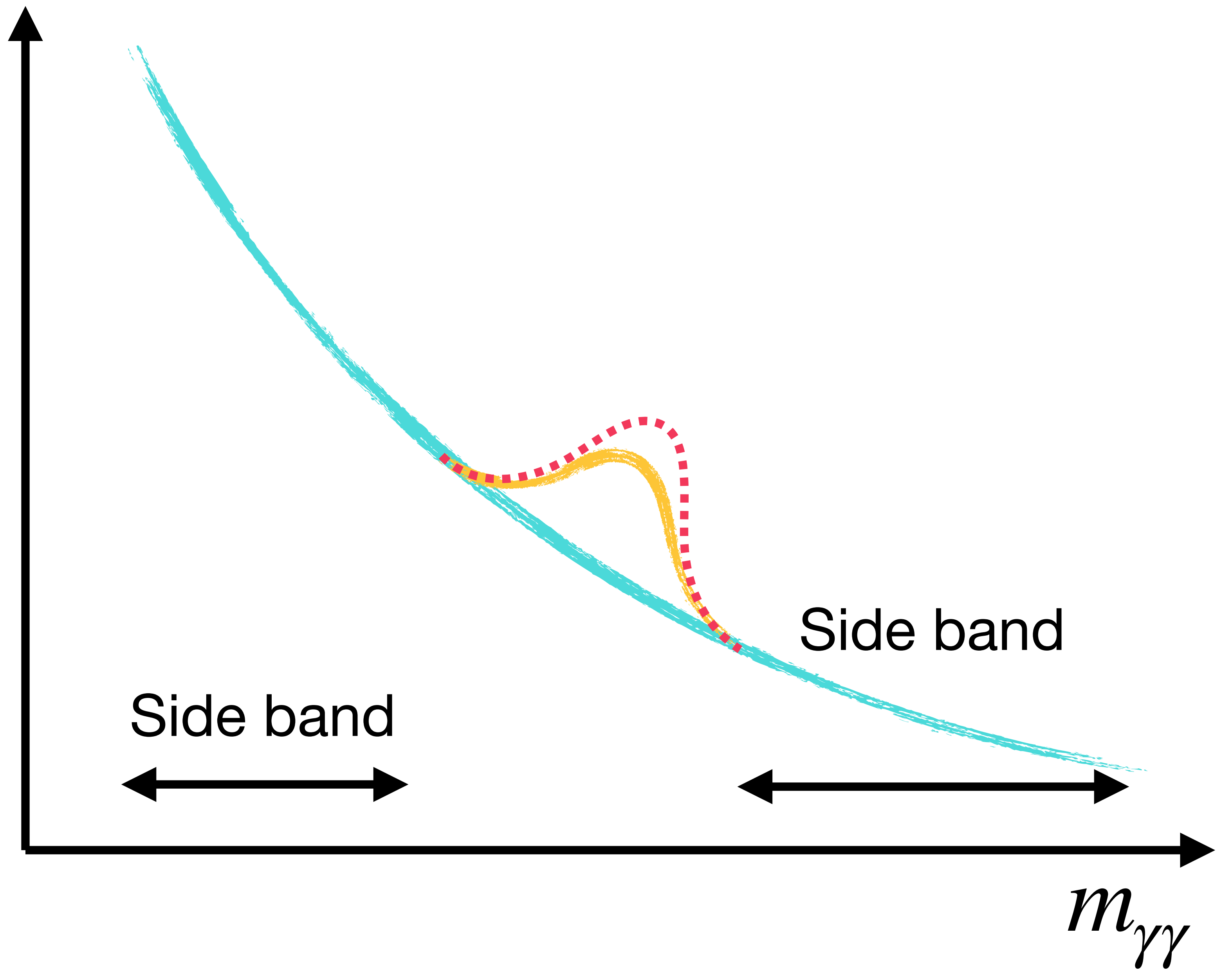

Diphoton Background

Functional form used to model the background:

- Fitted to background template normalised to data sideband;
- Bias from the function choice estimated through "*Spurious Signal*":
  - Signal event yield extracted from a S+B fit to the background-only distribution;
- Functions minimising the number of parameters and spurious signal is retained :
  - $exp(\alpha \cdot m_{\gamma\gamma})$ retained for all categories.

Single Higgs HH signal

- Single Higgs and HH processes can be modelled with **double-sided Crystal Ball** function.
  - Extracted in each category;
  - ggF and VBF HH are merged (using $\kappa_\lambda = 1$);
  - Same shape applied to single Higgs.
- Yields determined from $\sigma \times BR$ and $eff. \times acc$.

  Theory Simulation

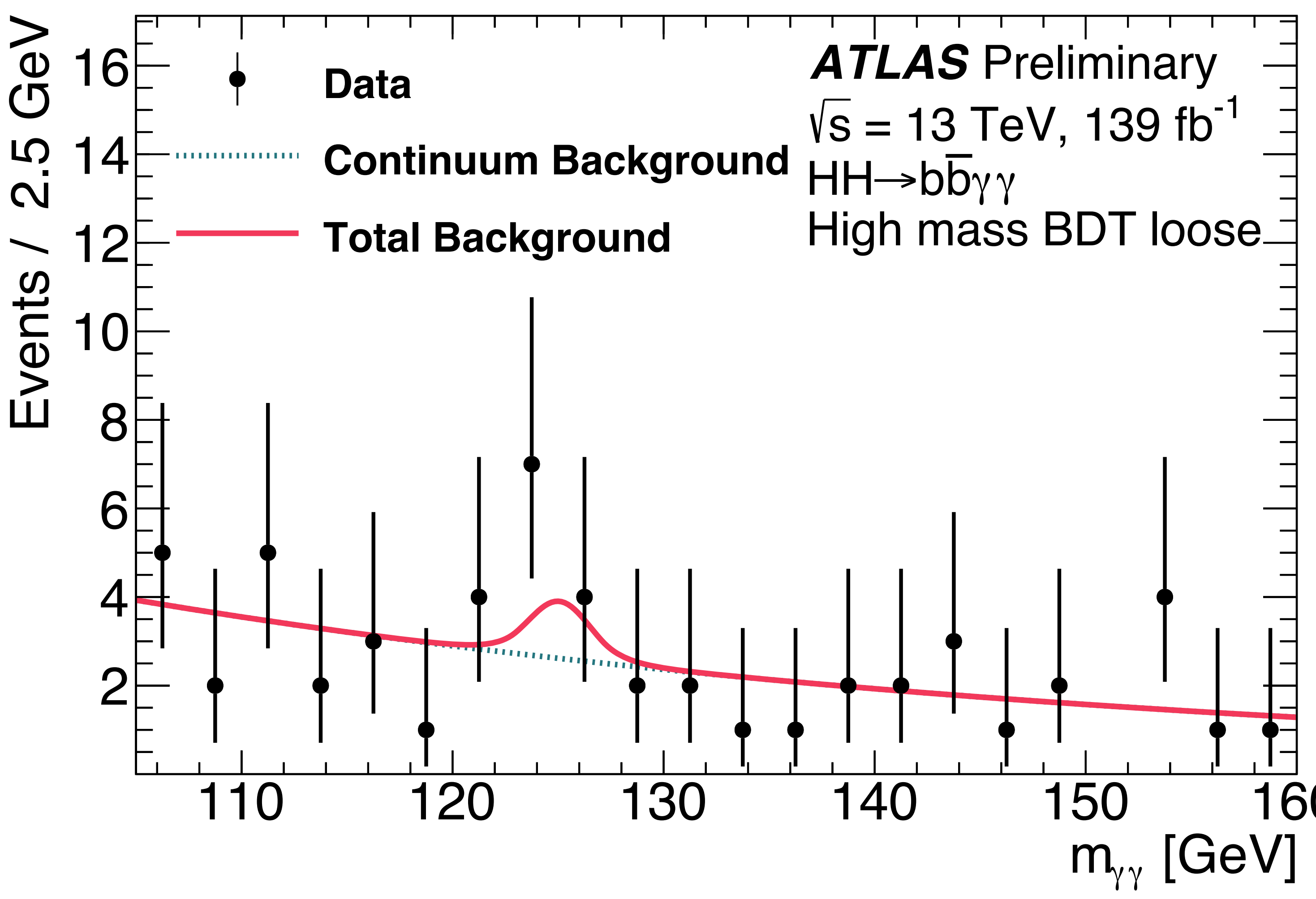

Category	σ_{68} [GeV]
High mass BDT tight	1.46 ± 0.01
High mass BDT loose	1.61 ± 0.02
Low mass BDT tight	1.72 ± 0.06
Low mass BDT loose	1.81 ± 0.03
Resonant m_X = 300 GeV	1.96 ± 0.02
Resonant m_X = 500 GeV	1.60 ± 0.01

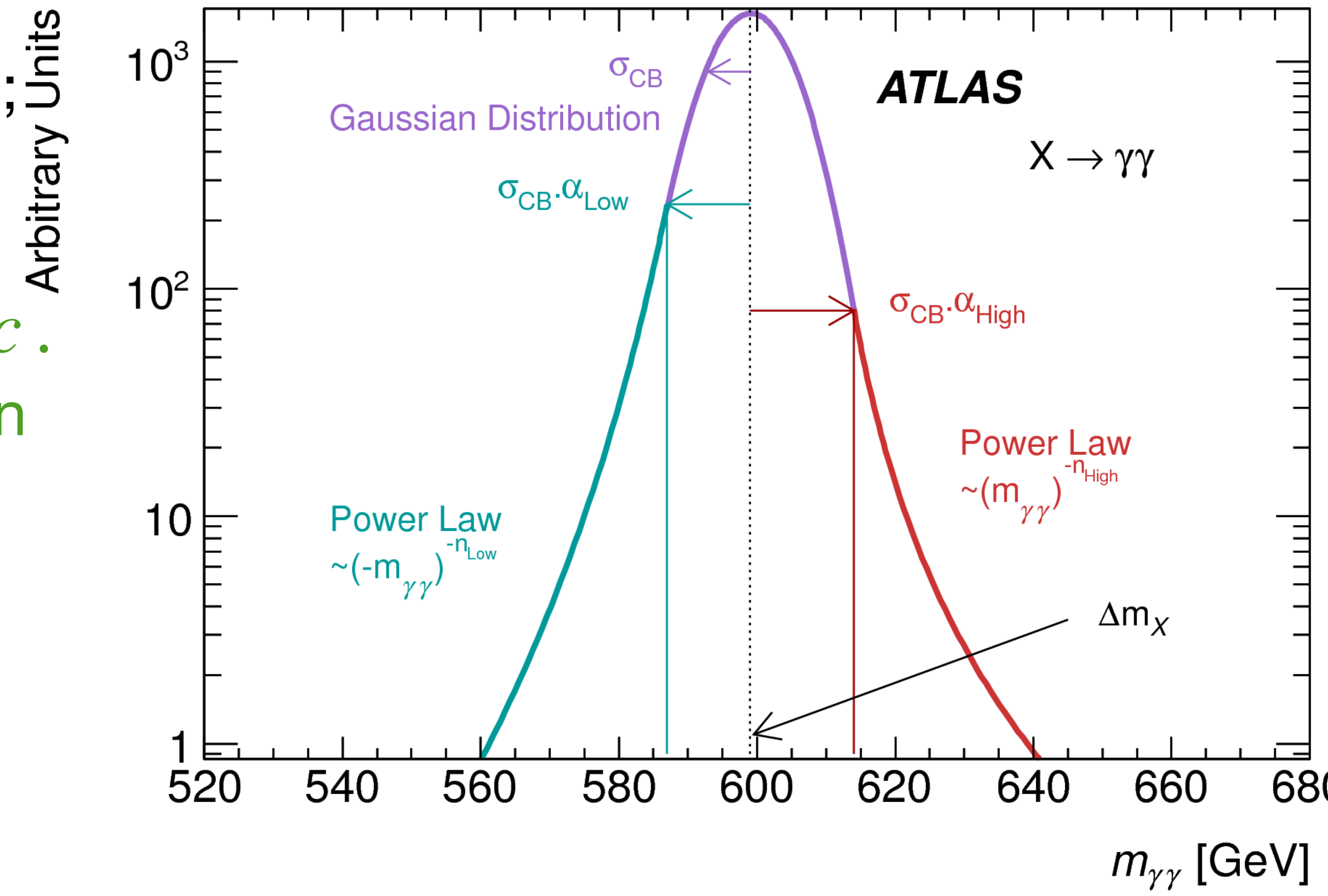

Results

NEW

$HH \rightarrow b\bar{b}\gamma\gamma$

Non Resonant

No significant excess found

$\sigma_{HH}^{ggF+VBF}$ **observed (expected)** limit is **4.1 (5.5)** times the SM prediction.

- Improved by factor 4 from $\mathscr{L} = 36\ \text{fb}^{-1}$;
- *Best result* from single channel *observed to date;*
- Statistically dominated.
- Limits are set on κ_λ: $-1.5 < \kappa_\lambda < 6.7$ observed
  $-2.4 < \kappa_\lambda < 7.7$ expected.

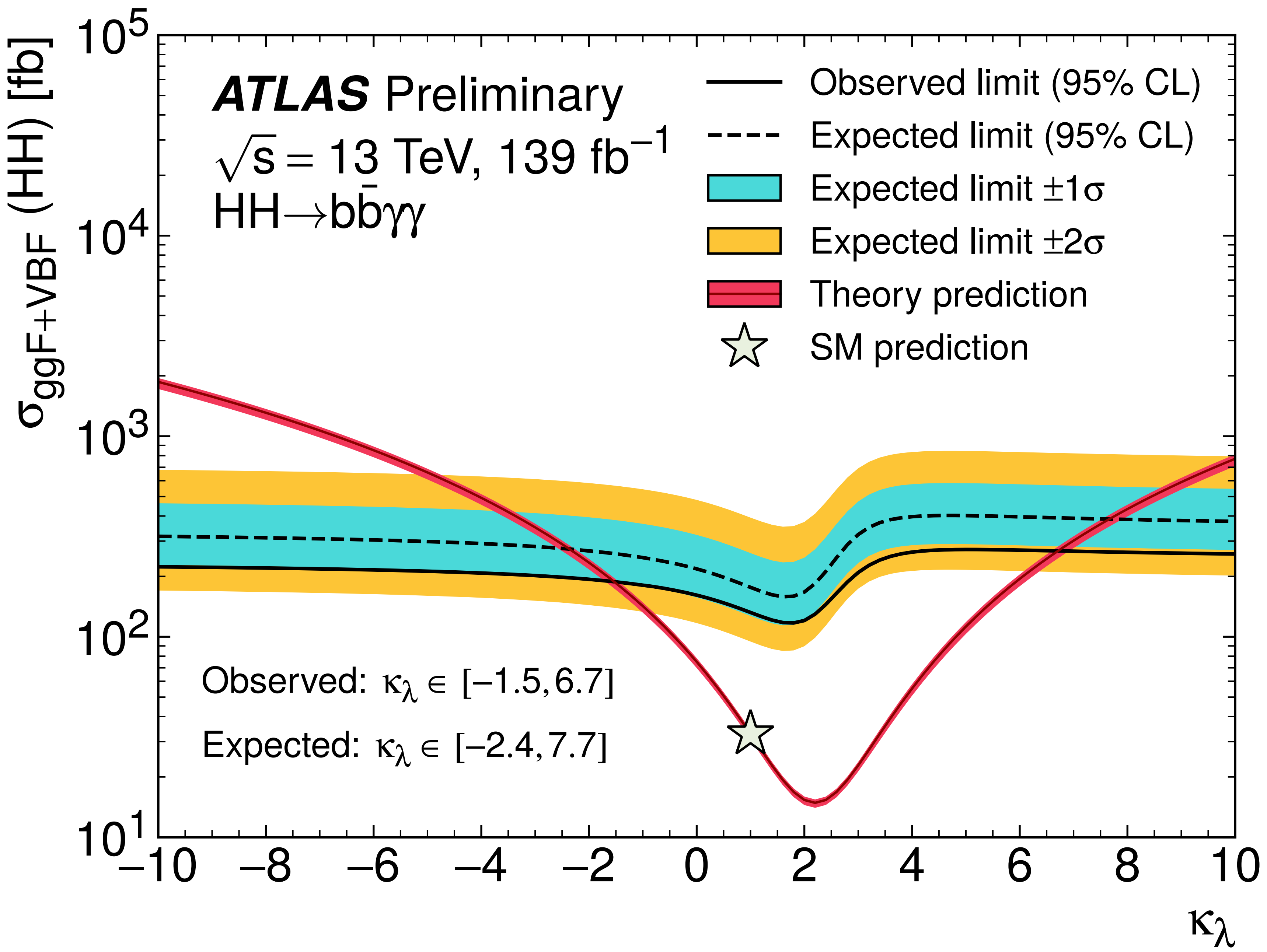

Resonant:

No significant excess found

Limits set on $\sigma(X \rightarrow HH)$ where X is a narrow-width scalar resonance:

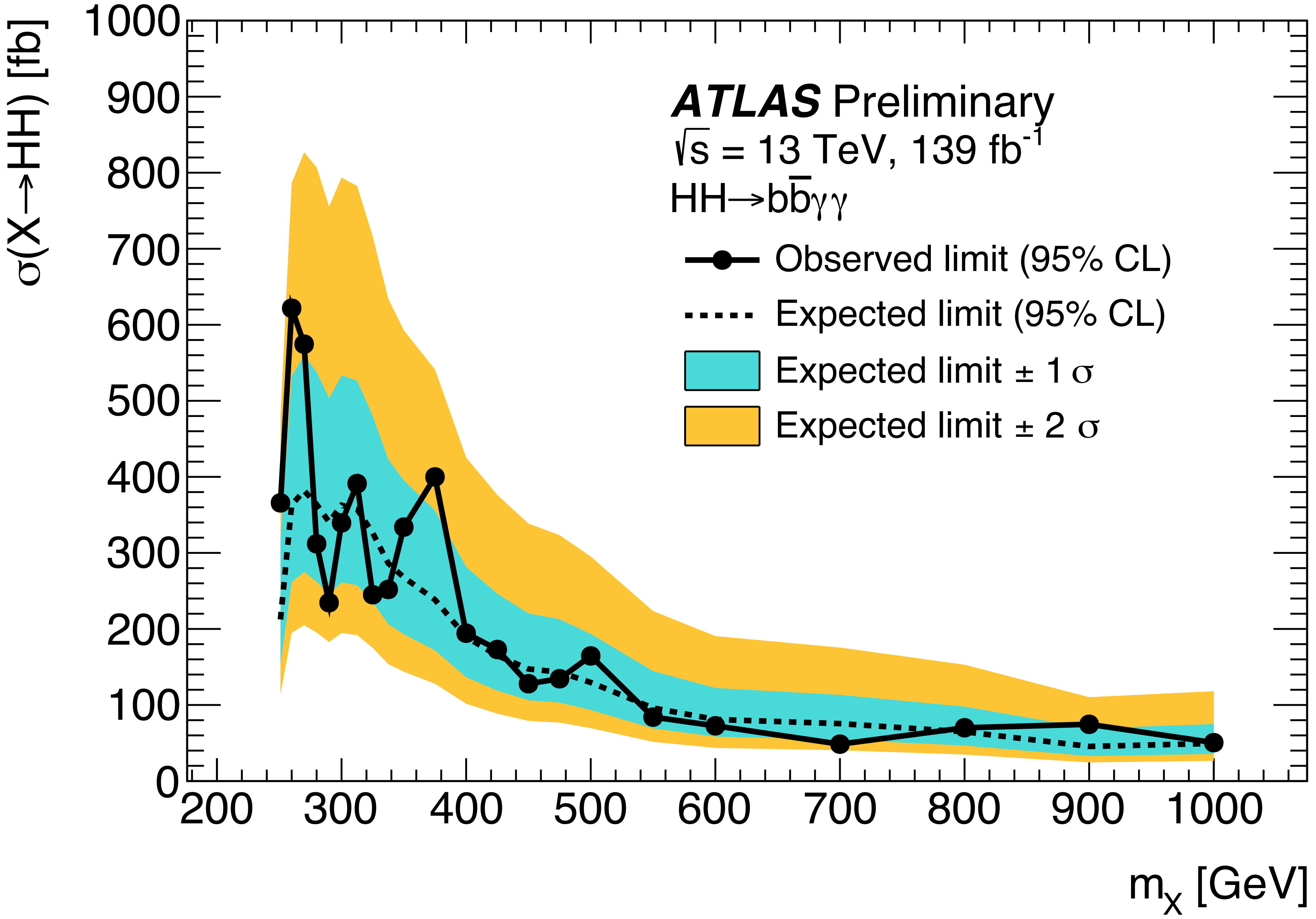

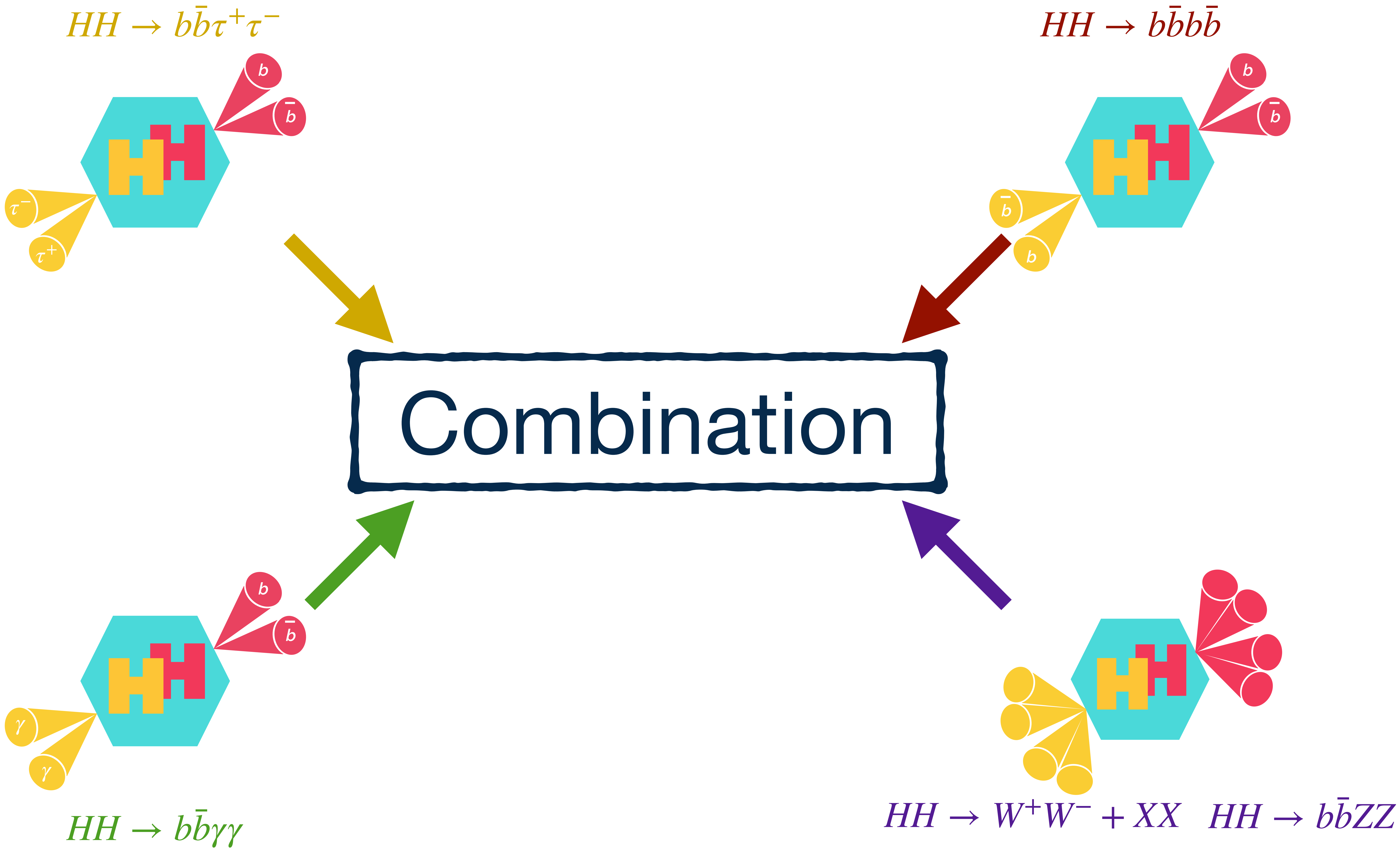

$HH \to b\bar{b}\tau^+\tau^-$
$HH \to b\bar{b}b\bar{b}$
Combination
$HH \to b\bar{b}\gamma\gamma$
$HH \to W^+W^- + XX$
$HH \to b\bar{b}ZZ$

Conclusion

Combinaison: $\mathscr{L} = 36\text{fb}^{-1}$ Phys. Lett. B 800 (2020) 135103

Combination done with most of the analyses with $\mathscr{L} = 36\text{fb}^{-1}$

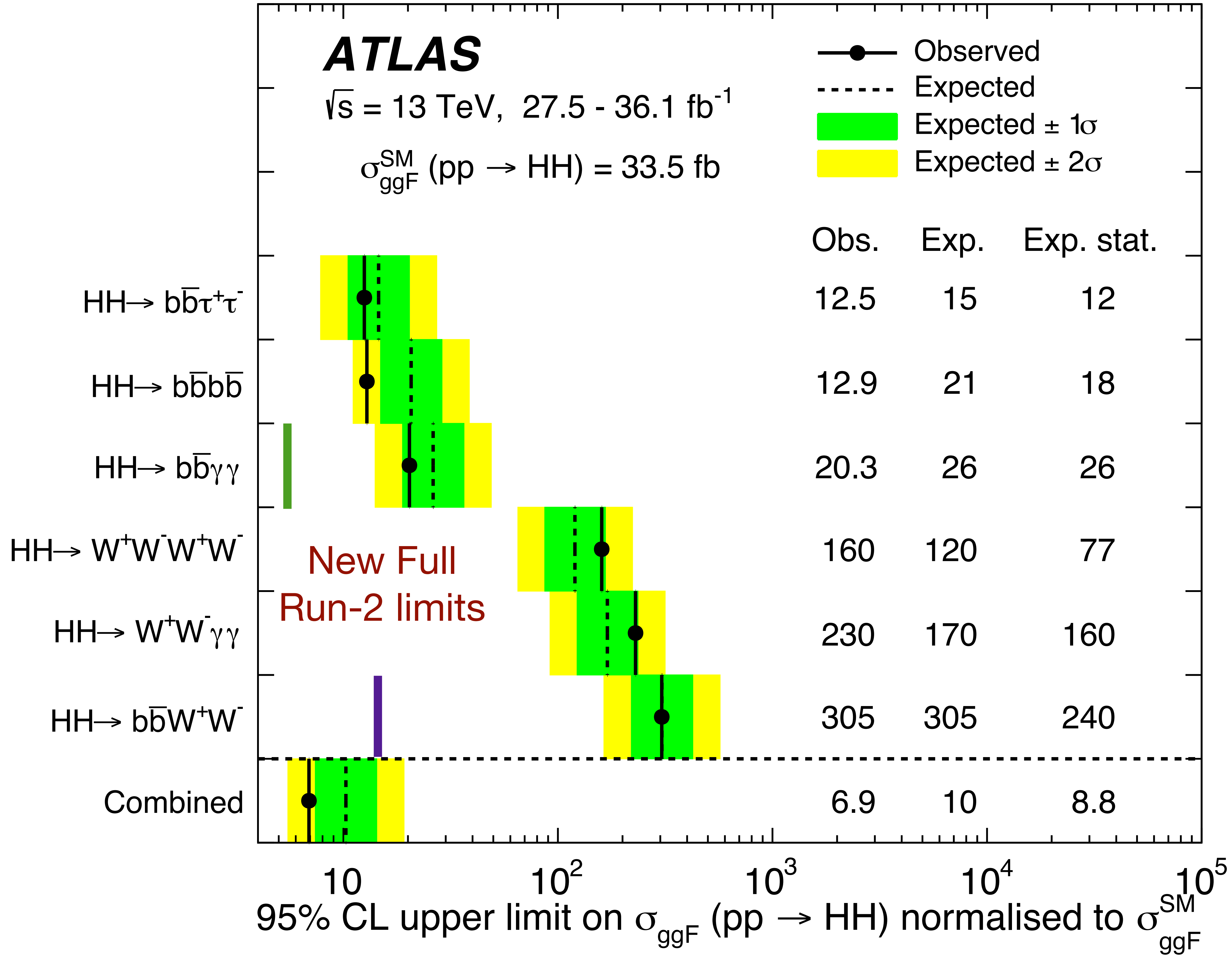

Additional results with $\mathscr{L} = 139\text{fb}^{-1}$:

$b\bar{b}l\nu l\nu$ final state (not presented today): Phys. Lett. B 801 (2020) 135145

observed (expected) limit is **14 (29)** times the SM prediction.

$b\bar{b}\gamma\gamma$ final state NEW

observed (expected) limit is **4.1 (5.5)** times the SM prediction.

↳ Single results outperforms the combination.

First look at **VBF**:

σ_{HH}^{VBF} **observed (expected)** limit is **840 (550)** times the SM prediction.

↳ Still very limited

Conclusion

Combination done with most of the analyses with $\mathscr{L} = 36\text{fb}^{-1}$

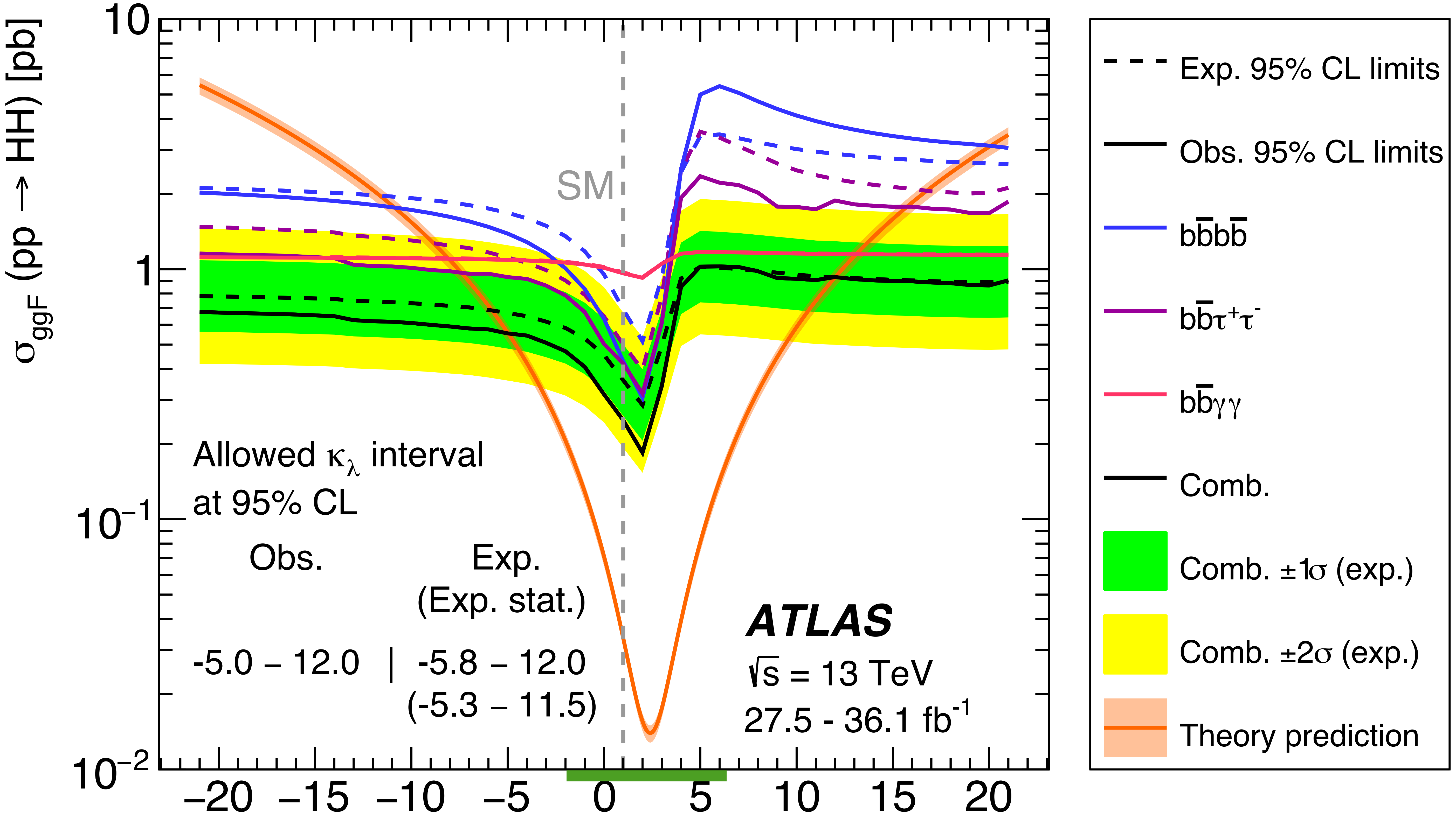

New Full Run-2 limits

Additional results with $\mathscr{L} = 139\text{fb}^{-1}$:

$b\bar{b}\gamma\gamma$ final state **NEW**

Limits are set on the κ_λ coupling modifier to:

$-1.5 < \kappa_\lambda < 6.7$ observed,

$-2.4 < \kappa_\lambda < 7.7$ expected.

↳ Single results outperforms the combination.

First look at **VBF**: $b\bar{b}b\bar{b}$ final state

Limits are set on the κ_{2V} coupling modifier to:

$-0.43 < \kappa_{2V} < 2.56$ observed,

$-0.55 < \kappa_{2V} < 2.72$ expected.

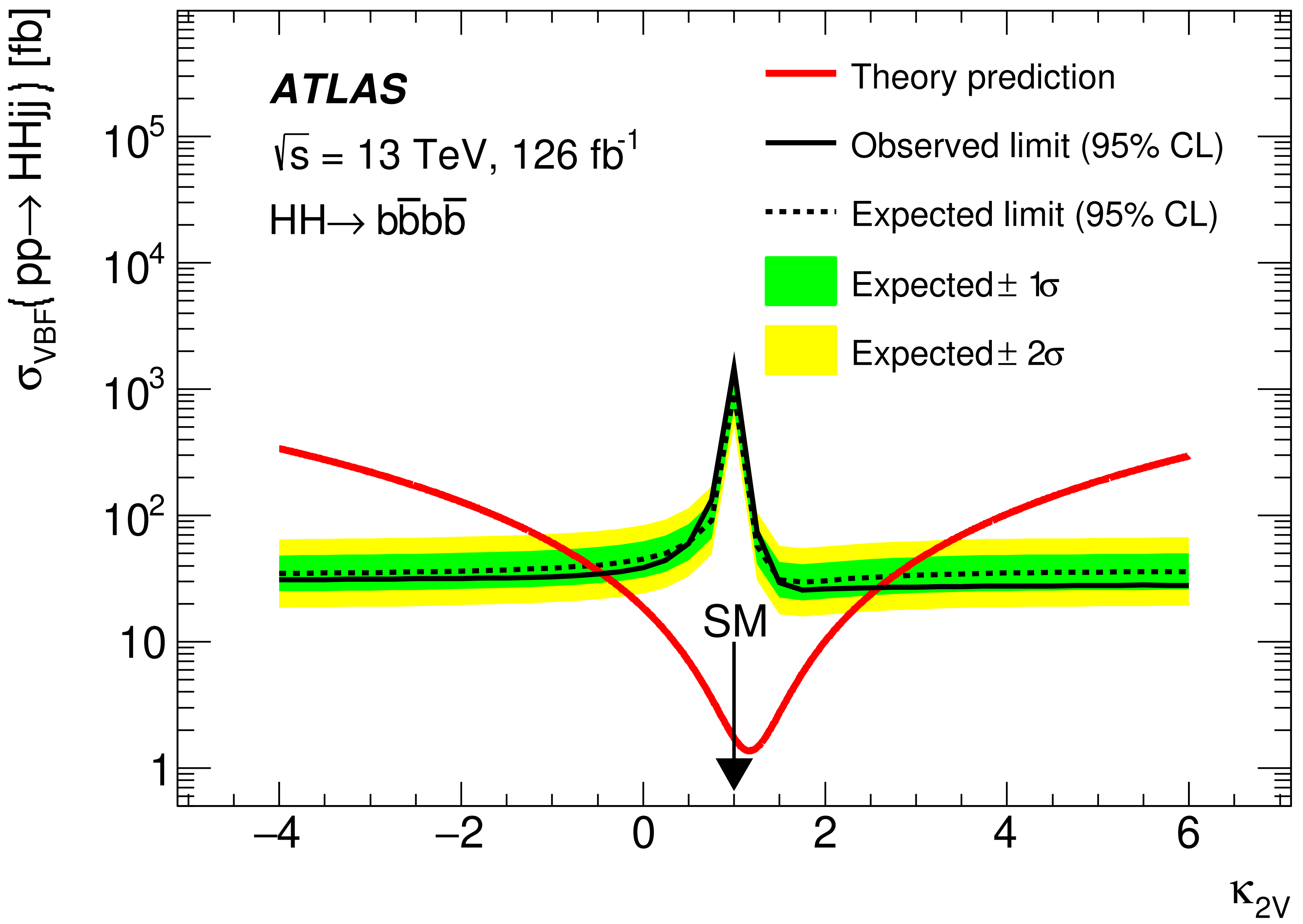

Conclusion

Combination done with most of the analyses with $\mathscr{L} = 36\text{fb}^{-1}$

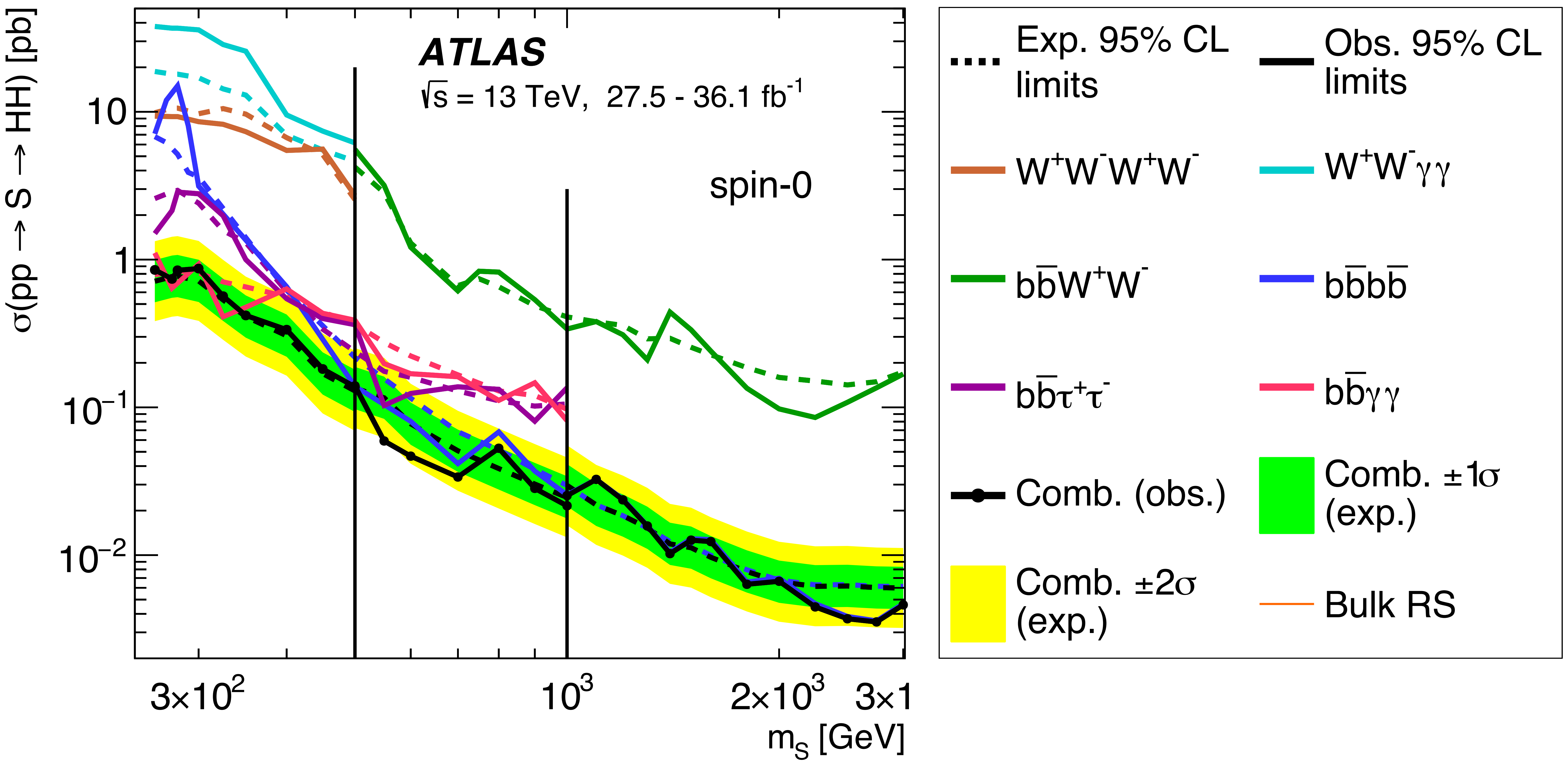

Additional results with $\mathscr{L} = 139\text{fb}^{-1}$:

$b\bar{b}\gamma\gamma$ final state NEW

observed (expected) limit is **610 fb** (251 GeV) **to 47 fb** (1000 GeV) (360-43 fb)

↳ Single results outperforms the combination in most of the mass range

$b\bar{b}\tau\tau$ Boosted final state

observed (expected) limit is **816 fb** (1000 GeV) **to 27 fb** (2500 GeV) (624-31 fb)

First look at Resonant **VBF**: $b\bar{b}b\bar{b}$ final state

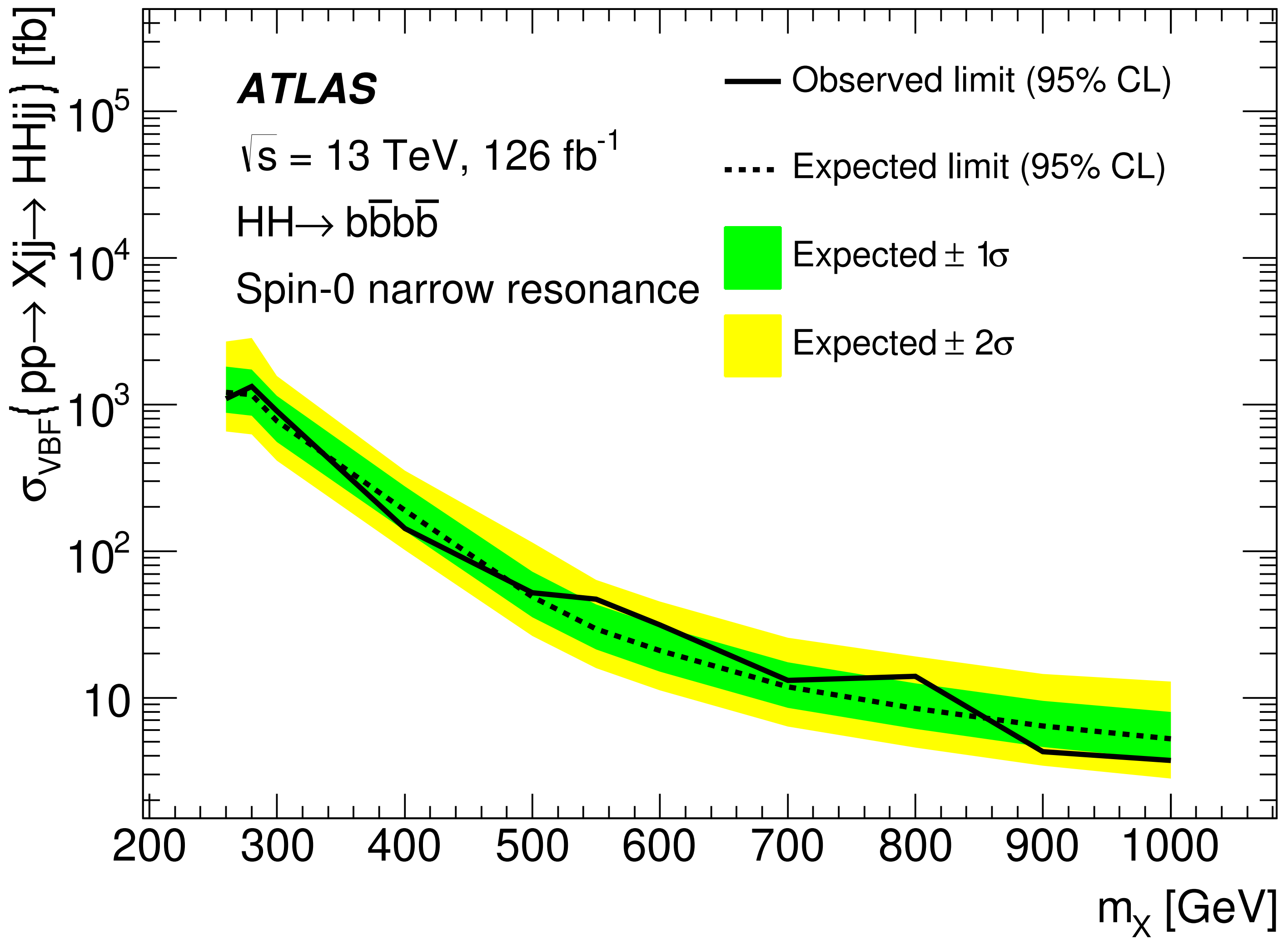

BACK-UP

HH: Higgs potential modification

[Phys. Rev. D 101, 075023]

$$V(H) \simeq \begin{cases} -m^2 H^\dagger H + \lambda (H^\dagger H)^2 + \frac{c_6 \lambda}{\Lambda^2}(H^\dagger H)^3, & \text{Elementary Higgs} \\ -a \sin^2(\sqrt{H^\dagger H}/f) + b \sin^4(\sqrt{H^\dagger H}/f), & \text{Nambu-Goldstone Higgs} \\ \lambda (H^\dagger H)^2 + \epsilon (H^\dagger H)^2 \log \frac{H^\dagger H}{\mu^2}, & \text{Coleman-Weinberg Higgs} \\ -\kappa^3 \sqrt{H^\dagger H} + m^2 H^\dagger H, & \text{Tadpole-induced Higgs} \end{cases}$$

- Nambu-Goldstone Higgs: pseudo Nambu-Goldstone boson emerging from strong dynamics at a high scale
- Coleman-Weinberg Higgs: EWSB is triggered by renormalization group (RG) running effects
- Tadpole-induced Higgs: EWSB is triggered by the Higgs tadpole

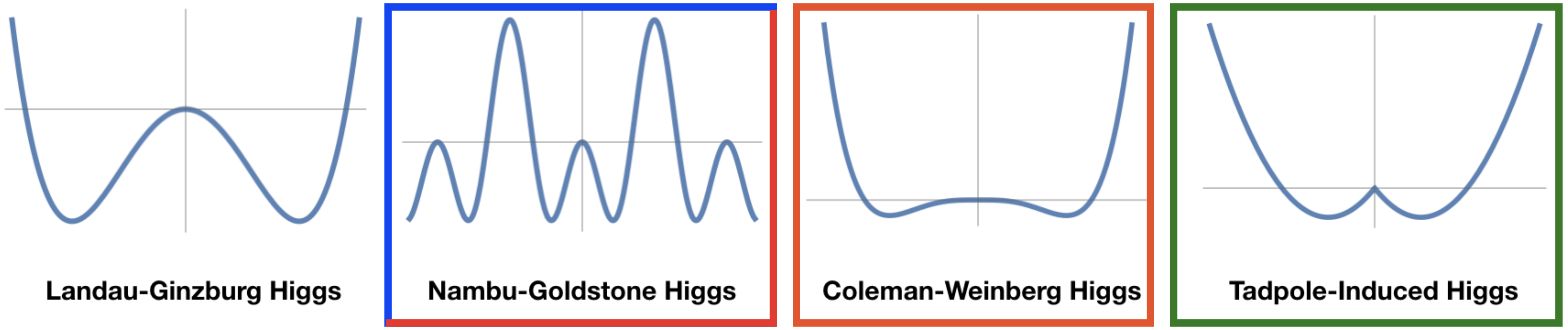

minimal composite Higgs model/composite twin Higgs model : different coupling to top quark

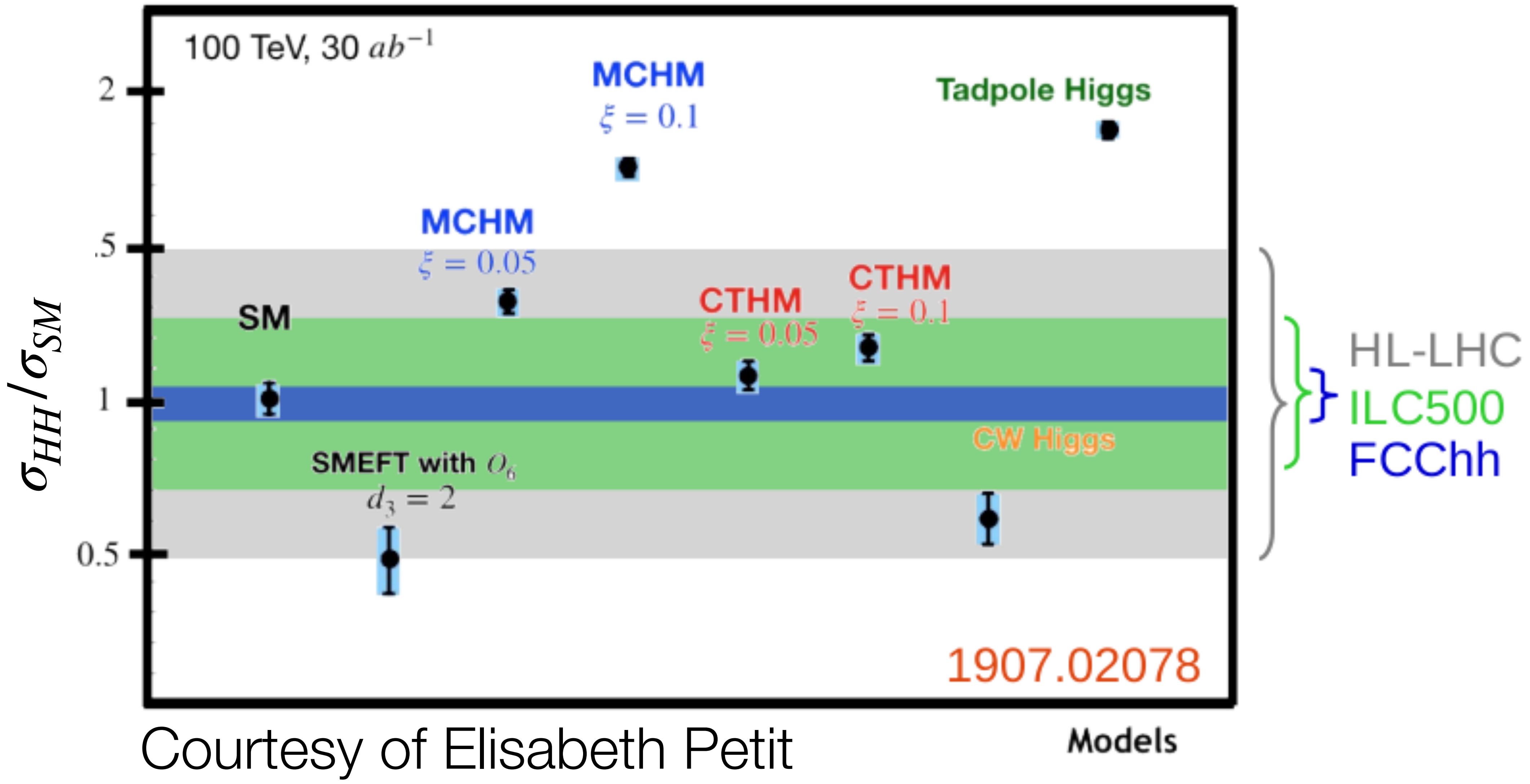

Courtesy of Elisabeth Petit

Single Higgs constrains

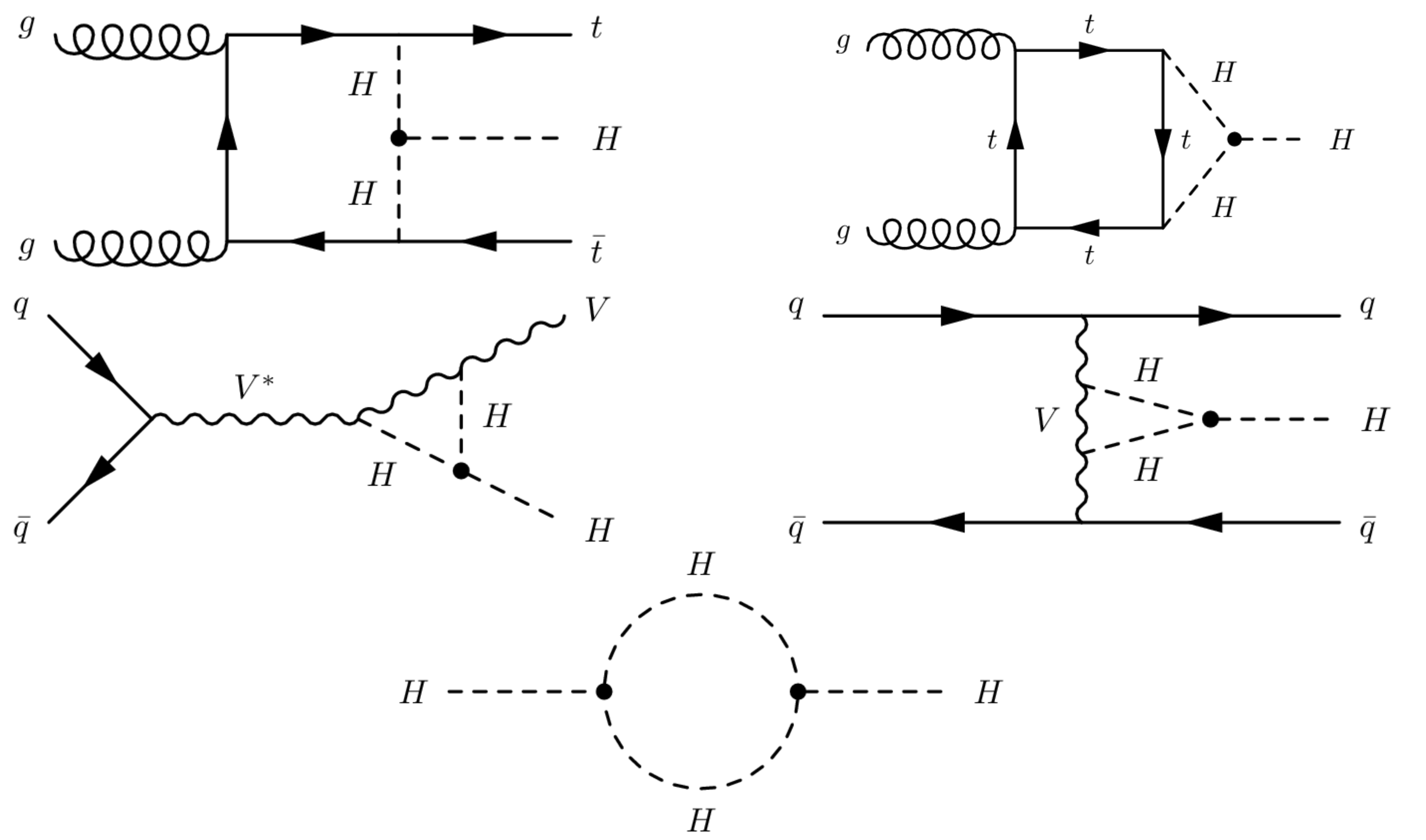

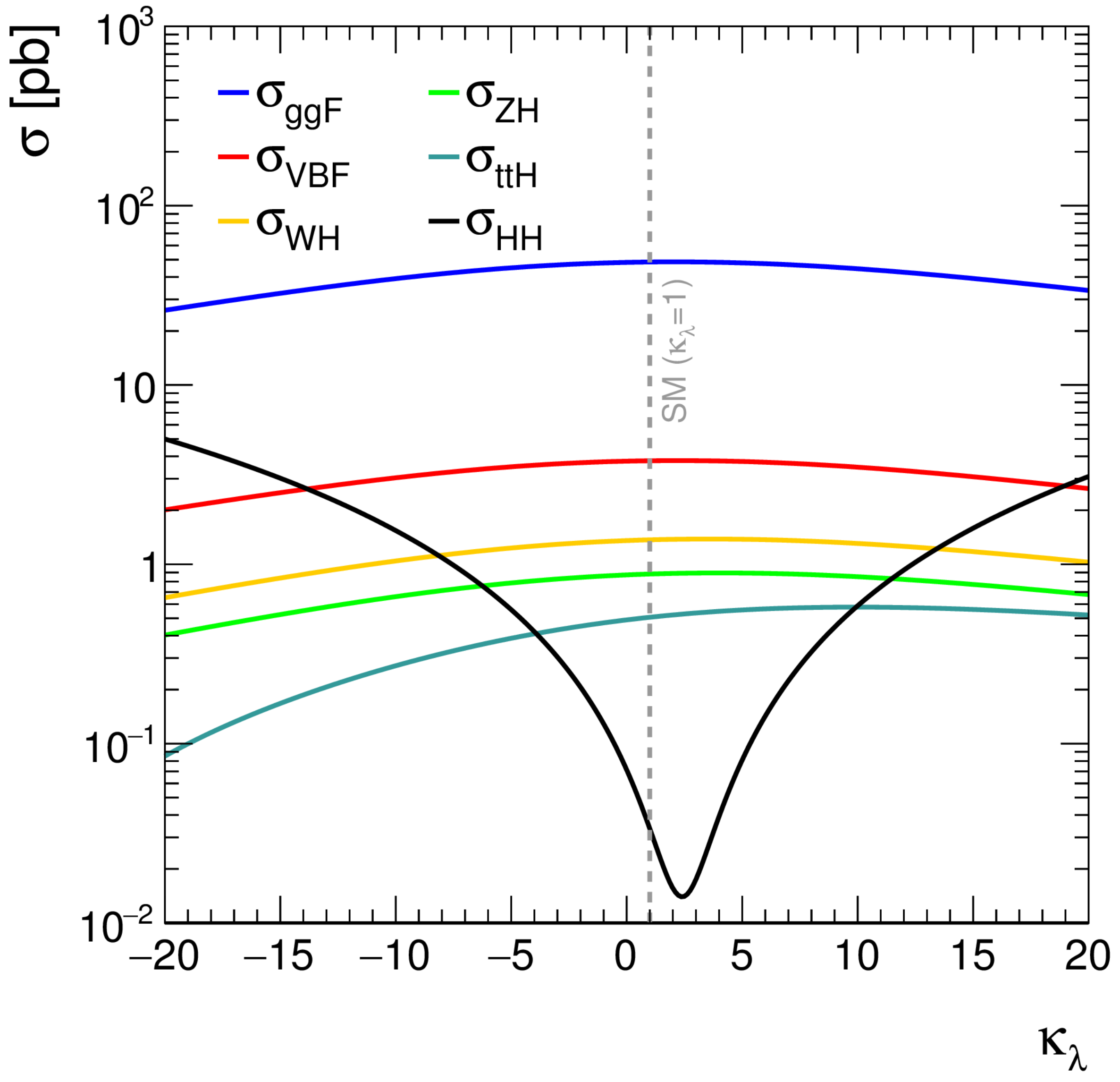

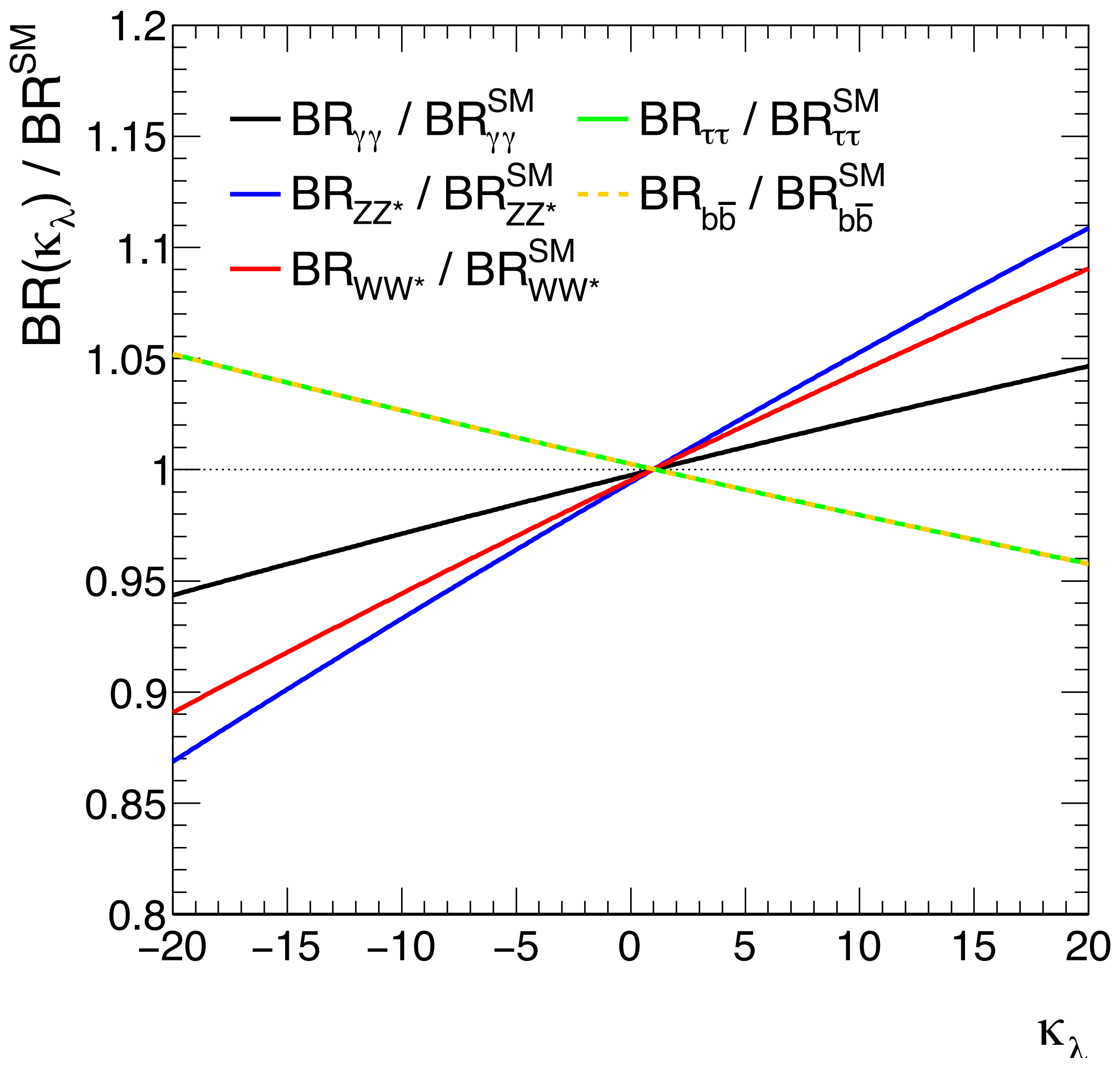

ATL-PHYS-PUB-2019-009

Combinaison of single Higgs channels with $\mathscr{L} = 80\text{fb}^{-1}$ yielding: $-3.2 < \kappa_\lambda < 11.9$

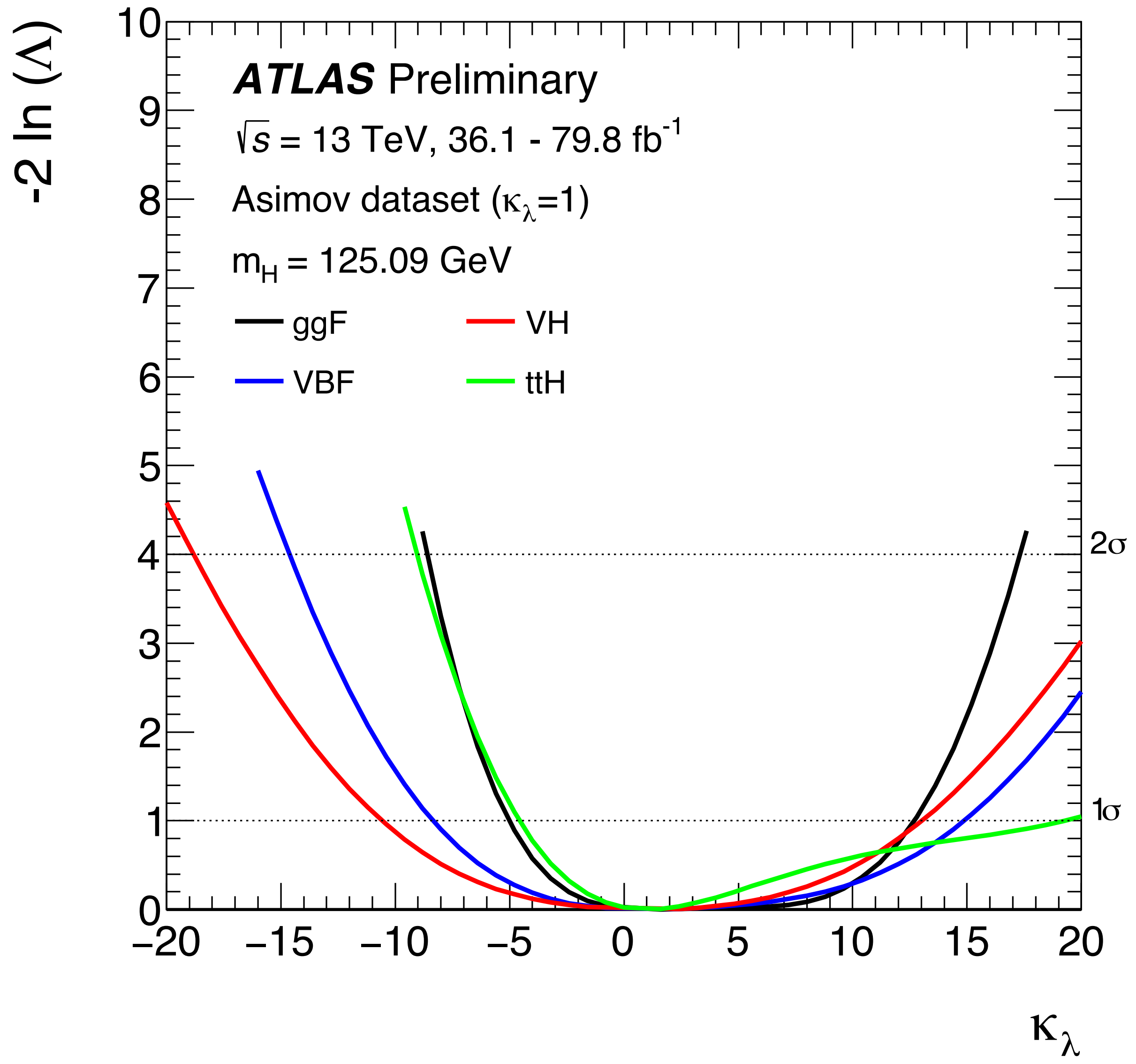

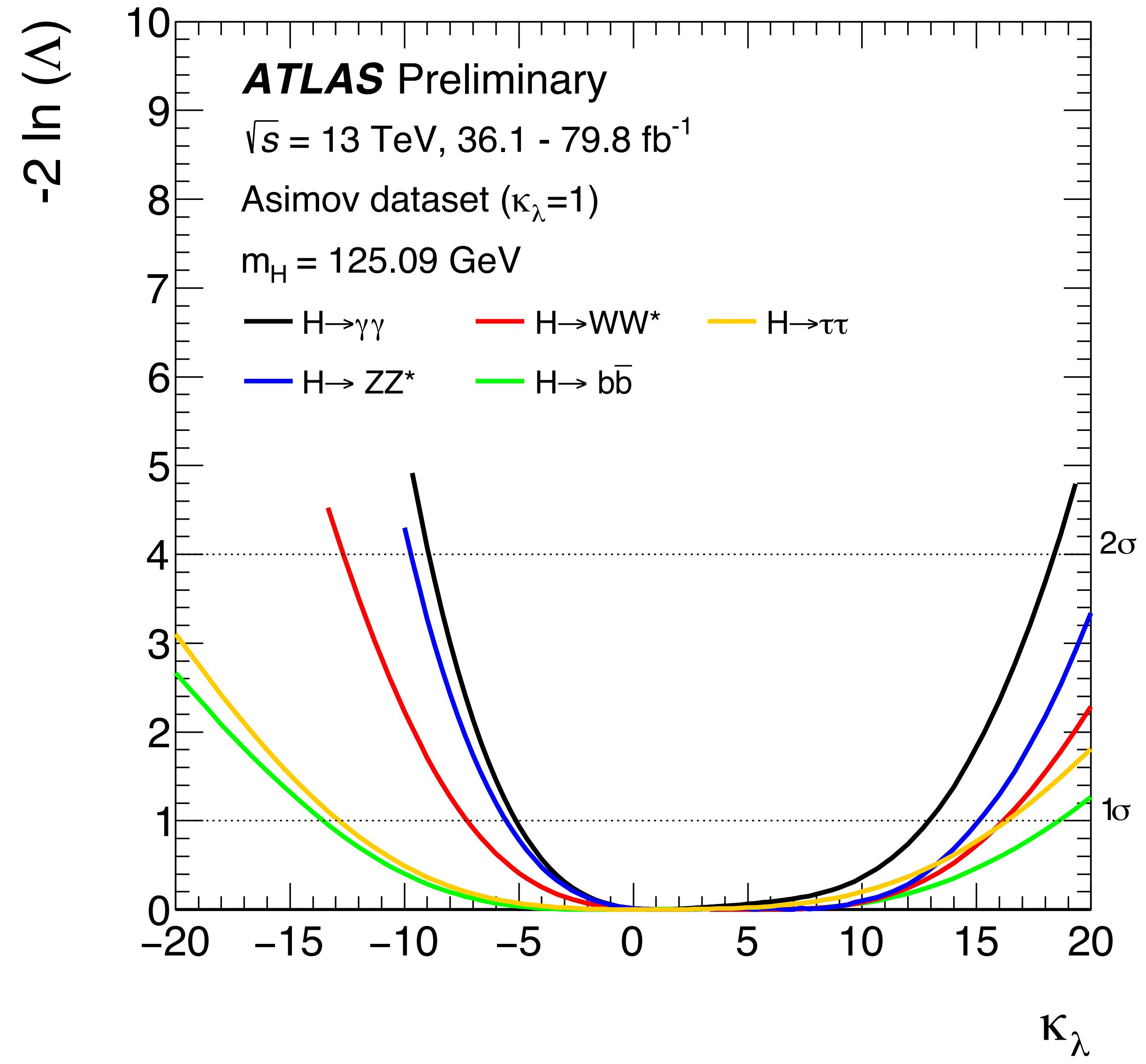

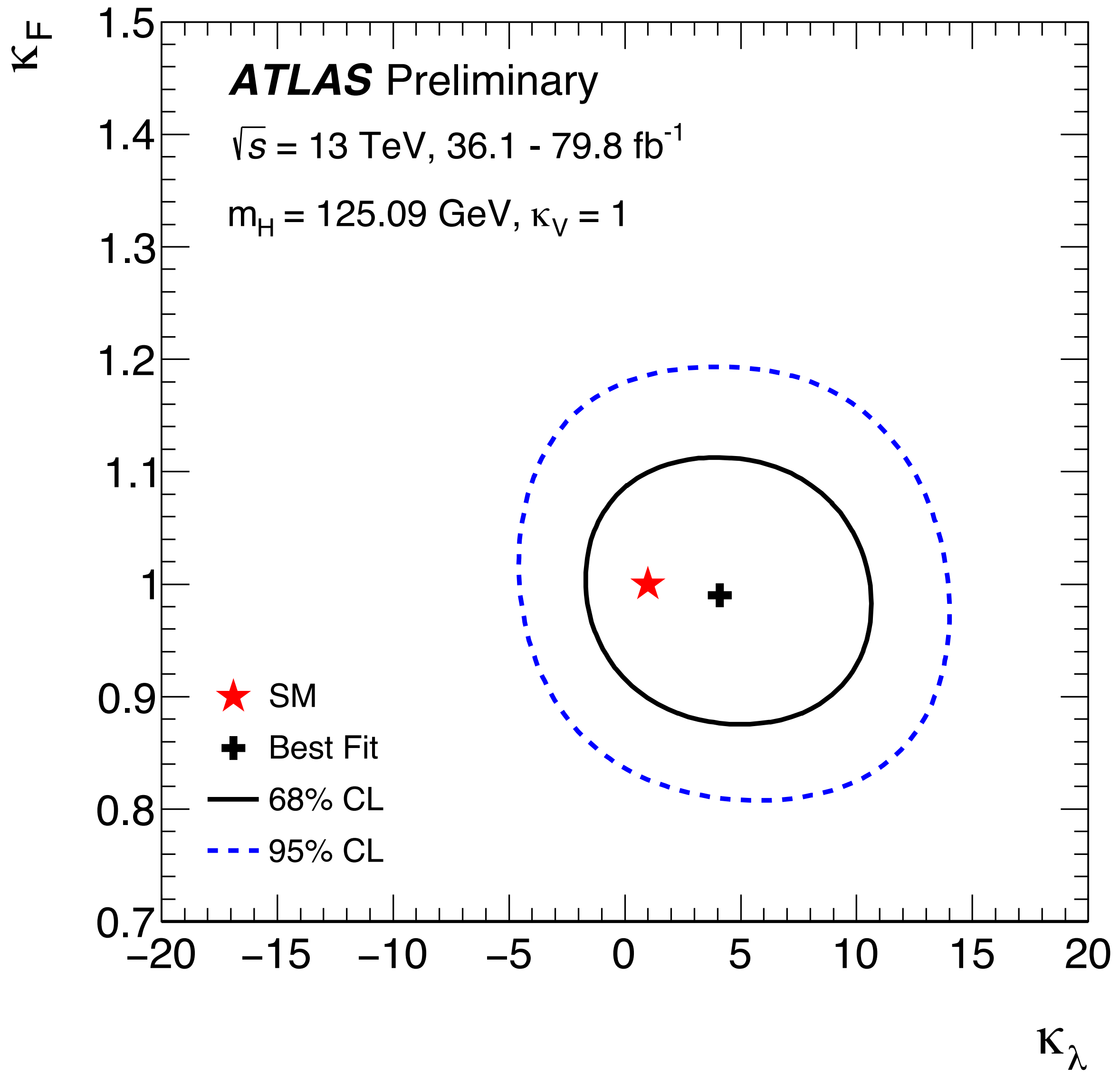

Object selection

Resolved: $\mathscr{L} = 36\text{fb}^{-1}$ Phys. Rev. Lett. 121, 191801
Boosted: $\mathscr{L} = 139\text{fb}^{-1}$ JHEP 11 (2020) 163

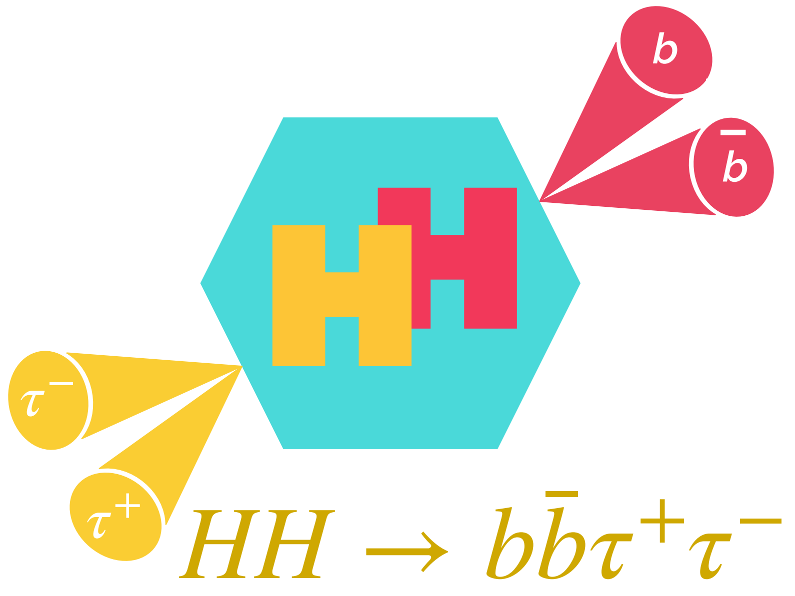

Trigger:

- **Resolved**: based on the tau decay chain:

$\tau_{\text{lep}}\tau_{\text{had}}$		$\tau_{\text{had}}\tau_{\text{had}}$
Single lepton	Single lepton + hadronic tau + additional jet	(Single hadronic tau) || (di-tau + additional jet)

- **Boosted**: Single large radius jet

Resolved:

- $\tau_{\text{lep}}\tau_{\text{had}}$: exactly 1 lepton + 1 hadronic τ of opposite charge
- $\tau_{\text{had}}\tau_{\text{had}}$: exactly two hadronic τs with opposite charge

+ reconstructed mass $m_{\tau\tau}^{MMC} > 60$ GeV

Boosted:

Novel BDT reconstruction and identification of di-τ in large R jets:

- $p_T^{large\ jet} > 300$ GeV
- ≤ 3 sub-jets, sum of track charge ± 1 in each sub-τ

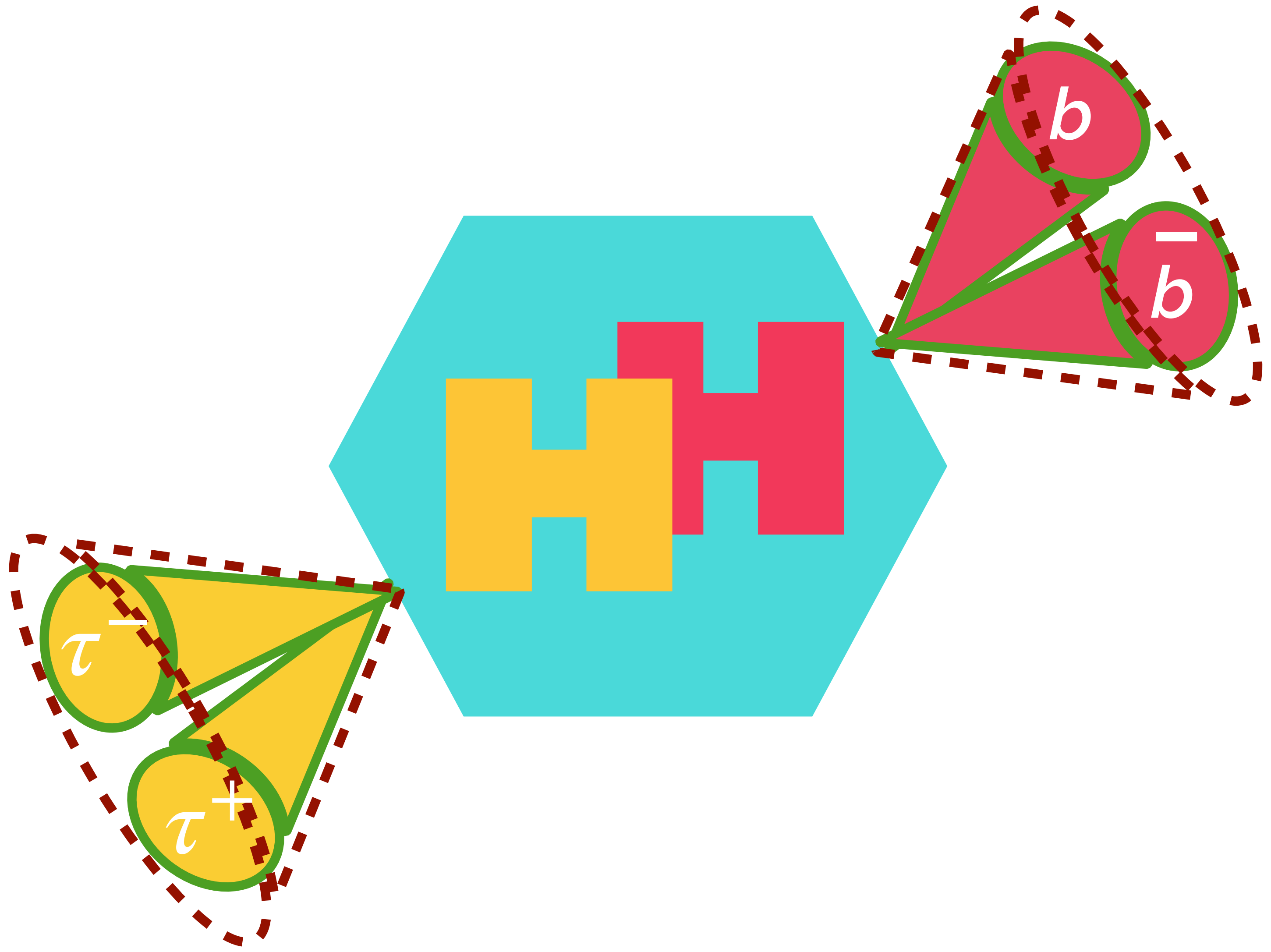

Resolved:

Exactly 2 b-jets with 70% working point:

- Leading jet $p_T > 45\ (80)$ GeV
- Sub-leading jet $p_T > 20$ GeV

Boosted:

- ≥ 1 large R jet with $p_T^{large\ jet} > 300$ GeV
- 2 variable radius b-tagged jets

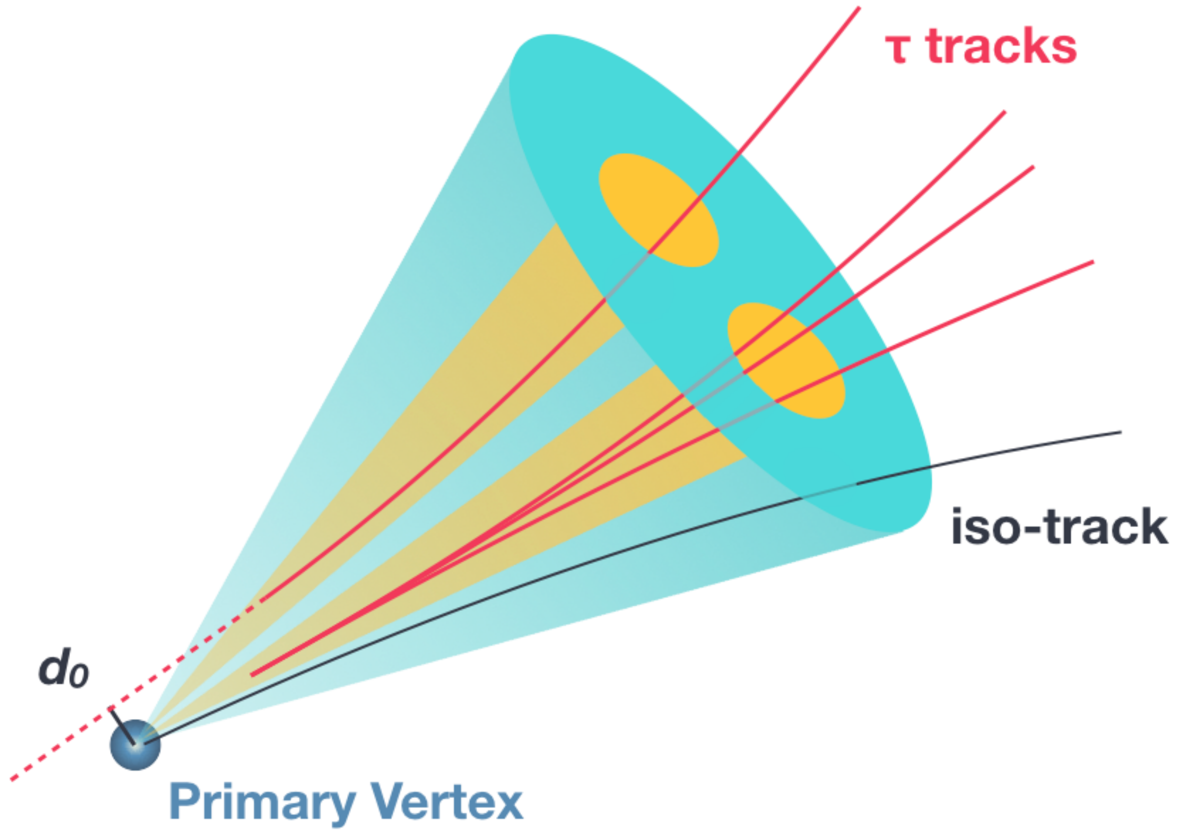

Bbtautau Boosted

Boosted di-tau BDT identification:

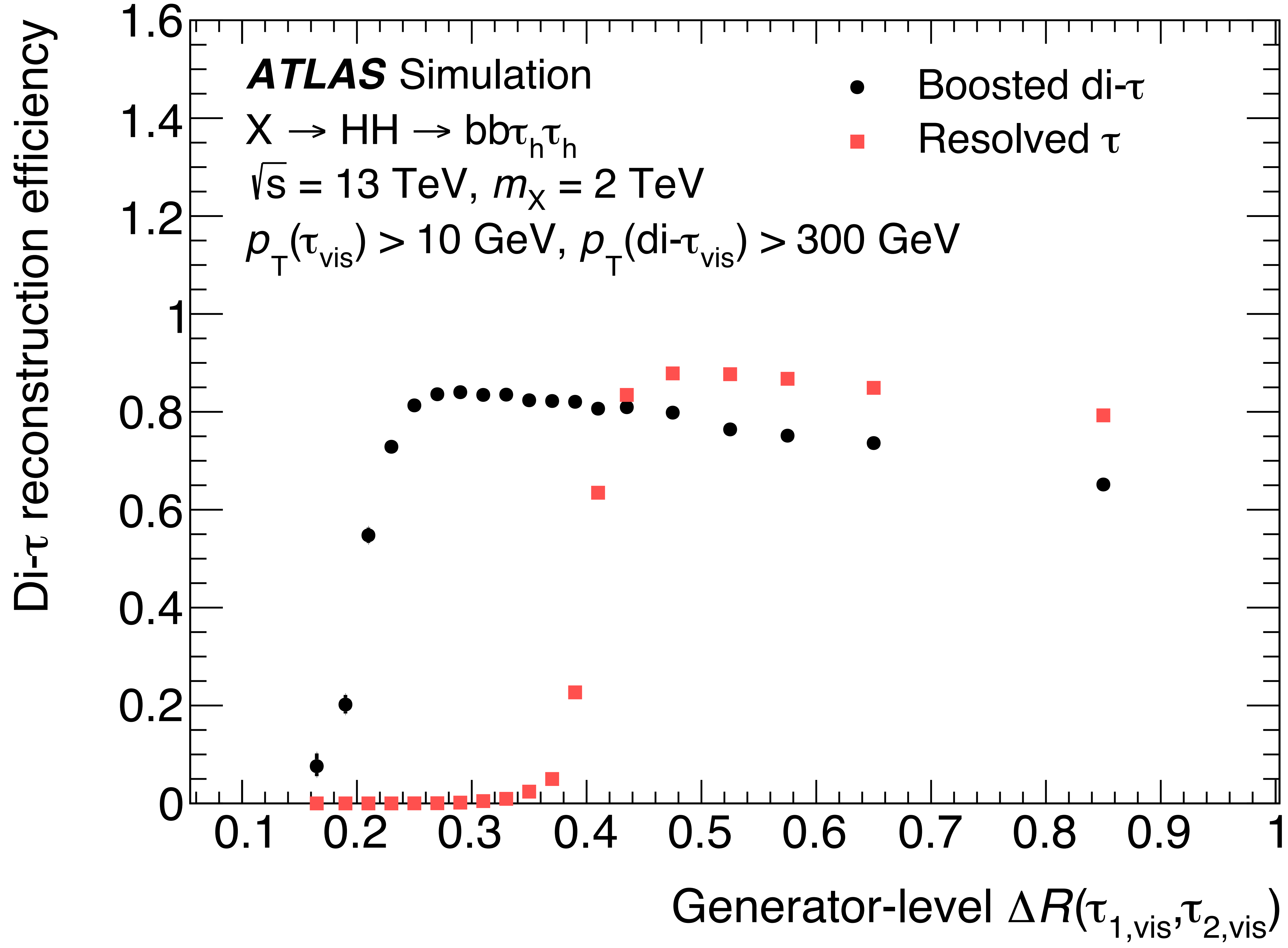

Variable	Definition
$E^{\mathrm{sj}_1}_{\Delta R<0.1}/E^{\mathrm{sj}_1}_{\Delta R<0.2}$ and $E^{\mathrm{sj}_2}_{\Delta R<0.1}/E^{\mathrm{sj}_2}_{\Delta R<0.2}$	Ratios of the energy deposited in the core to that in the full cone, for the sub-jets sj_1 and sj_2, respectively
$p_{\mathrm{T}}^{\mathrm{sj}_2}/p_{\mathrm{T}}^{\mathrm{LRJ}}$ and $(p_{\mathrm{T}}^{\mathrm{sj}_1}+p_{\mathrm{T}}^{\mathrm{sj}_2})/p_{\mathrm{T}}^{\mathrm{LRJ}}$	Ratio of the p_{T} of sj_2 to the di-τ seeding large-radius jet p_{T} and ratio of the scalar p_{T} sum of the two leading sub-jets to the di-τ seeding large-radius jet p_{T}, respectively
$\log(\sum p_{\mathrm{T}}^{\text{iso-tracks}}/p_{\mathrm{T}}^{\mathrm{LRJ}})$	Logarithm of the ratio of the scalar p_{T} sum of the iso-tracks to the di-τ seeding large-radius jet p_{T}
$\Delta R_{\max}(\text{track}, \mathrm{sj}_1)$ and $\Delta R_{\max}(\text{track}, \mathrm{sj}_2)$	Largest separation of a track from its associated sub-jet axis, for the sub-jets sj_1 and sj_2, respectively
$\sum[p_{\mathrm{T}}^{\text{track}}\Delta R(\text{track}, \mathrm{sj}_2)]/\sum p_{\mathrm{T}}^{\text{track}}$	p_{T}-weighted ΔR of the tracks matched to sj_2 with respect to its axis
$\sum[p_{\mathrm{T}}^{\text{iso-track}}\Delta R(\text{iso-track}, \mathrm{sj})]/\sum p_{\mathrm{T}}^{\text{iso-track}}$	p_{T}-weighted sum of ΔR between iso-tracks and the nearest sub-jet axis
$\log(m^{\text{tracks, sj}_1}_{\Delta R<0.1})$ and $\log(m^{\text{tracks, sj}_2}_{\Delta R<0.1})$	Logarithms of the invariant mass of the tracks in the core of sj_1 and sj_2, respectively
$\log(m^{\text{tracks, sj}_1}_{\Delta R<0.2})$ and $\log(m^{\text{tracks, sj}_2}_{\Delta R<0.2})$	Logarithms of the invariant mass of the tracks with $\Delta R < 0.2$ from the axis of sj_1 and sj_2, respectively
$\log(\lvert d^{\mathrm{sj}_1}_{0,\text{lead-track}}\rvert)$ and $\log(\lvert d^{\mathrm{sj}_2}_{0,\text{lead-track}}\rvert)$	Logarithms of the closest distance in the transverse plane between the primary vertex and the leading track of sj_1 and sj_2, respectively
$n^{\mathrm{sj}_1}_{\text{tracks}}$ and $n^{\text{sub-jets}}_{\text{tracks}}$	Number of tracks matched to sj_1 and to all sub-jets, respectively

$HH \to b\bar{b}\tau^+\tau^-$

Bbtautau Resolved

$HH \to b\bar{b}\tau^+\tau^-$

BDT input variables:

Variable	$\tau_{\text{lep}}\tau_{\text{had}}$ channel (SLT resonant)	$\tau_{\text{lep}}\tau_{\text{had}}$ channel (SLT nonresonant & LTT)	$\tau_{\text{had}}\tau_{\text{had}}$ channel
m_{HH}	✓	✓	✓
$m_{\tau\tau}^{\text{MMC}}$	✓	✓	✓
m_{bb}	✓	✓	✓
$\Delta R(\tau,\tau)$	✓	✓	✓
$\Delta R(b,b)$	✓	✓	✓
E_T^{miss}	✓		
E_T^{miss} ϕ centrality	✓		✓
m_T^W	✓	✓	
$\Delta\phi(H,H)$	✓		
$\Delta p_T(\text{lep}, \tau_{\text{had-vis}})$	✓		
Subleading b-jet p_T	✓		

Impact of systematics on SM limit:

Source	Uncertainty (%)
Total	±54
Data statistics	±44
Simulation statistics	±16
Experimental uncertainties	
Luminosity	±2.4
Pileup reweighting	±1.7
τ_{had}	±16
Fake-τ estimation	±8.4
b tagging	±8.3
Jets and E_T^{miss}	±3.3
Electron and muon	±0.5
Theoretical and modeling uncertainties	
Top	±17
Signal	±9.3
$Z \to \tau\tau$	±6.8
SM Higgs	±2.9
Other backgrounds	±0.3

Non resonant limits per channel:

		Observed	-1σ	Expected	$+1\sigma$
$\tau_{\text{lep}}\tau_{\text{had}}$	$\sigma(HH \to bb\tau\tau)$ [fb]	57	49.9	69	96
	$\sigma/\sigma_{\text{SM}}$	23.5	20.5	28.4	39.5
$\tau_{\text{had}}\tau_{\text{had}}$	$\sigma(HH \to bb\tau\tau)$ [fb]	40.0	30.6	42.4	59
	$\sigma/\sigma_{\text{SM}}$	16.4	12.5	17.4	24.2
Combination	$\sigma(HH \to bb\tau\tau)$ [fb]	30.9	26.0	36.1	50
	$\sigma/\sigma_{\text{SM}}$	12.7	10.7	14.8	20.6

BDTs

$HH \to b\bar{b}\gamma\gamma$

Non Resonant

Variable	Definition
Photon-related kinematic variables	
$p_T/m_{\gamma\gamma}$	Transverse momentum of the two photons scaled by their invariant mass $m_{\gamma\gamma}$
η and ϕ	Pseudo-rapidity and azimuthal angle of the leading and sub-leading photon
Jet-related kinematic variables	
b-tag status	Highest fixed b-tag working point that the jet passes
p_T, η and ϕ	Transverse momentum, pseudo-rapidity and azimuthal angle of the two jets with the highest b-tagging score
$p_T^{b\bar{b}}$, $\eta_{b\bar{b}}$ and $\phi_{b\bar{b}}$	Transverse momentum, pseudo-rapidity and azimuthal angle of b-tagged jets system
$m_{b\bar{b}}$	Invariant mass built with the two jets with the highest b-tagging score
H_T	Scalar sum of the p_T of the jets in the event
Single topness	For the definition, see Eq. (1)
Missing transverse momentum-related variables	
E_T^{miss} and ϕ^{miss}	Missing transverse momentum and its azimuthal angle

Resonant

Variable	Definition
Photon-related kinematic variables	
$p_T^{\gamma\gamma}$, $y^{\gamma\gamma}$	Transverse momentum and rapidity of the di-photon system
$\Delta\phi_{\gamma\gamma}$ and $\Delta R_{\gamma\gamma}$	Azimuthal angular distance and ΔR between the two photons
Jet-related kinematic variables	
$m_{b\bar{b}}$, $p_T^{b\bar{b}}$ and $y_{b\bar{b}}$	Invariant mass, transverse momentum and rapidity of the b-tagged jets system
$\Delta\phi_{b\bar{b}}$ and $\Delta R_{b\bar{b}}$	Azimuthal angular distance and ΔR between the two b-tagged jets
N_{jets} and $N_{b-\text{jets}}$	Number of jets and number of b-tagged jets
H_T	Scalar sum of the p_T of the jets in the event
Photons and jets-related kinematic variables	
$m_{b\bar{b}\gamma\gamma}$	Invariant mass built with the di-photon and b-tagged jets system
$\Delta y_{\gamma\gamma,b\bar{b}}$, $\Delta\phi_{\gamma\gamma,b\bar{b}}$ and $\Delta R_{\gamma\gamma,b\bar{b}}$	Distance in rapidity, azimuthal angle and ΔR between the di-photon and the b-tagged jets system

Post-fit plots

Non Resonant

BDT loose

BDT tight

Low mass

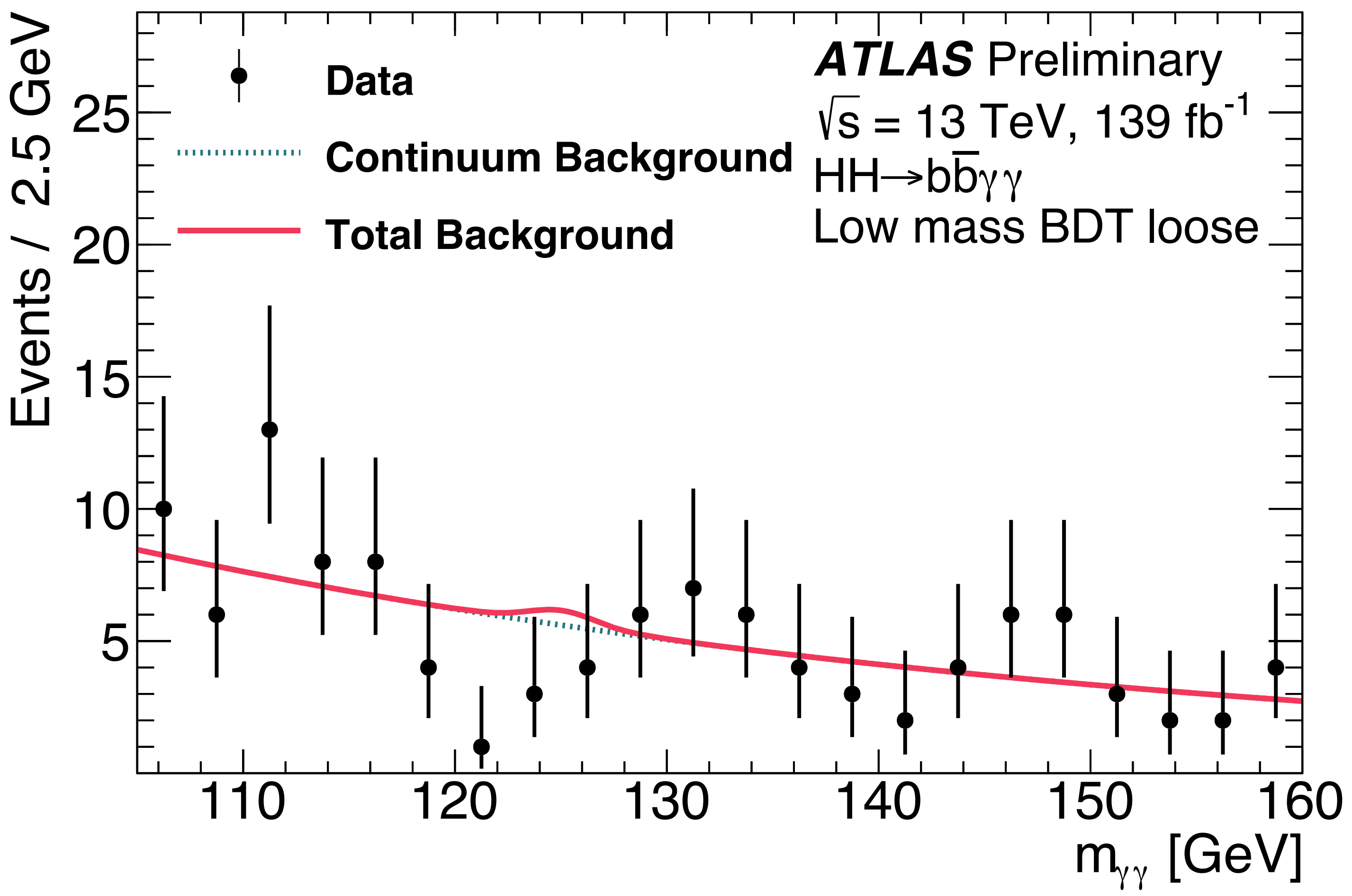

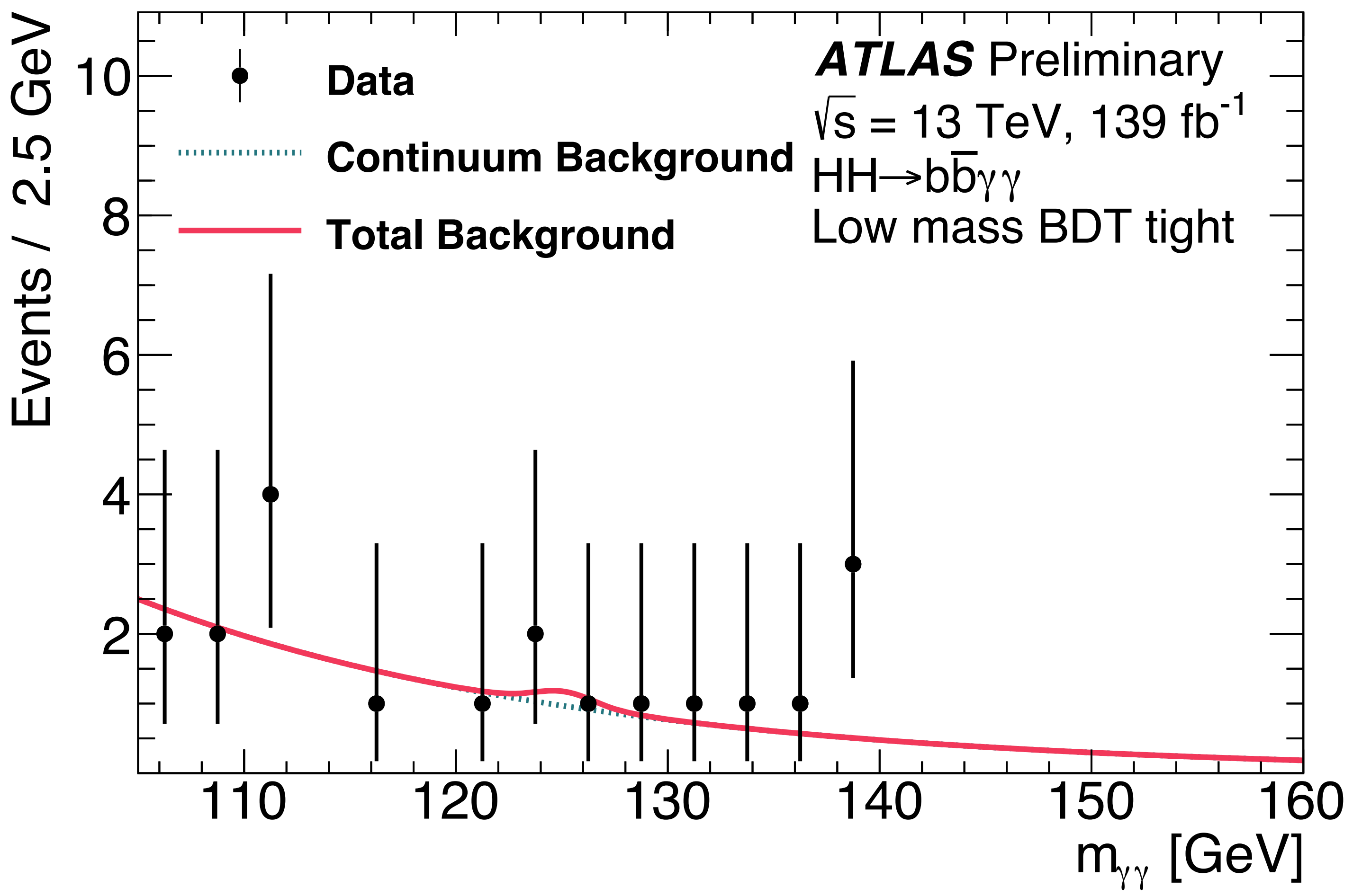

High mass

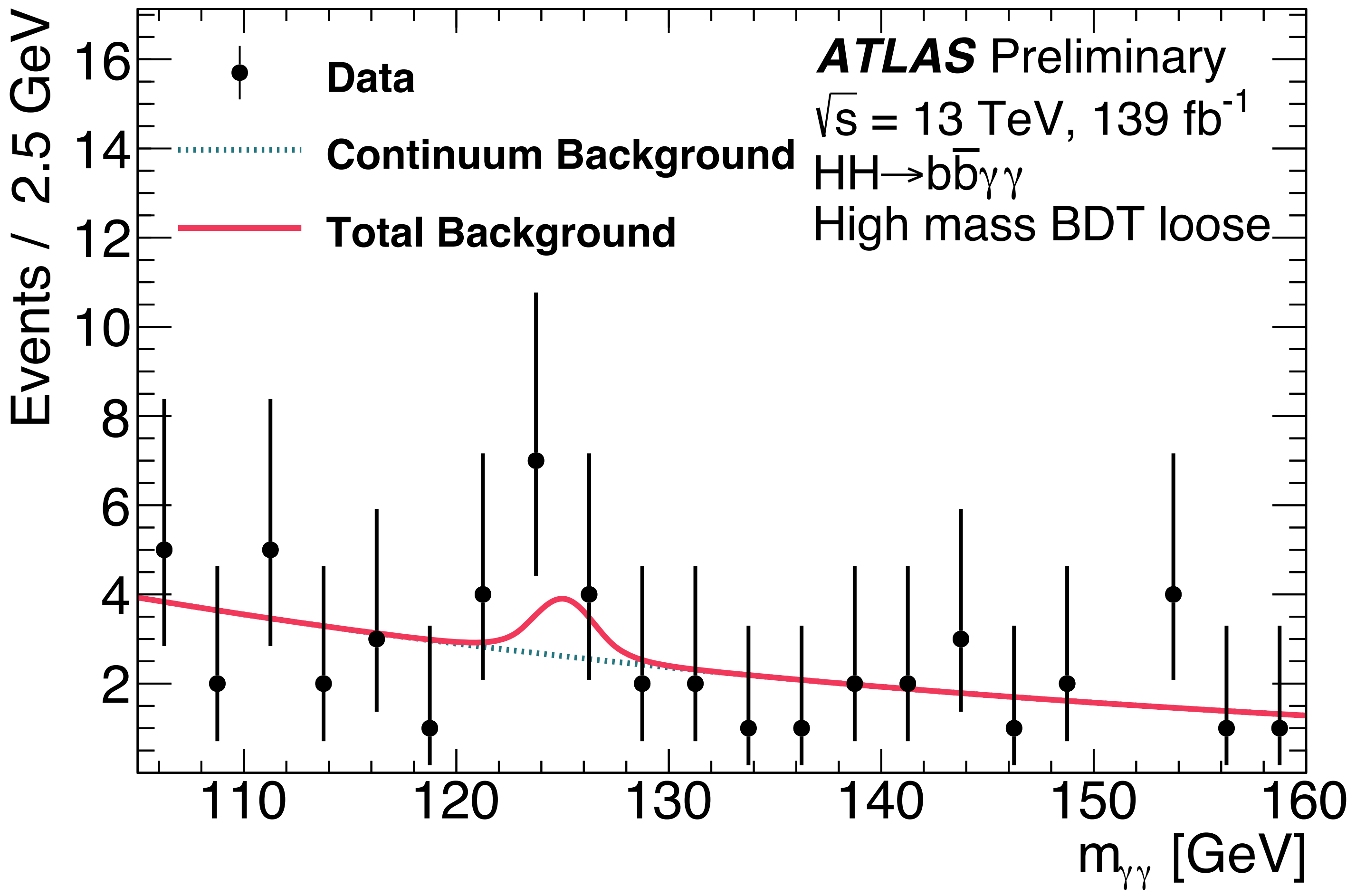

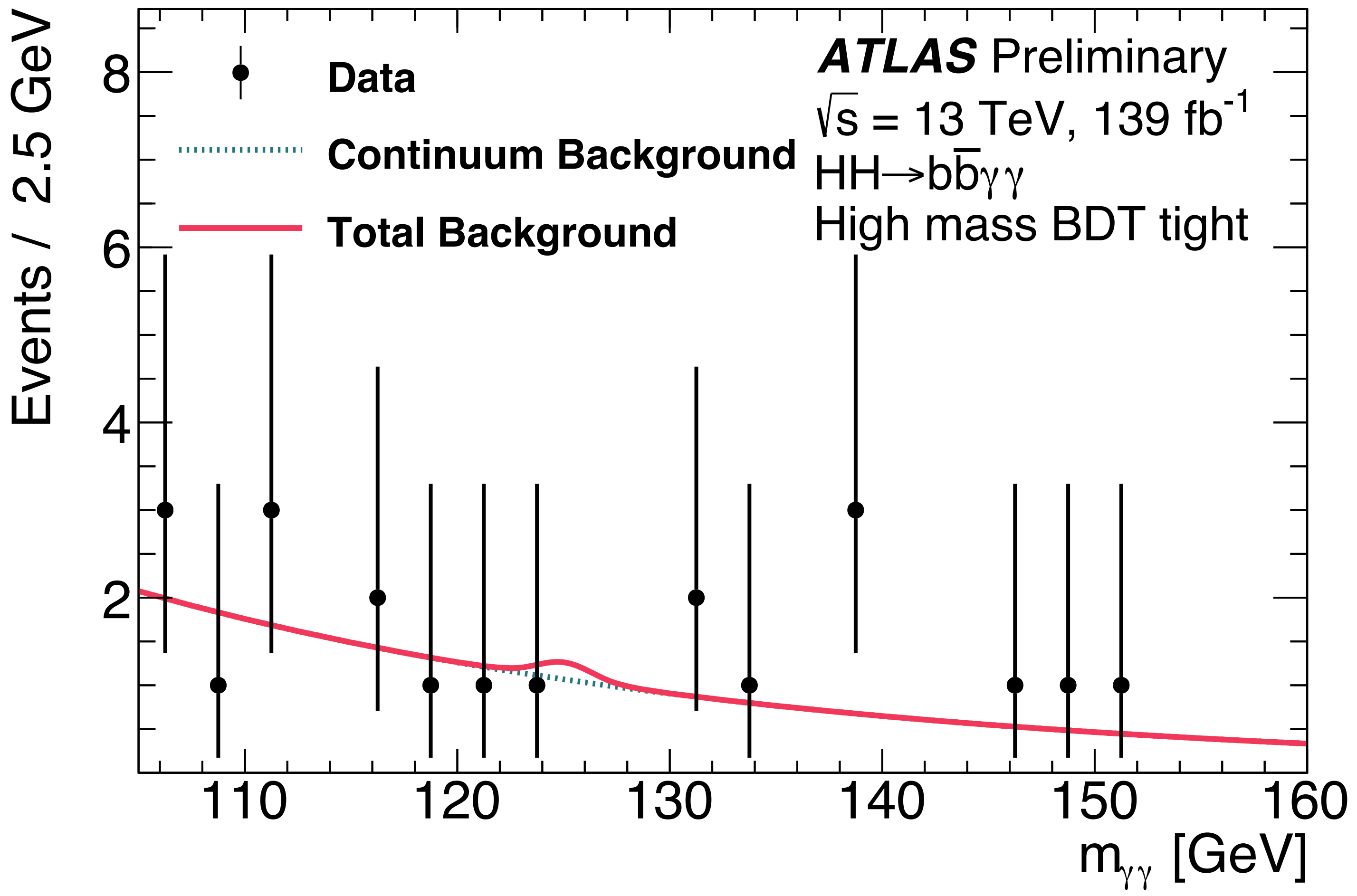

Resonant

$HH \rightarrow b\bar{b}\gamma\gamma$

Mx = 300 GeV

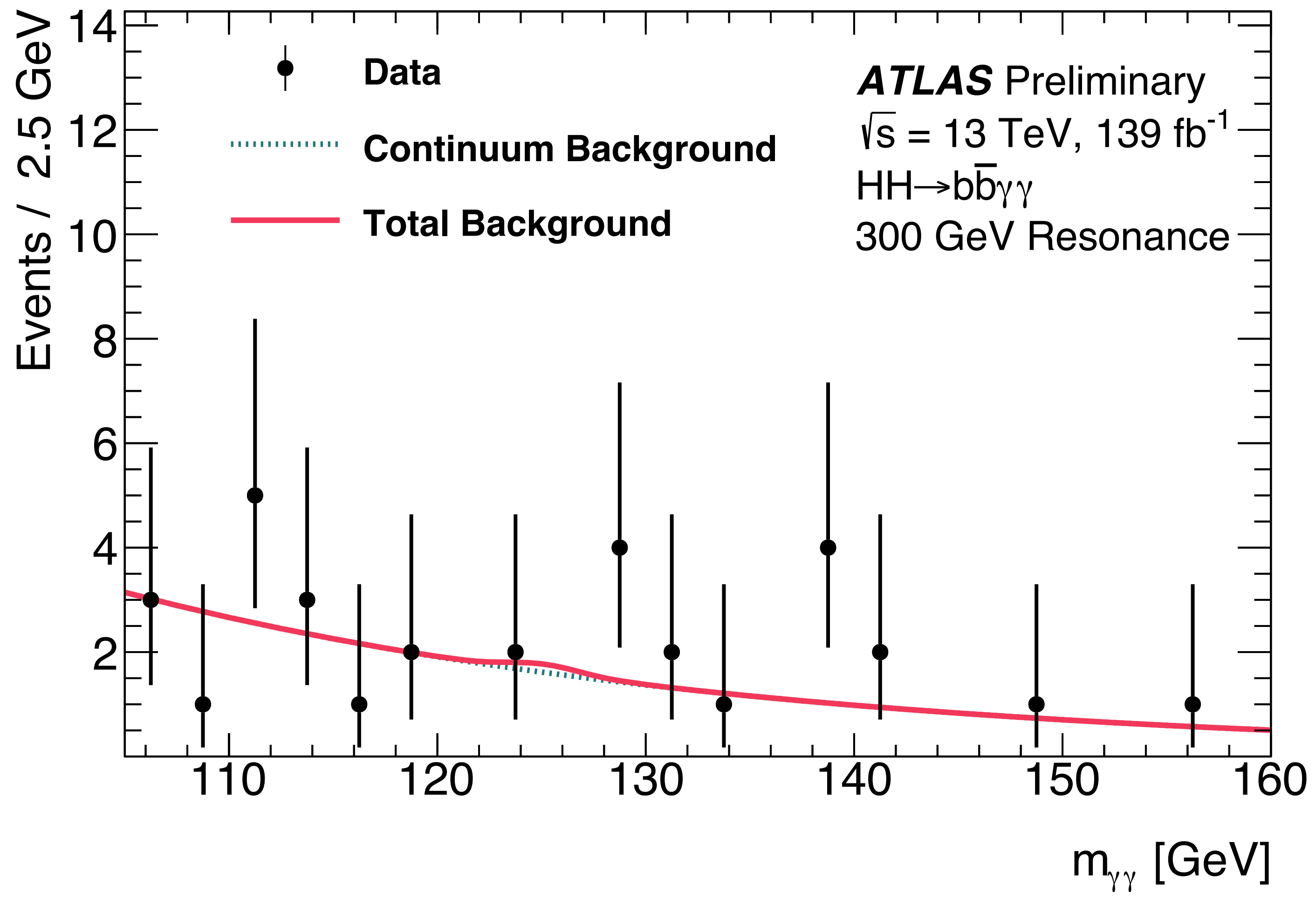

Mx = 500 GeV

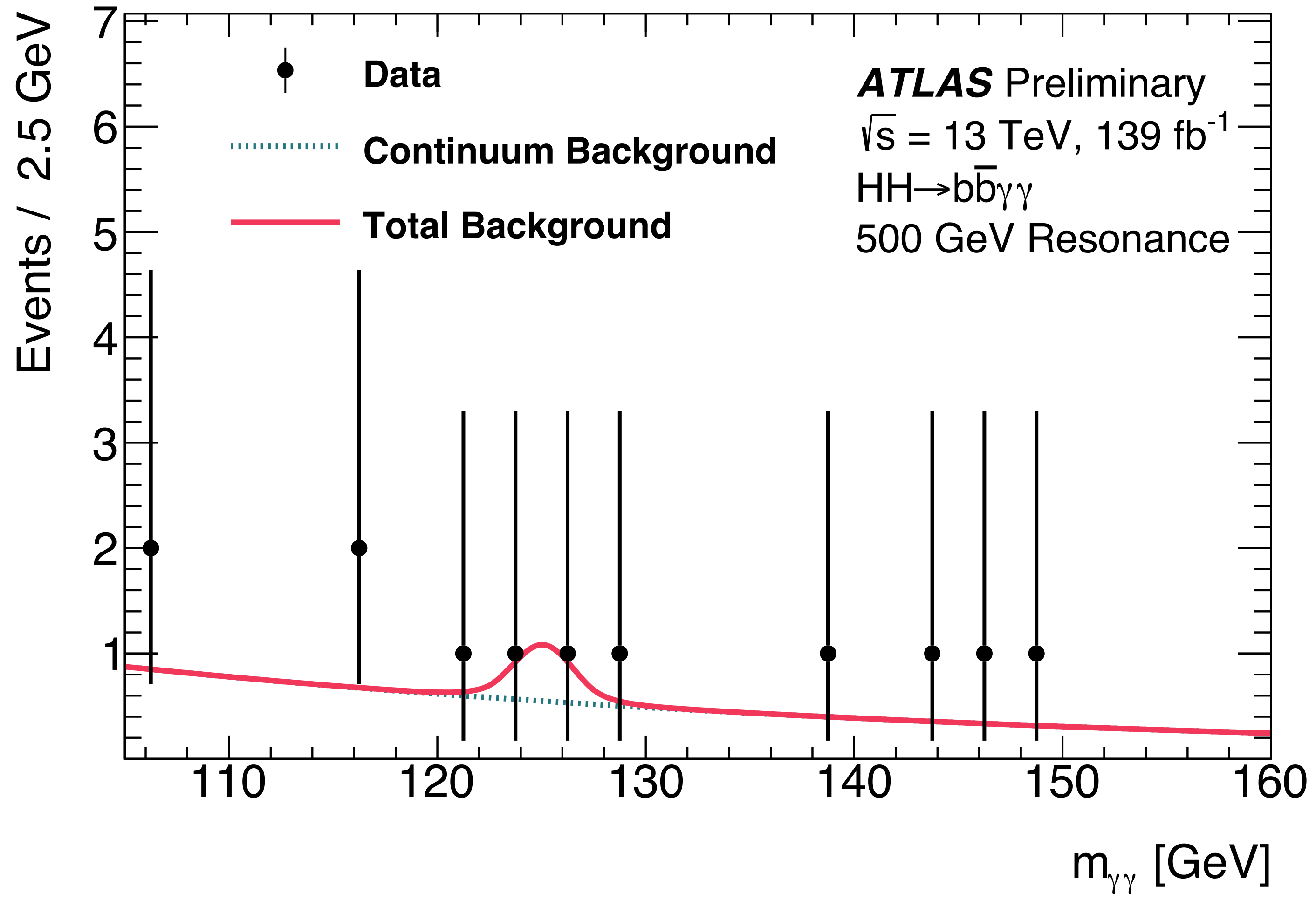

Yields and systematics

	High mass BDT tight	High mass BDT loose	Low mass BDT tight	Low mass BDT loose
Continuum background	4.9 ± 1.1	9.5 ± 1.5	3.7 ± 1.0	24.9 ± 2.5
Single Higgs boson background	0.670 ± 0.032	1.57 ± 0.04	0.220 ± 0.016	1.39 ± 0.04
ggF	0.261 ± 0.028	0.44 ± 0.04	0.063 ± 0.014	0.274 ± 0.030
$t\bar{t}H$	0.1929 ± 0.0045	0.491 ± 0.007	0.1074 ± 0.0033	0.742 ± 0.009
ZH	0.142 ± 0.005	0.486 ± 0.010	0.04019 ± 0.0027	0.269 ± 0.007
Rest	0.074 ± 0.012	0.155 ± 0.020	0.008 ± 0.006	0.109 ± 0.016
SM HH signal	0.8753 ± 0.0032	0.3680 ± 0.0020	$(49.4 \pm 0.7) \cdot 10^{-3}$	$(78.7 \pm 0.9) \cdot 10^{-3}$
ggF	0.8626 ± 0.0032	0.3518 ± 0.0020	$(46.1 \pm 0.7) \cdot 10^{-3}$	$(71.8 \pm 0.9) \cdot 10^{-3}$
VBF	0.01266 ± 0.00016	0.01618 ± 0.00018	$(3.22 \pm 0.08) \cdot 10^{-3}$	$(6.923 \pm 0.011) \cdot 10^{-3}$
Alternative $HH(\kappa_\lambda = 10)$ signal	6.36 ± 0.05	3.691 ± 0.038	4.65 ± 0.04	8.64 ± 0.06
Data	2	17	5	14

	$m_X = 300$ GeV	$m_X = 500$ GeV
Continuum background	5.6 ± 2.4	3.5 ± 2.0
Single Higgs boson background	0.339 ± 0.009	0.398 ± 0.010
SM HH background	$(20.6 \pm 0.5) \cdot 10^{-3}$	0.1932 ± 0.0015
$X \rightarrow HH$ signal	5.771 ± 0.031	5.950 ± 0.026
Data	6	4

		Relative impact of the systematic uncertainties in %	
Source	Type	Non-resonant analysis HH	Resonant analysis $m_X = 300$ GeV
Experimental			
Photon energy scale	Norm. + Shape	5.2	2.7
Photon energy resolution	Norm. + Shape	1.8	1.6
Flavor tagging	Normalization	0.5	< 0.5
Theoretical			
Heavy flavor content	Normalization	1.5	< 0.5
Higgs boson mass	Norm. + Shape	1.8	< 0.5
PDF+α_s	Normalization	0.7	< 0.5
Spurious signal	Normalization	5.5	5.4

Selection

$b\bar{b}l\nu l\nu$ final state : $\mathscr{L} = 139\text{fb}^{-1}$ | Phys. Lett. B 801 (2020) 135145
$b\bar{b}l\nu q\bar{q}$ final state : $\mathscr{L} = 36\text{fb}^{-1}$ | JHEP 04 (2019) 092
$\gamma\gamma WW^*$ final state : $\mathscr{L} = 36\text{fb}^{-1}$ | Eur. Phys. J. C 78 (2018) 1007
WW^*WW^* final state : $\mathscr{L} = 36\text{fb}^{-1}$ | JHEP 05 (2019) 124

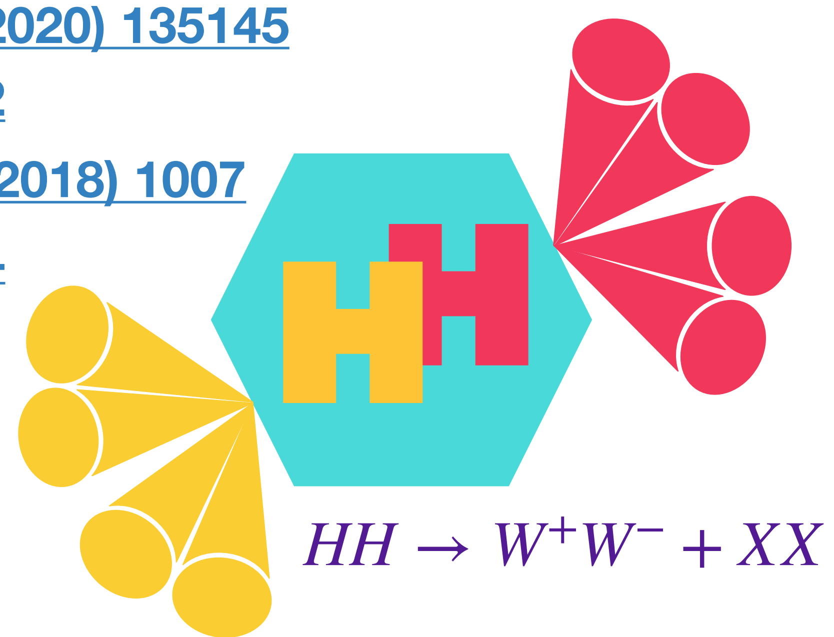

$b\bar{b}l\nu q\bar{q}$ final state

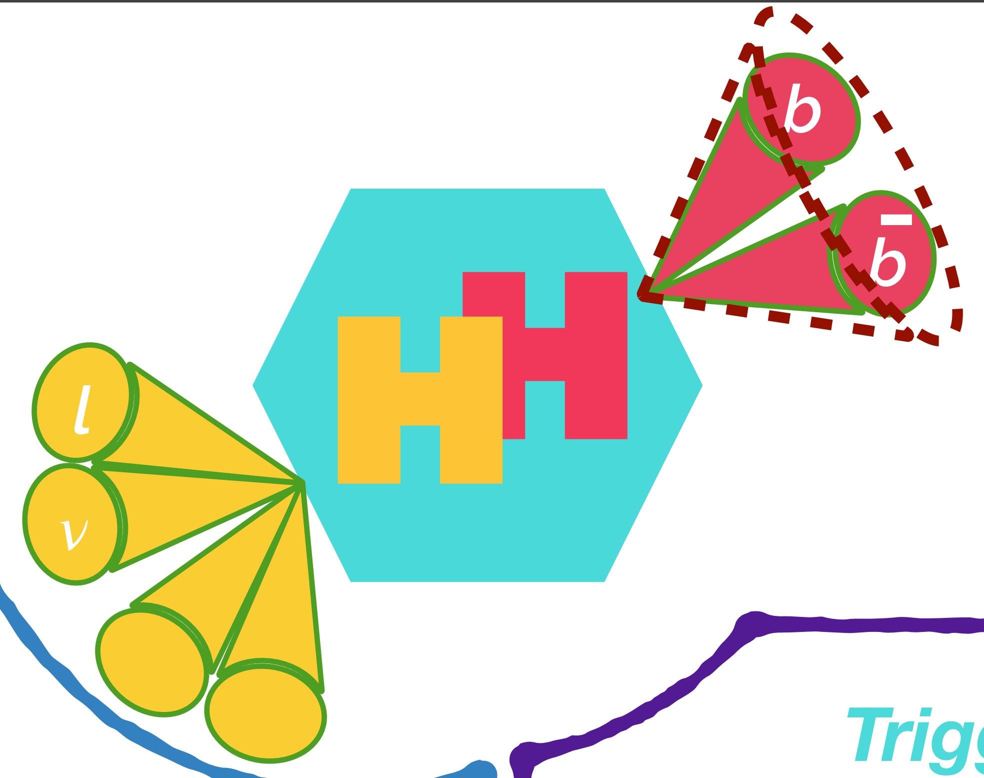

Trigger:
Single lepton triggers

Event selection:

$H \to b\bar{b}$:

- Resolved: exactly 2 b-tagged jets @ 85%
- Boosted: One large R jet with $\Delta R(jet, l) > 1.0$ and mass (90, 140) GeV, with 2 VR b-tagged jets @ 85%

$H \to WW^* \to l\nu q\bar{q}$:

- Resolved:
  - ≥ 1 high quality lepton.
  - ≥ 2 additional jets, pair chosen with minimising $\Delta R(jet, jet)$
  - Kinematic fit to find the neutrino momentum assuming $m_H = 125$ GeV
- Boosted: same as in resolved.

Signal regions:

- Resolved: cuts applied on kinematic and geometrical variables to define 1 non-resonant category + 1 resonant category/mass point
- Boosted: $E_T^{miss} > 50$ GeV

Fit: m_{HH} in different categories

$b\bar{b}l\nu l\nu$ final state

Resolved

Trigger:
Single lepton supplemented with di-lepton triggers

Event selection:

- $H \to b\bar{b}$:
  - Exactly 2 b-tagged jets @ 70 %.
  - $m_{b\bar{b}}$ in (110,140) GeV
- $H \to WW^* \to l\nu l\nu$:
  - Exactly 2 opposite charge high quality leptons.
  - Due to spin-correlation, m_{ll} in (20, 60) GeV.
  - Categories: based on flavour.
- *Deep neural Network:*
  - To remove dominant backgrounds
  - Trained on $HH \to b\bar{b}WW^*$, but output sensitive to $HH \to b\bar{b}ZZ^*$ and $HH \to b\bar{b}\tau\tau$

Fit: single bin in different categories

Results

$b\bar{b}l\nu l\nu$ final state : $\mathscr{L} = 139\text{fb}^{-1}$ Phys. Lett. B 801 (2020) 135145
$b\bar{b}l\nu q\bar{q}$ final state : $\mathscr{L} = 36\text{fb}^{-1}$ JHEP 04 (2019) 092
$\gamma\gamma WW^*$ final state : $\mathscr{L} = 36\text{fb}^{-1}$ Eur. Phys. J. C 78 (2018) 1007
WW^*WW^* final state : $\mathscr{L} = 36\text{fb}^{-1}$ JHEP 05 (2019) 124

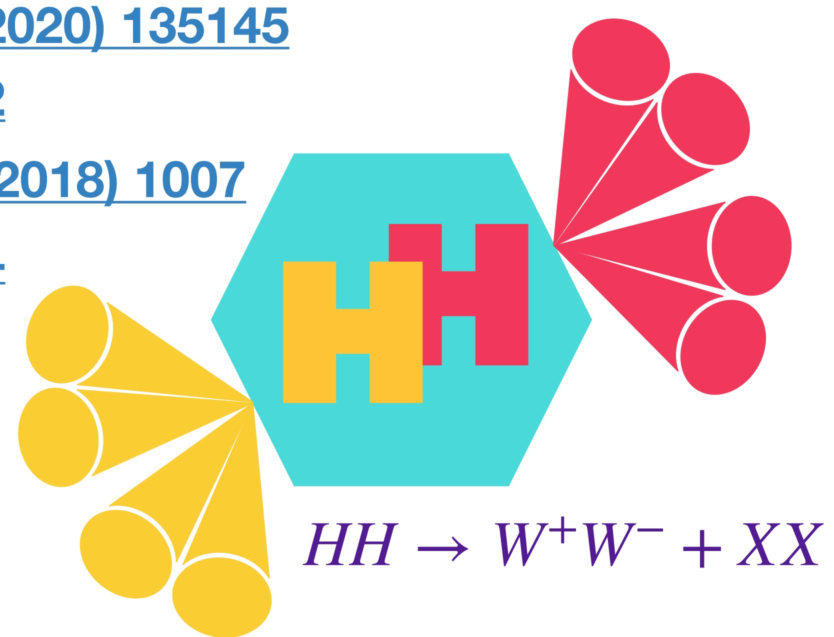

$b\bar{b}l\nu q\bar{q}$ final state

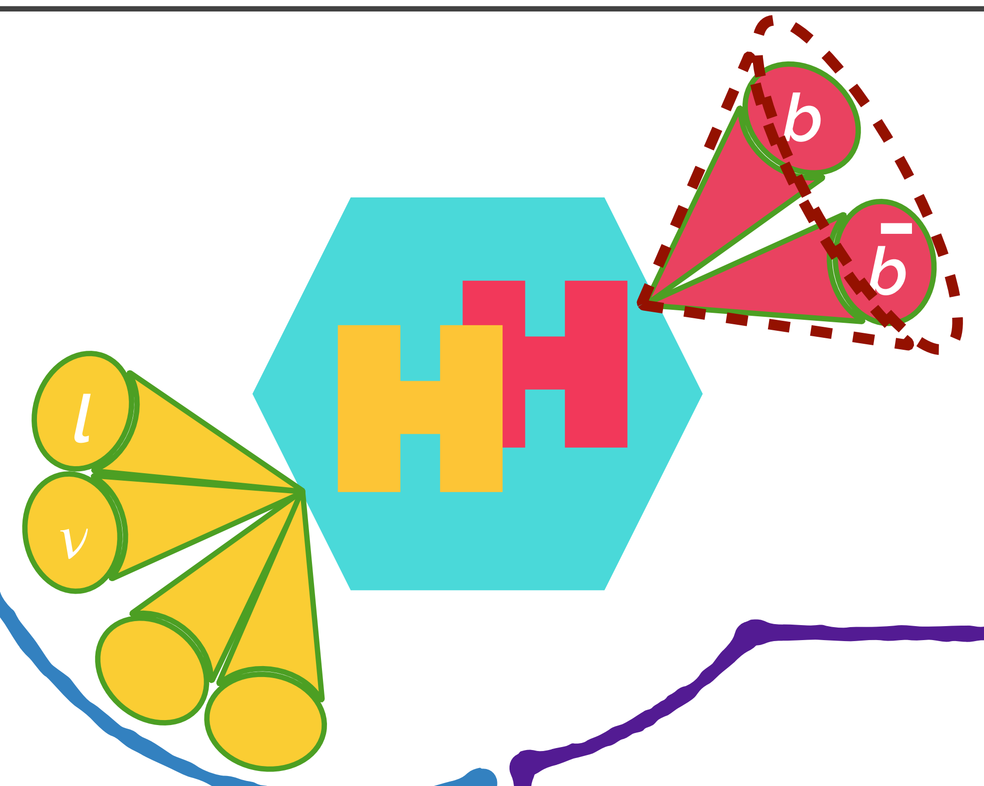

Non-resonant Resolved

σ_{HH}^{ggF} **observed (expected)** limit is **300 (190)** times the SM prediction.

Resonant: Resolved Boosted

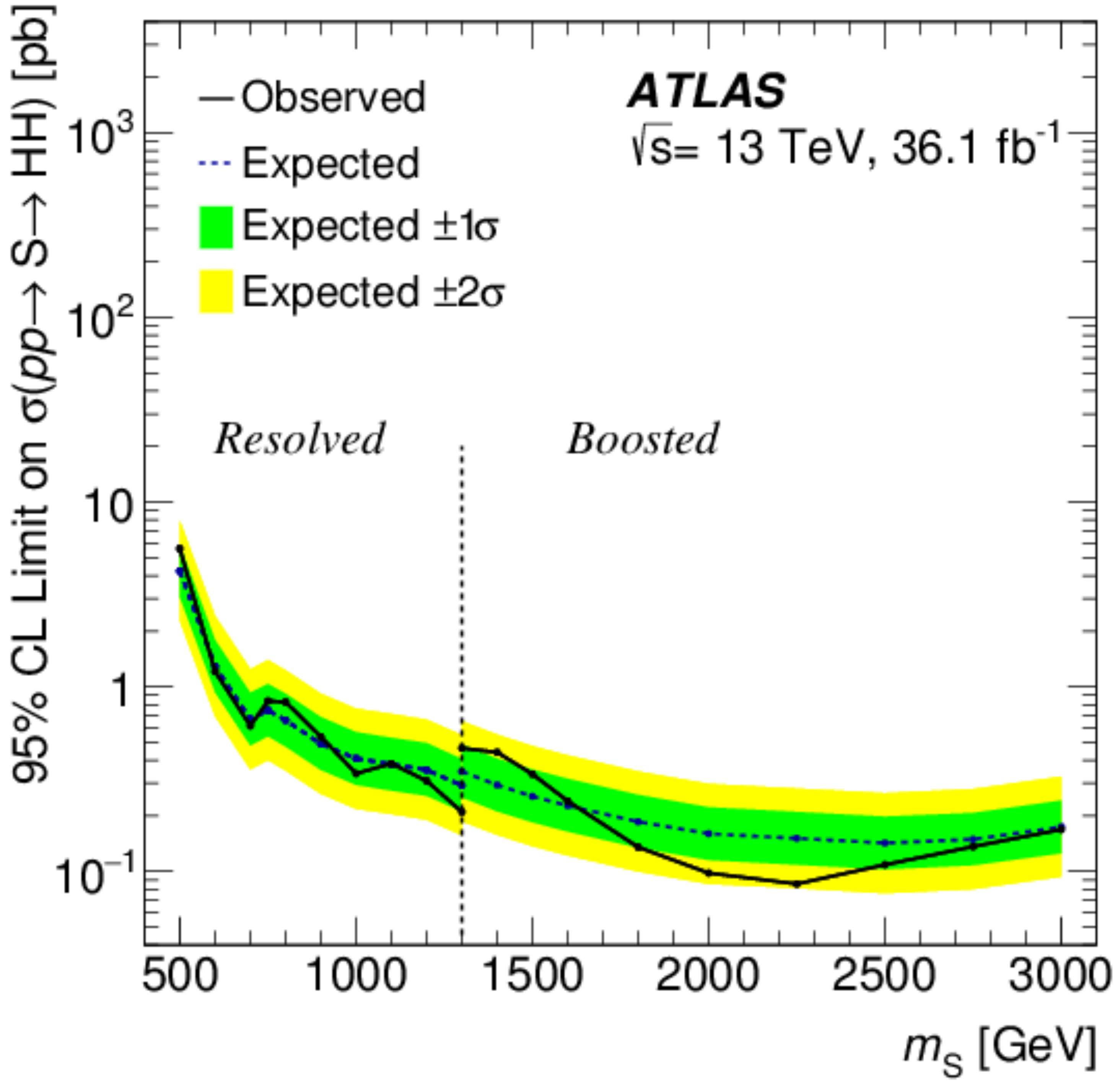

Limits set on $\sigma(X \to HH)$ where X is a narrow-width scalar resonance

$b\bar{b}l\nu l\nu$ final state Resolved

Non-resonant

σ_{HH}^{ggF} **observed (expected)** limit is **14 (29)** times the SM prediction.